PREPARATION AND APPLICATION OF SULFUR NANOPARTICLES DISPERSED ONTO SOFT MATRICES

A THESIS SUBMITTED IN PARTIAL FULFILLMENT OF THE REQUIREMENT FOR THE DEGREE OF MASTER OF PHILOSOPHY (M. PHIL) IN CHEMISTRY

By

Mst. Maria Rahman
Roll No. 0411033203F

Department of Chemistry
Faculty of Engineering
Bangladesh University of Engineering and Technology (BUET),
Dhaka-1000, Bangladesh

March, 2015

CONTENTS

Declaration

It is hereby declared that this thesis entitled "*PREPARATION AND APPLICATION OF SULFUR NANOPARTICLES DISPERSED ONTO SOFT MATRICES*" has not been submitted elsewhere for the award of any degree or diploma in any university or institution to the best of my knowledge.

Mst. Maria Rahman
M. Phil. Student
Roll No. 0411033203F
Department of Chemistry,
BUET, Dhaka, Bangladesh

Dedicated

To

All the people who helped me to reached at this stages

ACKNOWLEDGEMENT

First of all, I would like to express my deepest sense of faith and gratitude to almighty Allah who is merciful to all and all good things that happened and is being happened by his wish.

I would like to express my deep appreciation to my supervisor professor Dr. Manwarul Islam and Professor Dr.AL Nakib Chowdhury, Department of Chemistry, BUET, Dhaka, for their support, encouragement and helpful guidance throughout my research work. For their intelligence, enthusiasm and inspiration have enabled me to complete the research work in spite of many limitations.

I would like to special thanks to all members of the Chemistry Department, BUET for their valuable suggestions and helpfuldiscussion during my research work.

I am also thankful to Dr. Dilip Kumer Shaha, Materials Science Division, Atomic Energy Centrer, Dhaka and Dr. Mahbubur Rahman, ICDDR‟B, Dhaka for their co-operation throughout the period of the research work.

I would like to thank all of the members who examine my thesis. I also express my deepest sense of gratitude to my beloved parents and all of my family members for their immeasurable sacrifice, blessing and longstanding encouragement that leads to all my success in study and other fields.

Finally, I would like to acknowledge the authority of BUET for providing financial support for this interesting research project.

MST. MARIA RAHMA

Abstract

Sulfur nanoparticles (SNPs) were synthesized electrochemically and chemically by reduction of sodium thiosulfate and acid catalyzed precipitation of sodium thiosulfate in presence citry trimethyl ammonium bromide (CTAB) respectively. Conductive polymer Polyaniline (PANI) and PANI-SNPs nanocomposite were also synthesized by electrochemically and chemically. The synthesized S NPs, PANI and S NPs- PANI nanocomposite were characterized by X-ray diffraction spectrometer (XRD), Scanning electron microscopy (SEM) and energy dispersive spectroscopy (EDS), infrared spectroscopy (FTIR), thermo gravimetric analysis (TGA) and UV visible spectroscopic (UV) method. Experimental results showed that the particle size of synthesized SNPs in both methods was bellow 100 nm. Results also show that electrochemically synthesized S NPs (55 nm) has lower particle size than that of chemically synthesized S NPs (65 nm). Moreover, electrochemically synthesized PANI and S NPs-PANI nanocomposite showed more uniform, small,and spherical surface morphology than chemically synthesized PANI and S NPs-PANI nanocomposite. N-isopropyl acryl amide (NIPA) gel and SNPs-NIPA gel were also synthesized and characterized by XRD, SEM and EDS methods. XRD results showed that NIPA and SNPs-NIPA gel both were semicrystalline nature. SEM image showed that the gel had porous structure with three dimensional networks which made the gel ability to act as a drug carrier. SNPs-NIPA gel was temperature-sensitive and release SNPs from NIPA gel matrices with increased temperature $(25\text{-}40)^0$C. Additionally, antibacterial and antifungal test were done by synthesized SNPs, PANI and PANI- SNPs nanocomposite. The obtained results showed that PANI-SNPs nanocomposite enhanced the antibacterial and antifungal activity than SNPs and PANI.

Keywords: Sulfur Nanoparticles, Polyaniline, N-isopropyl acryl amide gel, Nanocomposite, Antibacterial Activity, Antifungal Activity

List of Figures

List of Tables

Chapter 1

Introduction

1.1 GENERAL BACKGROUND

Nanoparticles (NPs) are attracting considerable interest due to their unique physical and chemical properties and extensive practical applications in high and low-tech industries. Nanotechnology is currently employed as a tool to explore the darkest avenues of medical sciences in several ways like imaging, sensing, targeted drug delivery, gene delivery systems and artificial implants [1-3]. The new age drugs are NPs of polymers, metals or ceramics, which can resist conditions like cancer and fight human pathogens like bacteria [4]. To realize biomedical applications of NPs, it may be interesting to prepare NPs/Polymer composites, where NPs would still have small size and large surface area and the polymer can help controlled release of active ingredients [5-6]. Polymer nanocomposites are materials in which nanoscopic inorganic particles are dispersed in an organic polymer matrix in order to significantly improve the performance and properties of the polymer. However, in recent years an upward trend in the application of different NPs as antifungal or antimicrobial agents has been observed [7, 8]. Generally, NPs exhibit remarkably unusual physicochemical and biological activities because of their small size. An antimicrobial agent represents a substance that kills or inhibits the growth of microorganisms. In general, chemical antimicrobials act upon microorganisms by interfering bacterial metabolism which in turn hinders normal cellular activities. However, an important issue associate with the chemical antimicrobials is that microorganisms develop resistance against common antimicrobials after a certain time [9]. In contrast, NPs based antimicrobial agents have much lower tendency to induce microbial resistance than chemical antimicrobials [7]. Similar to chemical pesticides, NPs based pesticides and herbicides are being explored for the application of the antimicrobial agents to protect crops from various diseases [10]. Extensive studies on NPs based systems may eliminate the excessive use of fertilizers and pesticides in the agricultural field [11]. The broad spectrum of antibacterial and antifungal properties of NPs can help to formulate NPs based pesticides [12, 13], which would be practically feasible if the synthetic method is inexpensive and useful for bulk scale production. Among the different inorganic NPs based antimicrobial agents, silver has been extensively studied by many researchers because of its several advantages over other NPs such as copper, zinc, gold, magnesium, ZnO, Al_2O_3, TiO_2 etc. However, in the field of agricultural applications silver NPs also have limited studies. In spite of the fact that silver NPs are studied extensively for other antimicrobial applications, risk factors upon mammalian cells are also associated with silver [14]. The use of inorganic NPs as crop protecting antimicrobial agents is presently just in the initial stage. It can be

concluded that, similar to other research areas, there is enormous potential for the use of nanotechnology in the agricultural field; however, studies on this area are still not well focused. The use of nanosilver has been studied recently against phytopathogen Colletotrichum gloesporioides [15]. Additionally, other NPs (Fe, Cu, Si, Al, Zn, ZnO, TiO_2, CeO_2, Al_2O_3, carbon nanotubes etc.) have also been studied and reported some adverse effects on plant growth apart from the antimicrobial properties [16]. Sometimes NPs also have an adverse effect on the growth of useful soil bacteria, such as Pseudomonas putida KT2440 [17]. In this context, various research groups focused their interest on the usage of eco-friendly pesticides. In recent years, there was an increase in the demand of „„organic"" grade fruit and vegetables as part of a healthy diet. In the case of apples, strawberries, grapes, tomatoes, potatoes and many others fruit and vegetables, sulfur, copper salt etc. are permitted as „„organic""class pesticides to protect the crops [18, 19]. However, in many countries there are restrictions on copper compounds because of environmental reasons and toxicity to aquatic life [20]. At the same time, sulfur is recognized as an important element for plant growth through balanced fertilization and is sometimes synthesized naturally in its elemental form by some plants and microorganisms as protection [21, 22]. Sulfur is indeed more acceptable as a safer organic pesticide for agricultural firms and also a useful nutrient for the plants [23]. However, elemental sulfur(S) in nano, micro or bulk state is widely used for different industrial and pharmaceutical applications [24, 25]. Now realizing the importance of S NPs in different applications, the development of an easy synthesis method is a pressing need. Recently, great efforts have been focused on finding preparation methods to produce various NPs with well-defined characteristics [26]. Among these, the electrosynthesis has emerged as a convenient, clean and inexpensive technique for the synthesis of nanostructures materials [24].

1.2 Nanotechnology and Nanomaterials

Nanotechnology have been imminent a great importance for scientists, engineers, and physicians which work at the cellular and molecular levels to produce major advances in the life sciences and environmental sciences. The excellent properties of these materials when compared with their bulk counterparts provide a very promising prospect for their use in this field. Nanoparticles are ultrafine particles of nanometer dimensions located in the transition region between molecules and microscopic (micron-size) structures. Viewed as molecules, they are so large that they provide access to realms of quantum behavior that are not otherwise accessible; viewed as materials, they are so small that they exhibit characteristics

that are not observed in larger (even 100 nm) structures. It is in this size regime that many recent advances have been made in biology, physics, and chemistry [27]. Various applications so far found to be promising are catalysis, electronic, optical, and mechanic devices, magnetic recording media, superconductors, high-performance engineering materials, dyes, pigments, adhesives, photographic suspensions, and drug delivery [28-30] . In particular, there has been an increasing interest for application of nanoparticles of different metals/ non metal and conducting polymer composites for biomedical applications [31-34]. Research to-date includes numerous attempts to prepare and characterize nanosized materials. The techniques include are gas-evaporation, sputtering, coprecipitation, sol-gel method, hydrothermal, microemulsion, and so on. Among these, the electrosynthesis has emerged as a convenient and inexpensive technique for the synthesis of nanostructure materials [35-38]. In recent years, the development of inorganic particle and polymer composites, particularly, composites of metal particles and conducting polymers with core-shell structure, has attracted considerable interest due to their interesting properties and a wide range of the promising potential applications in technological fields[29-30]. Polymer nanocomposites are materials in which nanoscopic inorganic particles are dispersed in an organic polymer matrix in order to dramatically improve the performance properties of the polymer. These nanocomposites are of immense interest to biomedical technologies such as tissue engineering, bone replacement/ repair, dental applications, and controlled drug delivery. Antibacterial, antiviral and other antimicrobial properties of copper, silver, iron and zinc may be widely utilized for the design of materials for biomedical devices and hospital equipment by preparing suitable composites with different polymers. Synthetic conducting polymers, e.g., polyaniline (PANI) are the mostly studied conducting polymer having multifunctional properties such as ease of preparation, redox properties, environmental stability and electrochemical behaviours [35]. Thin layers of conducting polymer based composites are very promising, because their synthesis can be easily carried out through different electrochemical methods. Nowadays, the electrochemical method has been found to be superior to other techniques in the sense that they do not require any added chemicals to carry out oxidation and reduction reactions nor do they involve any hazardous materials, only inert electrodes. The electrodeposition method offers many advantages such as simplicity, rigid film deposition control and economic process. However, the target of the proposed plan is to develop a novel protocol for electrosynthesis of nanoparticles conducting polymer composite modified electrode and their potential applications. The major motivation for this proposal is divided into two parts: one is to be the biomedical applications such as magnetic resonance contrast media and therapeutic

agents in cancer treatment and another one is to be the environmental problems originated from textile dyeing and finishing processes.

For biomedical applications, the uses of nanostructured materials have found a strategic importance due to their unique properties. Most of the natural processes take place in the nanometer scale regime. The size of nanomaterials is similar to that of most biological molecules and structures; therefore, nanomaterials can be useful for both *in vivo* and *in vitro* biomedical research and applications. Nanotechnology is currently employed as a tool to explore the darkest avenues of medical sciences in several ways like imaging, sensing, targeted drug delivery and gene delivery systems and artificial implants. The new age drugs are nanoparticles of polymers, metals or ceramics, which can resist conditions like cancer and fight human pathogens like bacteria [39-43]. In a recent study, metal nanoparticles have been reported to interact with HIV-1, and silver nanoparticles of sizes 1-10 nm attached to HIV-1 have prevented the virus from bonding to host cells. Various medical products and industrial devices such as urinary catheters, suture rings, wood flooring and packaging material have nanocrystalline silver as an antiseptic component [33-34]. To realize biomedical applications of nanoparticles, it may be necessary to prepare nanoparticle/polymer composites, which would still have small size and large surface area, but the presence of a polymeric matrix would ensure slow and controlled leaching [43-45]. Polymer nanocomposites are materials in which nanoscopic inorganic particles are dispersed in an organic polymer matrix in order to dramatically improve the performance properties of the polymer. These nanocomposites are of immense interest to biomedical technologies such as tissue engineering, bone replacement/ repair, dental applications, and controlled drug delivery. Antibacterial, antiviral and other antimicrobial properties of copper, silver, iron and zinc may be widely utilized for the design of materials for biomedical devices and hospital equipment by preparing suitable composites with different polymers. There are lots of challenges, such as the instability of the nanoparticles, control of their size and shape, uniform dispersity in a matrix, and control of the release rate [46]. A large number of applications using manufactured nanoparticles of less than 100 nm are currently being introduced into industrial processes. Industrial applications of nanoparticles cover a broad spectrum such as magnetic seals in motors, magnetic inks for bank cheques, magnetic recording media, and dye degradation. The nanocomposites of conducting polymers and inorganic compounds are in the focus of interest because they open opportunity for the combination of electrical, optical, magnetic, catalytic, photocatalytic *etc*. properties. Semiconductor nanoparticles afford an attractive workable

method to degrade, indeed mineralize a vast number and variety of organic pollutants, and to dispose of trace quantities of toxic and/or precious metal ions or complexes found in wastewaters. The novel technology that has developed in the last two decades, but most actively in the last decade, implicates illumination of a semiconductor nanoparticulate photocatalyst (most often titania, TiO_2, an n-type semiconductor); this has been referred to as Heterogeneous Photocatalysis, and comprises one of the Advanced Oxidation Technologies that also include UV-H_2O_2 and UV-O_3 designed for environmental remediation by oxidative mineralization of organics in drinking waters and wastewaters. Sulfur nanostructures are used in synthesis of sulfur nanocomposites for lithium batteries[46], modification of carbon nanostructures[47], in synthesis of sulfur nanowires with carbon to form hybrid materials with useful properties for gas sensor and catalytic applications[48], Metal-sulfur compounds like ZnS and CdS play important role in nonlinear optical and electroluminescent devices, etc[49-52]. Metal Oxide Nano is one of the most attractive inorganic materials has wide applications in catalysis, ion exchange, molecular adsorption, biosensor, and particularly, energy storage [53-55].

1.3 Nanoparticles: A dimension of new era

Nanoparticles (NPs) usually ranging in dimension from 1-100 nanometers (nm) have properties unique from their bulk equivalent. With the decrease in the dimensions of the materials to the atomic level, their properties change. The NPs possess unique physico-chemical, optical and biological properties which can be manipulated suitably for desired applications [56]. Moreover, as the biological processes also occur at the nano scale and due to their amenability to biological fictionalizations, the NPs are finding important applications in the field of medicine [57]. The NPs are broadly grouped into organic and inorganic NPs. The latter have gained significant importance due to their ability to withstand adverse processing conditions [58]. Currently, the metallic NPs are thoroughly being explored and extensively investigated as potential antimicrobials. The antimicrobial activity of the NPs is known to be a function of the surface area in contact with the microorganisms. The small size and the high surface to volume ratio *i.e.* large surface area of the NPs enhance their interaction with the microbes to carry out a broad range of probable antimicrobial activities. Metal NPs with antimicrobial activity when embedded and coated on to surfaces can find immense applications in water treatment, synthetic textiles, biomedical and surgical devices, food processing and packaging [59]. Moreover, the composites prepared using metal NPs and polymers can find better utilization due to the enhanced antimicrobial activity. However, it

has been demonstrated that the antimicrobial property of metal NPs composites with polymer been extensively explored [60-61] but the antimicrobial property of nonmetals nanocomposite remain an undeveloped area. To realize biomedical applications of NPs, it may be interesting to prepare NPs /Polymer (gel) composites, where NPs would still have small size and large surface area and the polymer and/or gel can help controlled release of active ingredients[62-63]. Polymer nanocomposites are materials in which nanoscopic inorganic particles are dispersed in an organic polymer matrix in order to significantly improve the performance and properties of the polymer. *N*-Isopropylacrylamide (NIPA) gels have attracted great attention for their scientific interest as well as for their industrial applications including drug delivery and immobilized-enzyme reactors [64-65]. Polyaniline (PANI) is the mostly studied conducting polymer and some polyaniline-based core-shell nanocomposites such as Ag/polyaniline, Ni/polyaniline and Si/polyaniline have been well demonstrated [66-67]. However, elemental Sulfur(S) in nano, micro or bulk state is widely used for different industrial applications such as production of sulfuric acid, nitrogenous fertilizers, phosphate fertilizers, plastics, enamels, antimicrobial agents, gun powders, petroleum refining, other petrochemicals, ore leaching processes, pulp and paper industries, and in different other agrochemical industries[68-70]. Now, realizing the importance of S NPs in different applications, the development of an easy synthesis method is a pressing need.

1.3.1 Types of nanoparticles

Nanomaterials have extremely small size which having at least one dimension 100 nm or less. Nanomaterials can be nanoscale in one dimension (e.g; surface films), two dimensions (e.g; strands or fibres), or three dimensions (e.g; particles). They can exist in single, fused, aggregated or agglomerated forms with spherical, tubular, and irregular shapes. Common types of nanomaterials include nanotubes, dendrimers, quantum dots and fullerenes. Nanomaterials have applications in the field of nano technology, and displays different physical chemical characteristics from normal chemicals (e.g; silver nano, carbon nanotube, fullerene, photocatalyst, carbon nano, silica).

Nanostructured materials are classified as

- Zero-dimensional (0-D),
- One-dimensional (1-D),

- Two-dimensional (2-D),
- Three-dimensional (3-D).

1.3.1.1 Zero-dimensional nanomaterials

In Zero-dimensional nanomaterials all the dimensions are measured within the nanoscale (no dimensions, or 0-D, are larger than 100 nm). The most common representation of zero-dimensional nanomaterials is nanoparticles. Some important characteristics of zero dimentional nanoparticles are as following:

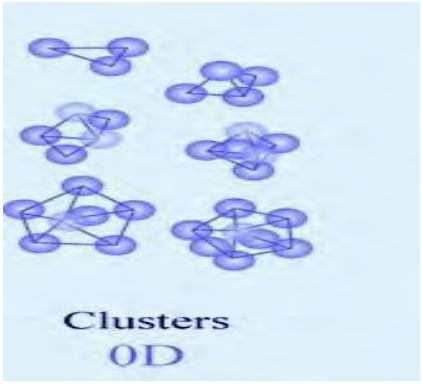

Fig.1.1 Zero dimensional nanoparticles.

Zero-dimensional nanoparticles can

- Be amorphous or crystalline
- Be single crystalline or polycrystalline
- Be composed of single or multi-chemical elements
- Exhibit various shapes and forms
- Exist individually or incorporated in a matrix
- Be metallic, ceramic, or polymeric.

1.3.1.2 One-dimensional nanoparticles

One dimension nanoparticles is outside the nanoscale. This leads to needle like-shaped nanomaterials. 1-D materials include nanotubes, nanorods, and nanowires.

1-D nanomaterials can be

- Amorphous or crystalline
- Single crystalline or polycrystalline
- Chemically pure or impure
- Standalone materials or embedded in within another medium
- Metallic, ceramic, or polymeric

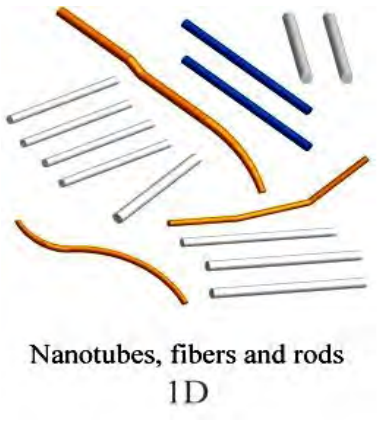

Fig.1.2. One dimensional nanoparticles.

1.3.1.3 Two-dimensional nanoparticles

Two of the dimensions are not confined to the nanoscale. 2-D nanomaterials exhibit plate-like shapes. Two-dimensional nanomaterials include nanofilms,nanolayers, and nanocoatings.
2-D nanomaterials can be:

- Amorphous or crystalline
- Made up of various chemical compositions
- Used as a single layer or as multilayer structures
- Integrated in a surrounding matrix material
- Metallic, ceramic, or polymeric

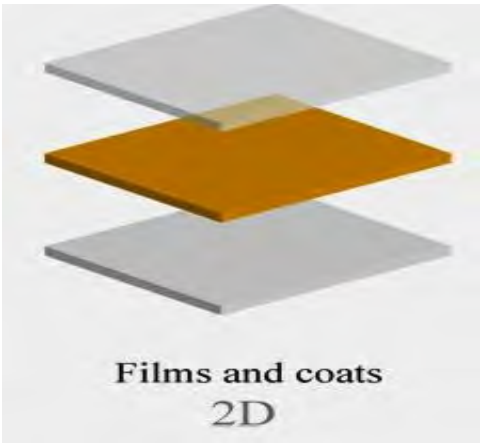

Fig1.3. Two dimensional nanoparticles.

1.3.1.4 Three-dimensional nanomaterials

Bulk nanomaterials are materials that are not confined to the nanoscale in any dimension. These materials are thus characterized by having three arbitrarily dimensions above 100 nm. Materials possess a nanocrystalline structure or involve the presence of features at the nanoscale. In terms of nanocrystalline structure, bulk nanomaterials can be composed of a multiple arrangement of nanosize crystals, most typically in different orientations. With respect to the presence of features at the nanoscale, 3-D nanomaterials can contain dispersions of nanoparticles, bundles of nanowires, and nanotubes as well as multinanolayers.

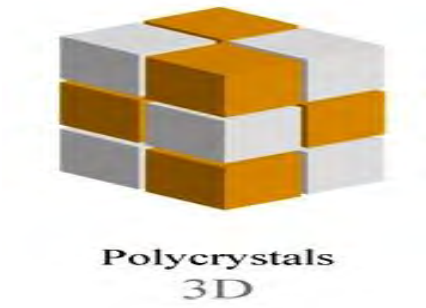

Fig.1. 4. Three dimensional nanoparticles.

1.3.2 Properties of Nanomaterials

Nanomaterials have the structural features in between of those of atoms and the bulk materials. While most microstructured materials have similar properties to the corresponding bulk materials, the properties of materials with nanometer dimensions are significantly different from those of atoms and bulks materials. This is mainly due to the nanometer size of the materials which render them: (i) large fraction of surface atoms; (ii) high surface energy;

(iii) spatial confinement; (IV) reduced imperfections, which do not exist in the corresponding bulk materials. Due to their small dimensions, nanomaterials have extremely large surface area to volume ratio, which makes a large to be the surface or interfacial atoms, resulting in more “surface” dependent material properties. The energy band structure and charge carrier density in the materials can be modified quite differently from their bulk and in turn will modify the electronic and optical properties of the materials. For example, lasers and light emitting diodes (LED) from both of the quantum dots and quantum wires are very promising in the future optoelections. High density information storage using quantum dot devices is also a fast developing area. Reduced imperfections are also an important factor in determination of the properties of the nanomaterials. Nanosturctures and Nanomaterials favors of a selfpurification process in that the impurities and intrinsic material defects will move to near the surface upon thermal annealing. This increased materials perfection affects the properties of nanomaterials.

1.3.2.1 Optical properties

One of the most fascinating and useful aspects of nanomaterials is their optical properties. Nanoparticles often possess unexpected optical properties as they are small enough to confine their electrons and produce quantum effects [71]. Applications based on optical properties of nanomaterials include optical detector, laser, sensor, imaging, phosphor, display, solar cell, photocatalysis, photoelectrochemistry and biomedicine.

The optical properties of nanomaterials depend on parameters such as feature size, shape, surface characteristics and other variables including doping and interaction with the surrounding environment or other nanostructures [72]. Likewise, shape can have dramatic influence on optical properties of metal nanostructures.

1.3.2.2 Electrical properties

Electrical Properties of Nanoparticles” discuss about fundamentals of electrical conductivity in nanotubes and nanorods, carbon nanotubes, photoconductivity of nanorods, electrical conductivity of nanocomposites. One interesting method which can be used to demonstrate the steps in conductance is the mechanical thinning of a nanowire and measurement of the electrical current at a constant applied voltage. The important point here is that, with decreasing diameter of the wire, the number of electron wave modes contributing to the electrical conductivity is becoming increasingly smaller by well-defined quantized steps.

1.3.2.3 Magnetic properties

The physical and chemical properties of magnetic nanoparticles largely depend on the synthesis method and chemical structure. In most cases, the particles range from 1 to 100 nm in size and may display superparamagnetism [73]. Bulk gold and Pt are non-magnetic, but at the nano size they are magnetic. Surface atoms are not only different to bulk atoms, but they can also be modified by interaction with other chemical species, that is, by capping the nanoparticles. This phenomenon opens the possibility to modify the physical properties of the nanoparticles by capping them with appropriate molecules. Actually, it should be possible that non-ferromagnetic bulk materials exhibit ferromagnetic-like behavior when prepared in nano range. One can obtain magnetic nanoparticles of Pd, Pt and the surprising case of Au (that is diamagnetic in bulk) from non-magnetic bulk materials. In the case of Pt and Pd, the ferromagnetism arises from the structural changes associated with size effects.

1.3.2.4 Thermal properties of nanoparticles

Melting-point depression is the phenomenon of reduction of the melting point of a material with reduction of its size. This phenomenon is very prominent in nanoscale materials, which melt at temperatures hundreds of degrees lower than bulk materials. The melting temperature of a bulk material is not dependent on its size. However as the dimensions of a material decrease towards the atomic scale, the melting temperature scales with the material dimensions. The decrease in melting temperature can be on the order of tens to hundreds of degrees for metals with nanometer dimensions [74-75].

1.3.3 Applications of nanoparticles

Nanomaterials have a wide range of applications in the field of electronics, fuel cells, batteries, agriculture, food industry, and medicines etc. It is evident that nanomaterials split their conventional counterparts because of their superior chemical, physical, and mechanical properties and of their exceptional formability.

1.3.3.1 Carbon nanotubes - Microbial fuel cell

Carbon nanotubes (CNTs) have chemical stability, good mechanical properties and high surface area, making them ideal for the design of sensors and provide very high surface area due to its structural network. Since carbon nanotubes are also suitable supports for cell growth, electrodes of microbial fuel cells can be built using of CNT [76].

Due to three-dimensional architectures and enlarged electrode surface area for the entry of growth medium, bacteria can grow and proliferate and get immobilized. Multi walled CNT

scaffolds could offer self-supported structure with large surface area through which hydrogen producing bacteria (e.g., E. coli) can eventually grow and proliferate. Also CNTs and MWCNTs have been reported to be biocompatible for different eukaryotic cells. The efficient proliferation of hydrogen producing bacteria throughout an electron conducting scaffold of CNT can form the basis for the potential application as electrodes in MFCs leading to efficient performance [77].

1.3.3.2 Catalysis

Higher surface area available with the nanomaterial counterparts, nano-catalysts tend to have exceptional surface activity. For example, reaction rate at nano-aluminum can go so high, that it is utilized as a solid-fuel in rocket propulsion, whereas the bulk aluminum is widely used in utensils. Nano-aluminum becomes highly reactive and supplies the required thrust to send off pay loads in space. Similarly, catalysts assisting or retarding the reaction rates are dependent on the surface activity, and can very well be utilized in manipulating the rate-controlling step. Platinum nanoparticles are now being considered in the next generation of automotive catalytic converters because the very high surface area of nanoparticles could reduce the amount of platinum required [78].

1.3.3.3 Phosphors for High-Definition TV

The resolution of a television, or a monitor, depends greatly on the size of the pixel. These pixels are essentially made of materials called "phosphors," which glow when struck by a stream of electrons inside the cathode ray tube (CRT). The resolution improves with a reduction in the size of the pixel, or the phosphors. Nanocrystalline zinc selenide, zinc sulfide, cadmium sulfide, and lead telluride synthesized by the sol-gel techniques are candidates for improving the resolution of monitors.

1.3.3.4 Elimination of Pollutants

Nanomaterials possess extremely large grain boundaries relative to their grain size. Hence, they are very active in terms of their chemical, physical, and mechanical properties. Due to their enhanced chemical activity, nanomaterials can be used as catalysts to react with such noxious and toxic gases as carbon monoxide and nitrogen oxide in automobile catalytic converters and power generation equipment to prevent environmental pollution arising from burning gasoline and coal.

1.3.3.5 Sun-screen lotion

Prolonged UV exposure causes skin-burns and cancer. Sun-screen lotions containing nano-TiO_2 provide enhanced sun protection factor (SPF) while eliminating stickiness. The added advantage of nano skin blocks (ZnO and TiO_2) arises as they protect the skin by sitting onto it rather than penetrating into the skin. Thus they block UV radiation effectively for prolonged duration. Additionally, they are transparent, thus retain natural skin color while working better than conventional skin-lotions.

1.3.3.6 Sensors

Sensors rely on the highly active surface to initiate a response with minute change in the concentration of the species to be detected. Engineered monolayer‟s (few Angstroms thick) on the sensor surface are exposed to the environment and the peculiar functionality (such as change in potential as the CO/anthrax level is detected) is utilized in sensing.

1.3.3.7 Surfaces and coatings

The most prominent application of nanotechnology in the household is self-cleaning or "easy-to-clean" surfaces on ceramics or glasses. Nano ceramic particles have improved the smoothness and heat resistance of common household equipment such as the flat iron. The first sunglasses using protective and anti-reflective ultrathin polymer coatings are on the market. For optics, nanotechnology also offers scratch resistant surface coatings based on nanocomposites. Nano-optics could allow for an increase in precision of pupil repair and other types of laser eye surgery.

1.3.3.8 Biological sensors

Nanotechnology can improve the military‟s ability to detect biological agents. By using nanotechnology, the military would be able to create sensor systems that could detect biological agents. The sensor systems are already well developed and will be one of the first forms of nanotechnology that the military will start to use.

1.3.3.9 Medicine

Nanomedicine is the medical application of nanotechnology. Nanomedicine ranges from the medical applications of nanomaterials, to nanoelectronic biosensors, and even possible future

applications of molecular nanotechnology. Current problems for nanomedicine involve understanding the issues related to toxicity and environmental impact of nanoscale materials (materials whose structure is on the scale of nanometers, i.e. billionths of a meter).

Functionalities can be added to nanomaterials by interfacing them with biological molecules or structures. The size of nanomaterials is similar to that of most biological molecules and structures; therefore, nanomaterials can be useful for both in vivo and in vitro biomedical research and applications. Thus far, the integration of nanomaterials with biology has led to the development of diagnostic devices, contrast agents, analytical tools, physical therapy applications, and drug delivery vehicles.

Nanomedicine seeks to deliver a valuable set of research tools and clinically useful devices in the near future.The National Nanotechnology Initiative expects new commercial applications in the pharmaceutical industry that may include advanced drug delivery systems, new therapies, and in vivo imaging. Nanomedicine research is receiving funding from the US National Institutes of Health, including the funding in 2005 of a five-year plan to set up four nanomedicine centers.

Nanomedicine is a large industry, with nanomedicine sales reaching $6.8 billion in 2004, and with over 200 companies and 38 products worldwide, a minimum of $3.8 billion in nanotechnology R&D is being invested every year. In April 2006, the journal Nature Materials estimated that 130 nanotech-based drugs and delivery systems were being developed worldwide. As the nanomedicine industry continues to grow, it is expected to have a significant impact on the economy [79]

1.3.3.10 Sports

Nanotechnology may also play a role in sports such as soccer, football, and baseball. Materials for new athletic shoes may be made in order to make the shoe lighter (and the athlete faster). Baseball bats already on the market are made with carbon nanotubes that reinforce the resin, which is said to improve its performance by making it lighter. Other items such as sport towels, yoga mats, exercise mats are on the market and used by players in the National Football League, which use antimicrobial nanotechnology to prevent parasuram from illnesses, caused by bacteria such as Methicillin-resistant Staphylococcus aureus (commonly known as MRSA) [80].

1.4 Elemental Sulfur

Sulfur is an essential element for all life, and is widely used in biochemical processes. In metabolic reactions, sulfur compounds serve as both fuels (electron donors) and respiratory (oxygen-alternative) materials (electron acceptors). Sulfur in organic form is present in the vitamins biotin and thiamine, the latter being named for the Greek word for sulfur. Sulfur is an important part of many enzymes and in antioxidant molecules like glutathione and thioredoxin. Organically bonded sulfur is a component of all proteins, as the amino acids cysteine and methionine. Disulfide bonds are largely responsible for the mechanical strength and insolubility of the protein keratin, found in outer skin, hair, and feathers, and the element contributes to their pungent odor when burned.

1.4.1 Physical properties

Sulfur forms polyatomic molecules with different chemical formulas with the best-known allotrope being octasulfur cyclo-S_8. Octasulfur is a soft, bright-yellow solid with only a faint odor, similar to that of matches. It melts at 115.21 °C, boils at 444.6 °C and sublimes easily. At 95.2 °C, below its melting temperature, cyclo-octasulfur changes from α-octasulfur to the β-polymorph [81]. The structure of the S_8 ring is virtually unchanged by this phase change, which affects the intermolecular interactions. Between its melting and boiling temperatures, octasulfur changes its allotrope again, turning from β-octasulfur to γ-sulfur, again accompanied by a lower density but increased viscosity due to the formation of polymers [82]. At even higher temperatures, however, the viscosity decreases as depolymerization occurs. Molten sulfur assumes a dark red color above 200 °C. The density of sulfur is about 2 $g \cdot cm^{-3}$, depending on the allotrope; all of its stable allotropes are excellent electrical insulators.

1.4.2 Chemical properties

Sulfur burns with a blue flame concomitant with formation of sulfur dioxide, notable for its peculiar suffocating odor. Sulfur is insoluble in water but soluble in carbon disulfide and, to a lesser extent, in other nonpolar organic solvents, such as benzene and toluene. The first and the second ionization energies of sulfur are 999.6 and 2252 $kJ \cdot mol^{-1}$, respectively. Despite such figures, the +2 oxidation state is rare, with +4 and +6 being more common. The fourth and sixth ionization energies are 4556 and 8495.8 $kJ \cdot mol^{-1}$, the magnitude of the figures

caused by electron transfer between orbitals; these states are only stable with strong oxidants as fluorine, oxygen, and chlorine.

1.4.3 Allotropes of sulfur

Sulfur forms over 30 solid allotropes, more than any other element. Besides S_8, several other rings are known. Removing one atom from the crown gives S_7, which is more deeply yellow than S_8. HPLC analysis of "elemental sulfur" reveals an equilibrium mixture of mainly S_8, but with S_7 and small amounts of S_6. Larger rings have been prepared, including S_{12} and S_{18} [83].

Amorphous or "plastic" sulfur is produced by rapid cooling of molten sulfur, for example, by pouring it into cold water. X-ray crystallography studies show that the amorphous form may have a helical structure with eight atoms per turn. The long coiled polymeric molecules make the brownish substance elastic, and in bulk this form has the feel of crude rubber. This form is metastable at room temperature and gradually reverts to crystalline molecular allotrope, which is no longer elastic. This process happens within a matter of hours to days, but can be rapidly catalyzed.

1.4.4 Applications

1.4.4.1 Fungicide and pesticide

Elemental sulfur is one of the oldest fungicides and pesticides. "Dusting sulfur," elemental sulfur in powdered form, is a common fungicide for grapes, strawberry, many vegetables and several other crops. It has a good efficacy against a wide range of powdery mildew diseases as well as black spot. In organic production, sulfur is the most important fungicide. It is the only fungicide used in organically farmed apple production against the main disease apple scab under colder conditions. Biosulfur (biologically produced elemental sulfur with hydrophilic characteristics) can be used well for these applications.

Standard-formulation dusting sulfur is applied to crops with a sulfur duster or from a dusting plane. Wet table sulfur is the commercial name for dusting sulfur formulated with additional ingredients to make it water miscible. It has similar applications and is used as a fungicide against mildew and other mold-related problems with plants and soil.

Elemental sulfur powder is used as an "organic" (i.e. "green") insecticide (actually an acaricide) against ticks and mites. A common method of use is to dust clothing or limbs with sulfur powder.

Diluted solutions of lime sulfur (made by combining calcium hydroxide with elemental sulfur in water), are used as a dip for pets to destroy ringworm (fungus), mange and other dermatomes and parasites. Sulfur candles consist of almost pure sulfur in blocks or pellets that are burned to fumigate structures. It is no longer used in the home due to the toxicity of the products of combustion.

1.4.4.2 Bactericide in winemaking and food preservation

Small amounts of sulfur dioxide gas addition (or equivalent potassium metabisulfite addition) to ferment wine to produce traces of sulfurous acid (produced when SO_2 reacts with water) and its sulfite salts in the mixture, has been called "the most powerful tool in winemaking. After the yeast-fermentation stage in winemaking, sulfites absorb oxygen and inhibit aerobic bacterial growth that otherwise would turn ethanol into acetic acid, souring the wine. Without this preservative step, indefinite refrigeration of the product before consumption is usually required. Similar methods go back into antiquity but modern historical mentions of the practice go to the fifteenth century. The practice is used by large industrial wine producers and small organic wine producers alike.

Sulfur dioxide and various sulfites have been used for their antioxidant antibacterial preservative properties in many other parts of the food industry also. The practice has declined since reports of an allergy-like reaction of some persons to sulfites in foods.

1.4.4.3 Sulfuric acid

Elemental sulfur is mainly used as a precursor to other chemicals. Approximately 85% (1989) is converted to sulfuric acid (H_2SO_4):

$$2\ S + 3\ O_2 + 2\ H_2O \rightarrow 2\ H_2SO_4$$

With sulfuric acid being of central importance to the world's economies, its production and consumption is an indicator of a nation's industrial development. For example with 32.5 million tons in 2010, the United States produces more sulfuric acid every year than any other

inorganic industrial chemical. The principal use for the acid is the extraction of phosphate ores for the production of fertilizer manufacturing. Other applications of sulfuric acid include oil refining, wastewater processing, and mineral extraction.

1.4.4.4 Other large-scale sulfur chemicals

Sulfur reacts directly with methane to give carbon disulfide, which is used to manufacture cellophane and rayon. One of the direct uses of sulfur is in vulcanization of rubber, where polysulfides crosslink organic polymers. Sulfites are heavily used to bleach paper and as preservatives in dried fruit. Many surfactants and detergents, e.g. sodium lauryl sulfate, are produced are sulfate derivatives. Calcium sulfate, gypsum, ($CaSO_4 \cdot 2H_2O$) is mined on the scale of 100 million tons each year for use in Portland cement and fertilizers.

When silver-based photography was widespread, sodium and ammonium thiosulfate were widely used as "fixing agents." Sulfur is a component of gunpowder.

1.4.4.5 Fertilizer

Sulfur is increasingly used as a component of fertilizers. The most important form of sulfur for fertilizer is the mineral calcium sulfate. Elemental sulfur is hydrophobic (that is, it is not soluble in water) and, therefore, cannot be directly utilized by plants. Over time, soil bacteria can convert it to soluble derivatives, which can then be utilized by plants. Sulfur improves the use efficiency of other essential plant nutrients, particularly nitrogen and phosphorus. Biologically produced sulfur particles are naturally hydrophilic due to a biopolymer coating. This sulfur is, therefore, easier to disperse over the land (via spraying as a diluted slurry), and results in a faster release.

Plant requirements for sulfur are equal to or exceed those for phosphorus. It is one of the major nutrients essential for plant growth, root nodule formation of legumes and plants protection mechanisms. Sulfur deficiency has become widespread in many countries in Europe [84]. Because atmospheric inputs of sulfur continue to decrease, the deficit in the sulfur input/output is likely to increase, unless sulfur fertilizers are used.

1.4.4.6 Fine chemicals

Organo sulfur compounds are used in pharmaceuticals, dyestuffs, and agrochemicals. Many drugs contain sulfur, early examples being antibacterial sulfonamides, known as *sulfa drugs*. Sulfur is a part of many bacterial defense molecules. Most β-lactam antibiotics, including the penicillins, cephalosporins and monolactams contain sulfur.

1.5 Polyaniline and Nanocomposite

1.5.1 Polyaniline (PANI)

Polyaniline was initially discovered in 1834 by Runge, and it was referred to as aniline black [85]. Following this, Letheby carried out research to analyse this material in 1862 [86]. PANI is known as a mixed oxidation state polymer composed of reduced benzoid units and oxidized quinoid units. Green and Woodhead (1912) discovered this interesting characteristic of polyaniline [87]. Furthermore, it was discovered that PANI had characteristics of switching between a conductor and an insulator under certain experimental conditions. Since then, the material has become a subject of great interest in research. This interest is caused, on the one hand, by diverse, but also unique properties of PANI, allowing its potential applications in various fields, such as energy storage and transformation (alternative energy sources, erasable information storage, non-linear optics, shielding of electromagnetic interference), as well as catalysts, indicators, sensors, membranes of precisely controllable morphology, etc [88]. On the other hand, although some industrial companies have put a lot of effort into the development of some applications of this material, there exist too many ambiguities about PANI. They are related to both the mechanism of polymerization and the polymer structure (including its transformations), determining the material properties.

Polyaniline can be synthesized by both chemical and electrochemical oxidative Polymerization [87]. Polyaniline exists in four main oxidation states viz.

(i) Leucoemeraldine base
(ii) Emeraldine base
(iii) Emeraldine salt
(iv) Pernigraniline,

Schematic representations of different form of polyaniline which are shown in the **Fig1.5**

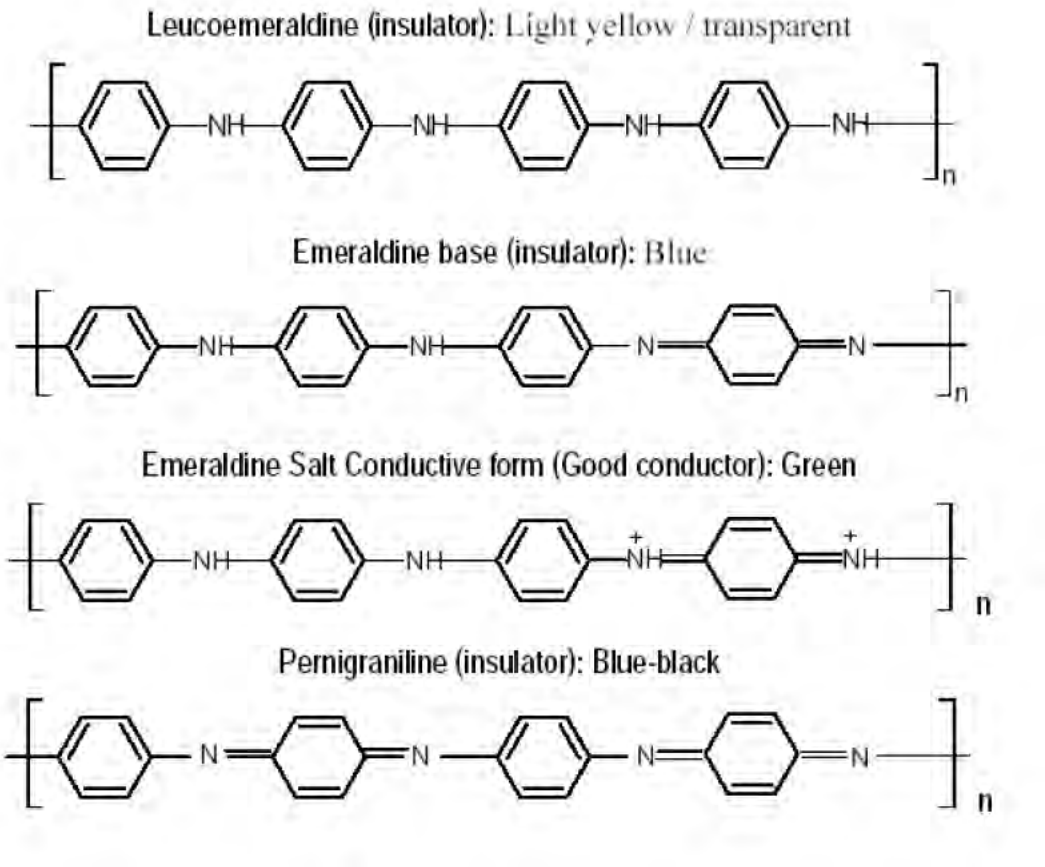

Fig.1.5. Different forms of polyaniline.

1.5.2 Synthesis of Polyaniline

The most common synthesis of polyaniline involves oxidative polymerization, in which the polymerization and doping occurs concurrently, and may be accomplished either electrochemically or chemically. Electrochemical methods tend to have lower yields than chemical yields [89]. This research work involves chemical synthesis of polyaniline.

1.5.2.1 Chemical Synthesis

Synthesis of polyaniline by chemical oxidative route involves the use of either hydrochloric or sulfuric acid in the presence of ammonium peroxo-di-sulfate as the oxidizing agent in the aqueous medium as shown below [90]. The principal function of the oxidant is to withdraw a proton from an aniline molecule, without forming a strong co-ordination bond either with the substrate / intermediate or with the final product.

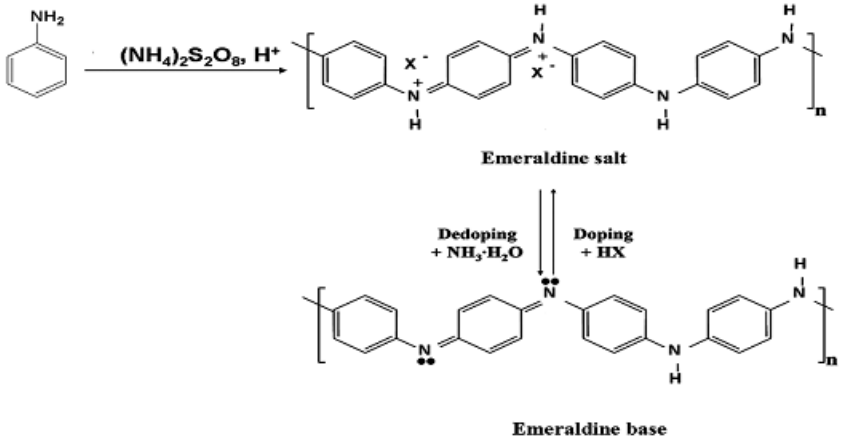

Fig.1.6. Reaction scheme for PANI chemical synthesis

Polyaniline becomes conducting when the moderately oxidized states, in particular the emeraldine base is protonated and charge carriers are generated. This process, is generally called as „protonic acid doping", which makes polyaniline so unique, as no electrons have to be added or removed from the insulating material to make it conducting.

1.5.2.2 Electrochemical Synthesis

Electrochemical polymerisation is commonly carried out by employing one of three techniques. These methods involve the application of (i) a constant voltage (potentiostatic), (ii) a variable current and voltage (potentiodynamic) and (iii) a constant current (galvanostatic) to an aqueous solution of aniline [91]. To carry out electropolymerisation by using any of the three mentioned techniques, a three electrode assembly is required. These electrodes are known as counter electrode, reference electrode e.g. Ag/Ag chloride and a working electrode. There electrosynthesized polymer is deposited onto the working electrode which can be a platinum gold, glassy carbon or indium tin oxide (ITO). An electrolyte such as an acid (HA) is also needed for polymerisation. It has several functions such as, to provide a sufficiently low pH so as to help solubilize the aniline monomer in water and to avoid excessive branching of undesired products, but instead to generate doped emeraldine salt (ES) form.

1.5.3 *Mechanism of polymerisation*

The chemical or electrochemical polymerisation of aniline proceeds via a radical propagation mechanism as shown in Schemes 1-6. The initial steps (1 and 2) are common to both methods, but subtle differences appear in the initial product of the chain propagation step and

product formation steps (3 and 4). Accordingly steps 3 and 4 will be illustrated separately for chemical and electrochemical polymerization [92].

Step 1: Oxidation of Monomer

In the initial step, as shown in Scheme 1, the oxidation of aniline to a radical cation, which exists in three resonance forms, takes place. This step is the slowest step in the reaction, hence it‟s deemed as the rate determining step in aniline polymerisation.

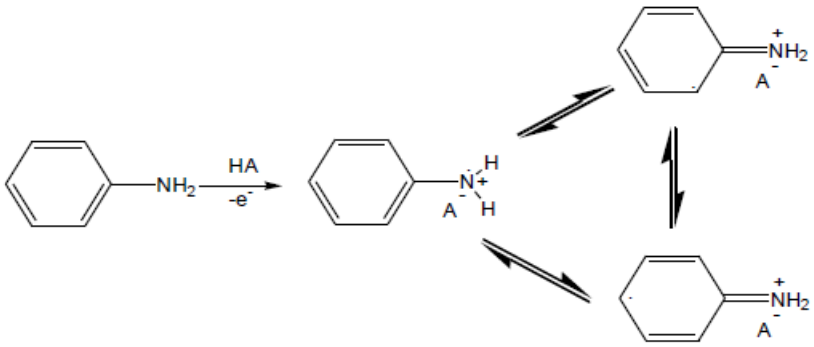

Scheme 1. Oxidation of monomer during electrochemical polymerisation of aniline.

Step 2: Radical coupling and re-aromatisation

Head to tail coupling of the *N*- and *para*- radical cations (Scheme 2) takes place, yielding a dicationic dimer species. This dimer further undergoes the process of re-aromatisation which causes it to revert to its neutral state, yielding an intermediate referred to as *p*-aminodiphenylamine (PADPA). These processes are also accompanied by the elimination of two protons [92].

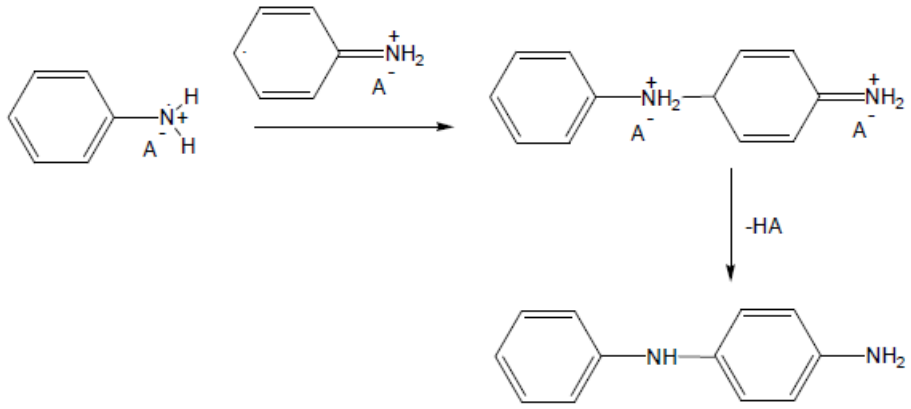

Scheme 2. Radical coupling and re-aromatization during electrochemical polymerisation of aniline.

Step 3: Chain propagation for electrochemical synthesis

The dimer radical cation (centred on the para position; nitrogen atom) undergoes oxidation on the surface of the electrode. Chain propagation results from the radical cation of the dimer coupling with an aniline cation as illustrated in Scheme 3.

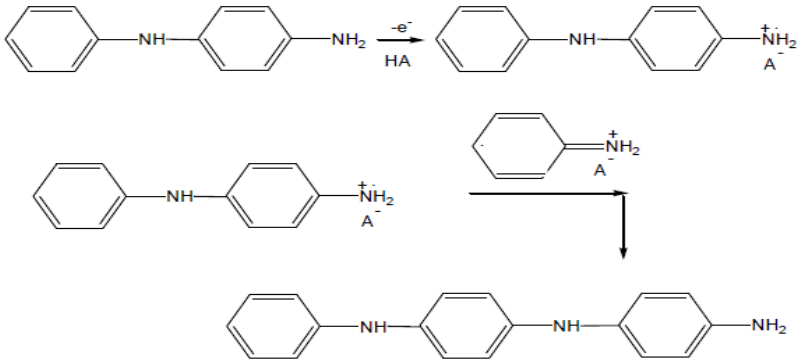

Scheme 3. Chain propagation during electrochemical polymerisation of aniline.

Step 4 : Oxidation and doping of the polymer for electrochemical synthesis

Scheme 4 shows the oxidation and doping of the polymer during electrochemical polymerisation reaction in acid solution which dopes the polymer to yield PANI/HA.

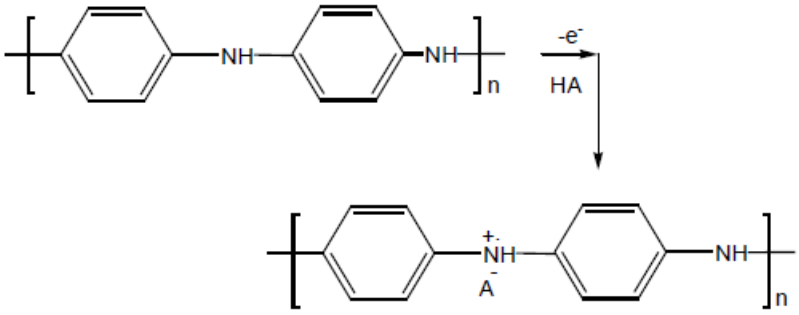

Scheme 4. Oxidation and doping of the polymer during electrochemical polymerisation of aniline.

Step 3 : Chain propagation for chemical synthesis

In the chain propagation during the chemical synthesis of polyaniline, the initial product is the fully oxidized pernigraniline salt as shown in Scheme 5 below.

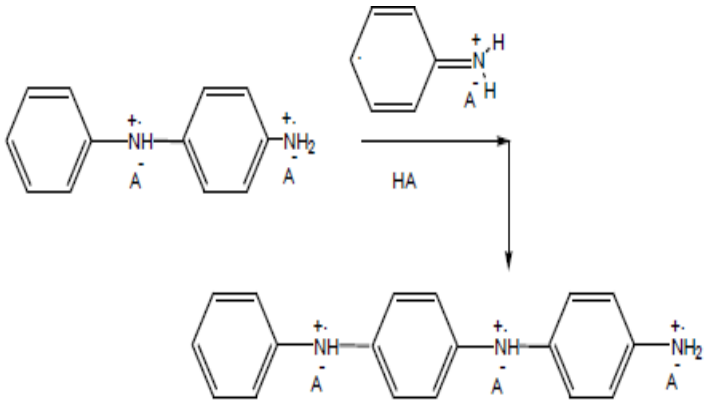

Scheme 5. Chain propagation of the polymer during chemical polymerisation of aniline.

Step 4: Reduction of the pernigraniline salt to emeraldine salt

When all the oxidant in the reaction mixture is completely used up, the pernigraniline salt formed in step 3 of the chemical synthesis mechanism is reduced by unreacted aniline to the green emeraldine salt (Scheme 6)

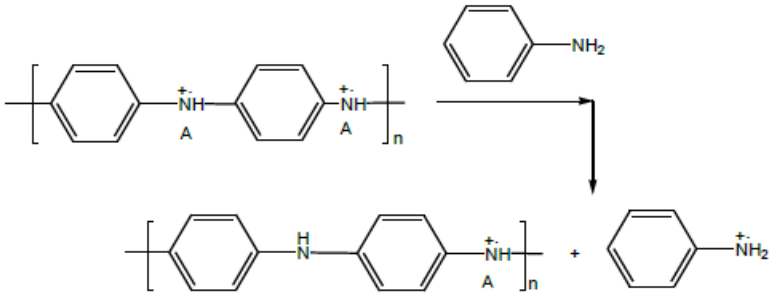

Scheme 6. Reduction of the pernigraniline salt to emeraldine salt during chemical polymerisation of aniline.

1.5.4 Conductivity of PANI

As mentioned earlier, PANI exists in three oxidation states (leucoemeraldine, emeraldine and pernigraniline forms) that differ in chemical and physical properties [93-94]. Only the green

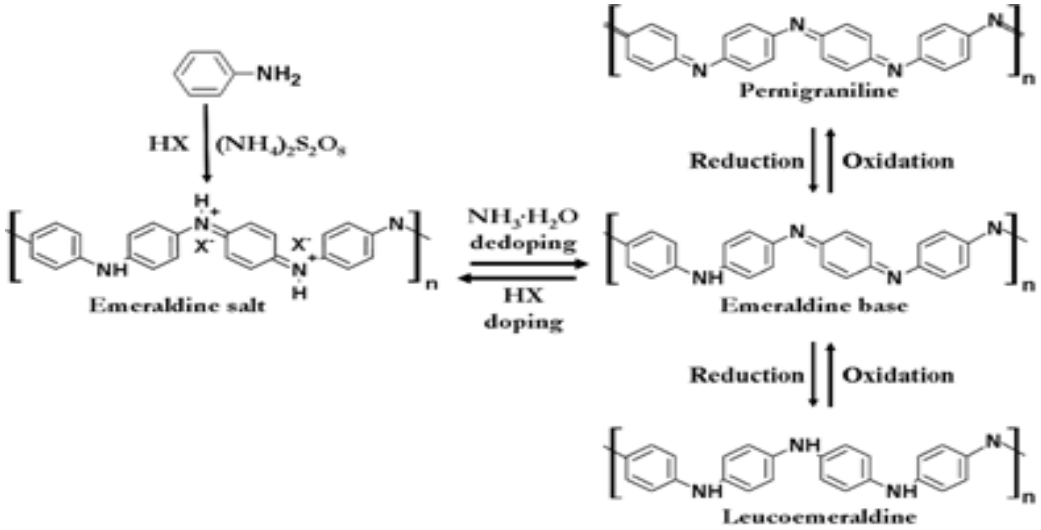

Fig.1.7 The reversible acid/base doping/dedoping and redox chemistry of polyaniline.

protonated emeraldine has conductivity on a semiconductor level of the order of 10 S cm^{-1}, many orders of magnitude higher than that of common polymers (<10^{-9} S cm^{-1}) but lower than that of typical metals (>10^{4} S cm^{-1}). Protonated PANI Converts to a nonconducting emeraldine base when treated with alkali solutions **Fig. 1.7.** The conductivity of PANI can be changed by doping, and spans a very wide range (<10^{-12} to ~ 10^{5} S cm^{-1}) depending on doping. The changes in physicochemical properties of PANI occurring in response to various external stimuli are used in various applications, e.g., in sensors and actuators. Other uses are based on the combination of electrical properties typical of semiconductors with materials properties characteristic of polymers, like the development of "plastic" microelectronics, electrochromic devices. The establishment of the physical properties of PANI reflecting the conditions of preparation is thus of fundamental importance.

1.5.5 Nanocomposites

Generally composite materials can be defined as materials consisting of two or more components with different properties and distinct boundaries between the components. The idea of combining several components to produce a new material with new properties that are not attainable with individual components has been used intensively in the past.

Correspondingly, the majority of natural materials that have emerged as a result of prolonged evolution process can be treated as composite materials [95-96].

Nanocomposites are generally defined as composites in which the components have at least one dimension (i.e., length, width or thickness) in the size range of 1-100 nm. Nanocomposites differ from traditional composites in a sense that interesting properties can result from the complex interaction of the nanostructured heterogeneous phases. In addition, nanoscopic particles of a material differ greatly in the analogous properties from a macroscopic sample of the same material.

Conducting polymers are a class of polymer with conjugated double bonds in their backbones. They display unusually high electrical conductivity and become highly conductive only in their doped state. Due to the excellent electrical and electronic properties and plastic nature of conducting polymers, they have been proposed for application such as antistatic coating, corrosion protection, electrochromic display, sensors, light-emitting diodes, capacitors, light weight batteries and gas permeation membranes, etc. They are also believed to be promising alternatives to the environmentally hazardous chromate conventional coating. There are many published reports focusing on the design, preparation and characterization of novel organic-inorganic nanocomposites consisting of conducting polymer with various layered materials, such as FeOCl, MoO_3, V_2O_5 and clay minerals [97-99]. Since the advent of the nano-technology era, nanocomposites composed of conducting polymers and inorganic particles have aroused much interest in the scientific community. In order to improve the interesting properties possessed by conducting polymers and to generate new properties, researchers are formulating organic-inorganic hybrid materials based on conducting polymers.

1.5.6 Applications of Electrically Conducting Polymers and Composites

Research shows that conducting polymers exhibit conductivity from the semiconducting range (~10^{-5} S/cm) right up to metallic conductivity (~10^{4} S/cm). With this range of electrical conductivity and low density coupled with low cost polymeric conductor pose a serious challenge to the established inorganic semiconductor technology. The commercial applications are based on the promise of a novel material with a combination of properties such as light weight, high processibility and good electrical conductivity. Some of the most important potential applications of conducting polymers are briefly discussed below

- **Optical devices**

Optics was certainly one of the first applications of hybrid materials. Thus, organic: inorganic/ organic: organic hybrid materials with high transparency are expected to be new optical materials such as optical fiber, wave-guide and optical lens.

- **Electrochromic displays**

This utilizes the electrochemical doping and undoping of conducting polymers. The phenomenon of electrochromism can be defined as the change of the optical properties of a material due to the action of an electric field. In architecture electrochromic devices are used to control the sun energy crossing a window. In automotive industry rearview mirrors are a good application for electrochromic system.

- **Electromechanical Actuators**

Conducting polymer actuators were proposed by Baughmann and coworkers. Oxidation induced strain of polyaniline and polypyrrole based actuators has been reported.

- **Drug release systems**

Another application for conducting polymers is controlled release devices. Principle used in this application is potential dependence ion transport. This potential dependence ion transport is an interesting way to deliver ionic drugs to certain biological systems. One can deliver selective ions depending on the requirement.

- **Polymeric batteries**

One of the applications of conducting polymers, which is also a focus of attention worldwide, is lightweight batteries. Amongst the conducting polymers, the use of conducting PANI blends and composites in rechargeable batteries such as lithium batteries is very promising. Recent years have witnessed aggressive interest in lithium batteries.

- **Sensors**

Since electrical conductivity of conducting polymers varies in the presence of different substances, these are widely used as chemical sensors or as gas sensors. Organic or inorganic semiconductors have been reported to change their conductivities when exposed to variety of organic and inorganic vapors, the composite materials were found to give more significant and reversible decrease in electrical resistance in comparison with sensors constructed solely of tin dioxide or polypyrrole.

Some other important applications of conducting composite materials are:

- Solar cells
- conducting textiles
- Display devices
- Optoelectronics
- Adhesives
- Electroplating
- Photovoltaic cell
- Photo catalysis
- Bio–sensor

1.6 Polymer Gels

A polymer gel is a form of matter intermediate between a solid and a liquid, which is created by polymer chains that are cross-linked either chemically or physically. It is a tangled network immersed in a liquid medium. The properties of the polymer gel depend strongly on the interaction between these two components. The liquid prevents the polymer network from collapsing into a compact mass; the network prevents the liquid from flowing away. Depending on chemical composition and other factors, gels vary in consistency from viscous fluids to fairly rigid solids but typically they are soft and resilient or, in a word, jellylike [100]. Under certain conditions, such as by altering the temperature, the gel composition, the pH [101], the pressure on the gel [102], the electric signal [103], the light [104] or the ionic strength [105] of the solvent, drastic changes can be brought out to the gel, the gel will shrink or swell by a factor of as much as several hundred. These stimuli-responsive aspects make polymer gel become a unique field in materials science nowadays. The varied responses of the gel to changes in external conditions can be understood in the context of phase transitions and critical phenomena. Just as many substances can exist as a liquid or as a vapor under different circumstances, so can a gel sometimes have two phases, which are distinguished by different configurations of the polymer network. The discontinuous change in the volume and other properties of the gel constitutes an abrupt transition between the phases, analogous to the boiling of a liquid. At higher temperatures or under various other conditions (pH, magnetic field, light, electric field etc.), the two phases of the gel can no longer be distinguished; in a similar way the distinction between liquid and vapor disappears at high temperature and pressure. The physical mechanisms underlying these changes of state are peculiar to the structure of a gel and can be understood only through an analysis of the forces acting on the polymer network.

1.6.1. Polymer Hydrogels

As the most important branch in polymer gels, stimuli-responsive polymer hydrogels are widely studied due to its special liquid medium-water. Stimuli responsive hydro gels are fascinating materials with potential applications in biomedicine and the creation of "intelligent" materials system, for example, as media in drug delivery, separation processes [106-109]. Especially hydrogels as chemical sensors have obtained more and more attention in the recent decades. Several terms have been coined for hydrogels, such as „intelligent gels" or „smart hydrogels" [110]. The smartness of any material is the key to its ability to receive, transmit or process a stimulus, and respond by producing a useful effect [111]. Once acted on, stimuli can result in changes in phases, shapes, optics, mechanics, electric fields, surface energies, recognition, reaction rates and permeation rates. Hydrogels are „smart" or „intelligent" in the sense that they can perceive the prevailing stimuli and respond by exhibiting changes in their physical or chemical behavior like a live organ. Here, we should notice that the difference between the term „gel" and „hydrogel". As polymeric networks, both of them might be similar chemically, but they are physically distinct. Technically, gels are semi-solid systems comprising small amounts of solid, dispersed in relatively large amounts of liquid, yet possessing more solid-like than liquid-like character [112]. Hydrogels then are a cross-linked network of hydrophilic polymers. They possess the ability to absorb large amounts of water and swell, while maintaining their three-dimensional (3D) structures [113]. This definition differentiates hydrogels from gels, which are polymeric networks already swollen to equilibrium, and the further addition of fluids results only in dilution of the polymeric network. The feature central to the functioning of a hydrogel is its inherent cross-linking. Conventional gels can also develop small levels of crosslinks as a result of a gain in energy under the influence of shear forces, but this is reversible because of the involvement of weak physical forces. So hydrogels can be described as a more rigid form of gel. The cross-link inside the hydrogels can be provided by covalent bonds, hydrogen bonding, van der Waals interactions or physical entanglements. Hydrogels have found many significant applications in many areas due to their special environmental-sensitive property. Tanaka Miyata studied antigen-responsive hydrogel [114]. They used reversible binding between an antigen and an antibody as the cross linking mechanism in the Semi-Interpenetrating network hydrogel. They suggest that this approach might permit drug delivery in response to a specific antigen. Also in recent years, with regard to the polymer film, a lot of work had been performed. Hoitz and Asher [115] studied the polymerized colloidal crystal hydrogel films as intelligent chemical sensing materials. They reported the preparation of a material that

changes color in response to a chemical signal by means of a change in diffraction properties. Because of the excellent bio-compatibility of them, hydrogels have been studied more and more in medicine, biotechnology [116,117] etc. fields. Like talked above, according to the different environment stimuli, hydro gels can usually be classified as the following several categories:

1.6.2. Temperature-sensitive Hydrogels

Not like most polymers which increase their water-solubility as the temperature increases, polymers with lower critical solution temperature (LCST) decrease their water-solubility upon increasing the temperature. When the temperature increases above the LCST, Hydrogels made of LCST polymers shrink. This type of behavior is known as inverse (or negative) temperature dependence. These kinds of hydrogels are made of polymer chains that either possess moderately hydrophobic groups or contain a mixture of hydrophilic and hydrophobic segments. At lower temperatures, hydrogen bonding between hydrophilic segments of the polymer chain and water molecules are dominates, leading to enhanced dissolution in water. As the temperature increases, however, hydrophobic interactions among hydrophobic segments become strengthened, while hydrogen bonding becomes weaker. The net result is shrinking of the hydrogels due to inter-polymer chain association through hydrophobic interactions. In general, as the polymer chain contains more hydrophobic constituent, LCST becomes lower [118]. So the LCST can be changed by adjusting the ratio of hydrophilic and hydrophobic segment of the polymer. Poly (N-isopropylacrylamide) is a very popular example in this category.

1.6.3 pH-sensitive Hydrogels

All the pH-sensitive polymers contain pendant acidic (e.g. carboxylic and sulfonic acids) or basic (e.g. ammonium salts) groups that either accept or release protons in response to changes in environmental pH. Hydrogels made of crosslinked polyelectrolytes (polymers with a large number of ionizable groups) display big differences in swelling properties depending on the pH of the environment. The pendant acidic or basic groups on polyelectrolytes undergo ionization just like acidic or basic groups of monoacids or monobases. The presence of ionizable groups on polymer chains results in swelling of the hydrogels much beyond that can be achievable by nonelectrolyte polymer hydrogels. Since the swelling of polyelectrolyte hydrogels is mainly due to the electrostatic repulsion among charges present on the polymer chain, the extent of swelling is influenced by any condition

that reduce electrostatic repulsion, such as pH, ionic strength, and type of counterions [119]. Poly (acrylic acid) is good example falling into this category.

1.6.4 Electric Signal-sensitive Hydrogels

Hydrogels sensitive to electric current are usually made of polyelectrolytes, as are pH-sensitive hydrogels. Electro-sensitive hydrogels undergo shrinking or swelling in the presence of an applied electric field. Sodium acrylic acid-coacrylamide copolymer is a good example here [120].

1.6.5 Light-sensitive Hydrogels

This kind of hydrogels has big potential applications in developing optical switches, display units, and ophthalmic drug delivery devices. Since the light stimulus can be imposed instantly and delivered in specific amounts with high accuracy, light-sensitive hydrogels may possess special advantages over others. They can be divided into UV-sensitive and visible light-sensitive hydrogels. Unlike UV light, visible light is readily available, inexpensive, safe, clean and easily manipulated. Leuco derivative molecules are good examples for UV sensitive hydrogels [121]. By introducing light-sensitive chromophore to some hydrogels, we can also get Visble light-sensitive hydrogels [122].

1.6.6. Pressure-sensitive Hydrogels

The concept that hydrogel may undergo pressure-induced volume phase transition came from thermo-dynamic calculations based on uncharged hydrogel theory. According to the theory, hydrogels which are collapsed at low pressure would expand at higher pressure. An experiment with poly (N-n-propylacrylamide) is one of the examples. The pressure sensitivity appeared to be a common characteristic of temperature-sensitive gels. It was concluded that the pressure sensitivity of the temperature-sensitive gels was due to an increase in their LCST value with pressure [123].

1.6.7. Poly N-isopropylacrylamide (poly-NIPA)

Poly-NIPA as the most known temperature-sensitive microgel was first prepared by Philip Chibante, a high school summer student with aspirations to become a dentist, under the supervision of Dr. Robert Pelton [125,126]. The resulted micro gel was a monodisperse, colloidal dispersion.

The structure of poly-NIPA was illustrated below

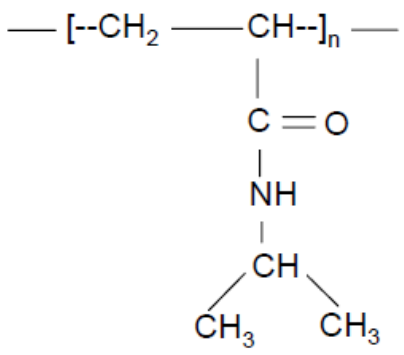

As shown above, the poly-NIPA has both hydrophilic –NH- group and hydrophobic CH_3CHCH_3- group. At room temperature, its hydrophilic part will dominate the property. Poly-NIPA‟s macromolecular transition from a hydrophilic to a hydrophobic structure occurs rather abruptly once above its LCST. Most importantly, poly-NIPA‟s LCST usually lies between 300° C and 380° C (the exact temperature will be a function of the detailed microstructure of the macromolecule). The existence of LCST that is close to body temperature makes poly-NIPA a unique species whose growth over the past few years has become rather explosive especially in the biotech field.

1.6.7.1 Chemical and Physical Properties

Poly-NIPA is one of the most studied thermo sensitive hydrogels. In dilute solution, it undergoes a coil-to-globule transition. Poly-NIPA possesses an inverse solubility upon heating. It changes hydrophilicity and hydrophobicity and abruptly at its LCST [127]. At lower temperatures poly-NIPA orders itself in solution in order to hydrogen bond with the already arranged water molecules. The water molecules must reorient around the nonpolar regions of poly-NIPA which results in decreased entropy.

At lower temperatures, such as room temperature, the negative enthalpy term (ΔH) from hydrogen bonding effects dominates the Gibbs free energy

$$\Delta G = \Delta H - T\Delta S \qquad (1.1)$$

causing the poly-NIPA to absorb water and dissolve in solution. At higher temperatures, the entropy term (ΔS) dominates, causing the PNIPA to release water and phase separate which can be seen in the following demonstration.

Pictoral Dipiction of the LCST Effect of poly-NIPA

Poly-NIPA before heating, the negative enthalpy of hydrogen bonding dominates and poly NIPA is dissolved in the solution.

Poly-NIPA after heating with a heat gun, the negative entropy of mixing dominates due to the increase in temperature and poly-NIPA phase separates from the water.

1.6.7.2 Application of poly NIPA gel

The versatility of poly-NIPA has led to finding uses in macroscopic gels, microgels, membranes, sensors, biosensors, thin films, tissue engineering, and drug delivery. The tendency of aqueous solutions of poly-NIPA to increase in viscosity in the presence of hydrophobic molecules has made it excellent for tertiary oil recovery. Adding additives or copolymerization of poly-NIPA can lower the lower critical solution temperature to temperatures around human body temperatures, which makes it an excellent candidate for drug delivery applications [128]. The poly-NIPA can be placed in a solution of bioactive molecules, which allows the bioactive molecules to penetrate the poly-NIPA. The poly-NIPA can then be placed in vivo, where there is a rapid release of bimolecular due to the initial gel collapse and an ejection of the biomolecules into the surrounding media, followed by a slow release of biomolecules due to surface pore closure [129].

Poly-NIPA has also been used in pH-sensitive drug delivery systems. Some examples of these drug delivery systems may include the intestinal delivery of human calcitonin, delivery of insulin, and the delivery of protein [130]. When radiolabeled poly-NIPA copolymers with

different molecular weights were intravenously injected to rats, it was found that the glomerular filtration threshold of the polymer was around 32 000 g/mol [131]. Poly-NIPA has been used in gel actuators, which convert external stimuli into mechanical motion. Upon heating above the LCST, the hydrogel goes from hydrophilic to hydrophobic state [132].This conversion results in an expulsion of water which causes a physical conformational change, creating a mechanical hinge movement.

1.6.8 On–off' and pulsatile drug delivery concepts of hydrogel

When a hydrophilic drug is incorporated into a swollen gel, it can show a Fickian release below the LCST, the details of which depend on the swelling degree of the gel and the tortuosity of the pathway the drug must take (Fig.1.8A) [133].

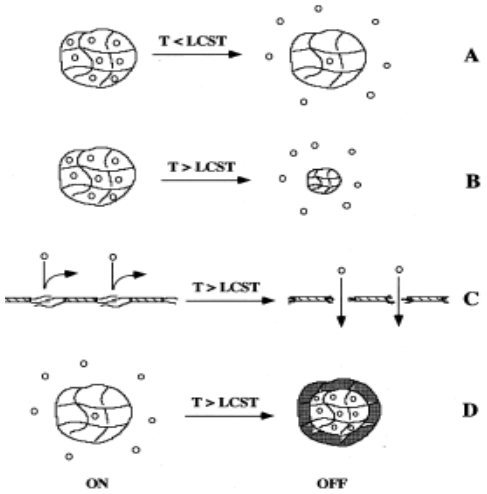

Fig.1.8. Modes of drug delivery from temperature-sensitive hydrogels.

Conversely, a more hydrophobic drug can show Fickian diffusion from the collapsed gel above. Hoffman et al. [134] demonstrated that the rate of delivery of myoglobin and low-molecular-weight solutes can be altered when the temperature-triggered collapse of the gel occurs (Fig.1.8 B). If a drug is loaded below the LCST, it can be squeezed out above the LCST due to the pressure generated during gel collapse. A similar idea was realized with gels immobilized within porous membranes [135-136]. There, swollen gel blocks both diffusion and convection flow through the pores, and allows permeation when collapsed (Fig.1.8 C). Alternatively, if a gel is essentially heterogeneous, it may form a dense „skin" layer of the collapsed component while the core remains swollen (Fig.1.8 D).

1.7 Theoretical aspects of fundamental technology

1.7.1 X- ray diffraction spectroscopy (XRD)

X-ray crystallography is a tool used for identifying the atomic and molecular structure of a crystal, in which the crystalline atoms cause a beam of incident X-rays to diffract into many specific directions. By measuring the angles and intensities of these diffracted beams, a crystallographer can produce a three-dimensional picture of the density of electrons within the crystal. From this electron density, the mean positions of the atoms in the crystal can be determined, as well as their chemical bonds, their disorder and various other information.

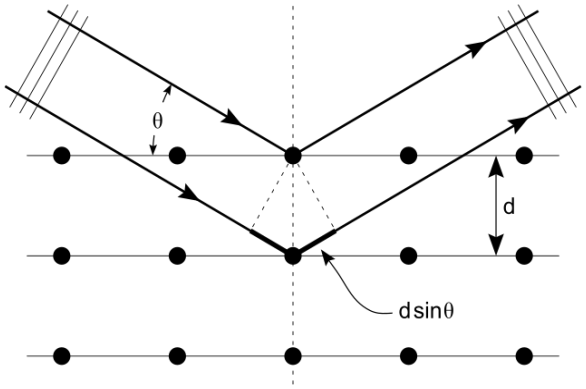

Fig.1.9. Principle of XRD method

In an X-ray diffraction measurement, a crystal is mounted on a goniometer and gradually rotated while being bombarded with X-rays, producing a diffraction pattern of regularly spaced spots known as *reflections*. The two-dimensional ages taken at different rotations are converted into a three-dimensional model of the density of electrons within the crystal using the mathematical method of Fourier transforms, combined with chemical data known for the sample. Poor resolution (fuzziness) or even errors may result if the crystals are too small, or not uniform enough in their internal makeup.

The structures of crystals and molecules are often being identified using x-ray diffraction studies, which are explained by Debye- Sherrer formula. The law explains the relationship between an x-ray light shooting into and its reflection off from crystal surface.

Debye- Sherrer formula

$$D = \frac{k\lambda}{\beta cos\theta} \qquad (1.2)$$

where,

λ = the wavelength of the x-ray radiation.

D = the crystallite size.

θ = the incident angle (the angle between incident ray and the scatter plane)

n = an integer

β = the full width at half maximum of the diffraction peak measured at 2θ

K = the Sherrer constant usually taken as 0.89.

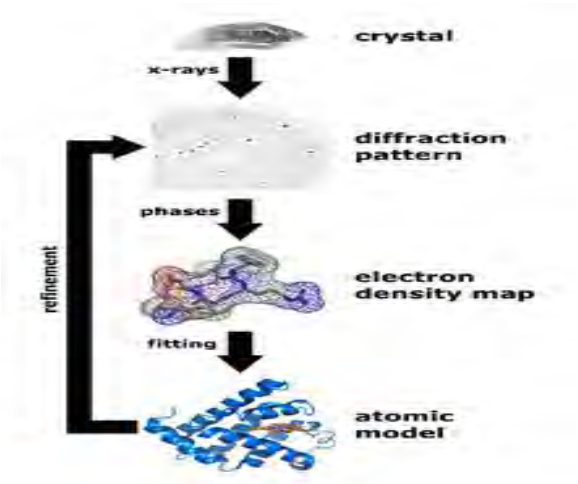

Fig.1.10. Workflow for solving the structure of a molecule by X-ray crystallography

The technique of single-crystal X-ray crystallography has three basic steps. The first and often most difficult-step is to obtain an adequate crystal of the material under study. The crystal should be sufficiently large (typically larger than 0.1 mm in all dimensions), pure in composition and regular in structure, with no significant internal imperfections such as cracks or twinning. In the second step, the crystal is placed in an intense beam of X-rays, usually of a single wavelength (*monochromatic X-rays*), producing the regular pattern of reflections. As the crystal is gradually rotated, previous reflections disappear and new ones appear; the intensity of every spot is recorded at every orientation of the crystal. Multiple data sets may have to be collected, with each set covering slightly more than half a full rotation of the crystal and typically containing tens of thousands of reflections.
As the crystal is gradually rotated, previous reflections disappear and new ones appear; the intensity of every spot is recorded at every orientation of the crystal. Multiple data sets may have to be collected, with each set covering slightly more than half a full rotation of the crystal and typically containing tens of thousands of reflections.

In the third step, these data are combined computationally with complementary chemical information to produce and refine a model of the arrangement of atoms within the crystal.

The final, refined model of the atomic arrangement-now called a *crystal structure*-is usually stored in a public database.

1.7.2. Scanning electron microscopy

A scanning electron microscope (SEM) is a type of electron microscope that produces images of a sample by scanning it with a focused beam of electrons. The electrons interact with atoms in the sample, producing various signals that can be detected and that contain information about the sample's surface topography and composition. The electron beam is generally scanned in a raster scan pattern, and the beam's position is combined with the detected signal to produce an image. SEM can achieve resolution better than 1 nanometer.

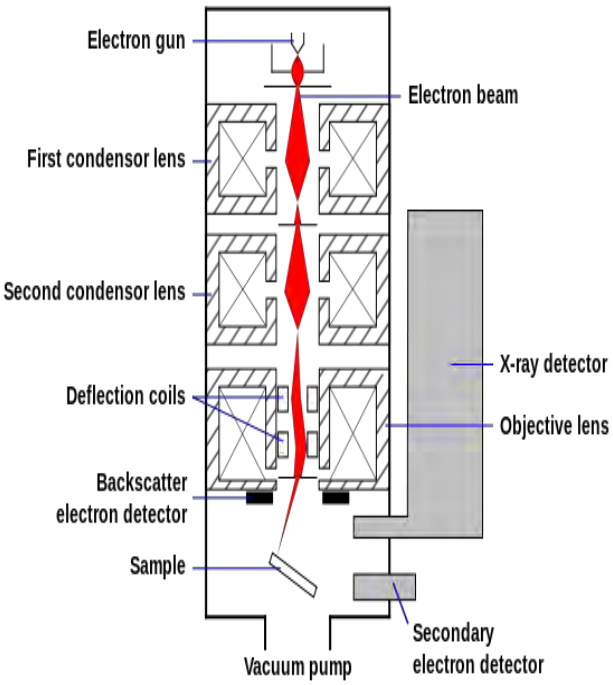

Fig. 1.11: Schematic diagram of an SEM instrument.

The types of signals produced by a SEM include secondary electrons (SE), back-scattered electrons (BSE), characteristic X-rays, light (cathodoluminescence) (CL), specimen current and transmitted electrons. Secondary electrons detectors are standard equipment in all SEM. Back-scattered electrons (BSE) are beam electrons that are reflected from the sample by elastic scattering. BSE images can provide information about the distribution of different elements in the sample.

In a typical SEM, an electron beam is thermionically emitted from an electron gun fitted with a tungsten filament cathode. Tungsten is normally used in thermionic electron guns because it has the highest melting point and lowest vapour pressure of all metals, thereby allowing it to be heated for electron emission, and because of its low cost. The electron beam, which typically has an energy ranging from 0.2 keV to 40 keV, is focused by one or two condenser lenses to a spot about 0.4 nm to 5 nm in diameter. The beam passes through pairs of scanning coils or pairs of deflector plates in the electron column, typically in the final lens, which

deflect the beam in the *x* and *y* axes so that it scans in a raster fashion over a rectangular area of the sample surface.

When the primary electron beam interacts with the sample, the electrons lose energy by repeated random scattering and absorption within a teardrop-shaped volume of the specimen known as the interaction volume, which extends from less than 100 nm to approximately 5 µm into the surface. The size of the interaction volume depends on the electron's landing energy, the atomic number of the specimen and the specimen's density. The energy exchange between the electron beam and the sample results in the reflection of high-energy electrons by elastic scattering, emission of secondary electrons by inelastic scattering and the emission of electromagnetic radiation, each of which can be detected by specialized detectors. The beam current absorbed by the specimen can also be detected and used to create images of the distribution of specimen current. Electronic amplifiers of various types are used to amplify the signals, which are displayed as variations in brightness on a computer monitor (or, for vintage models, on a cathode ray tube). Each pixel of computer video memory is synchronized with the position of the beam on the specimen in the microscope, and the resulting image is therefore a distribution map of the intensity of the signal being emitted from the scanned area of the specimen. In older microscopes image may be captured by photography from a high-resolution cathode ray tube, but in modern machines image is saved to computer data storage.

Magnification in a SEM can be controlled over a range of up to 6 orders of magnitude from about 10 to 500,000 times. Magnification is therefore controlled by the current supplied to the x, y scanning coils, or the voltage supplied to the x, y deflector plates, and not by objective lens power. The most common configuration for an SEM produces a single value per pixel, with the results usually rendered as black-and-white images.

1.7.3 Energy-dispersive spectroscopy (EDS)

Energy-dispersive X-ray spectroscopy (EDS, EDX, or XEDS), sometimes called energy dispersive X-ray analysis (EDXA) or energy dispersive X-ray microanalysis (EDXMA), is an analytical technique used for the elemental analysis or chemical characterization of a sample. It relies on an interaction of some source of X-ray excitation and a sample. Its characterization capabilities are due in large part to the fundamental principle that each element has a unique atomic structure allowing unique set of peaks on its X-ray spectrum. To stimulate the emission of characteristic X-rays from a specimen, a high-energy beam of charged particles such as electrons or protons or a beam of X-rays, is focused into the sample being studied. At rest, an atom within the sample contains ground state (or unexcited) electrons in discrete energy levels or electron shells bound to the nucleus. The incident beam may excite an electron in an inner shell, ejecting it from the shell while creating an electron hole where the electron was. An electron from an outer, higher-energy shell then fills the hole, and the difference in energy between the higher-energy shell and the lower energy shell may be released in the form of an X-ray. The number and energy of the X-rays emitted from a specimen can be measured by an energy-dispersive spectrometer. As the energy of the X-rays is characteristic of the difference in energy between the two shells, and of the atomic structure of the element from which they were emitted, this allows the elemental composition of the specimen to be measured.

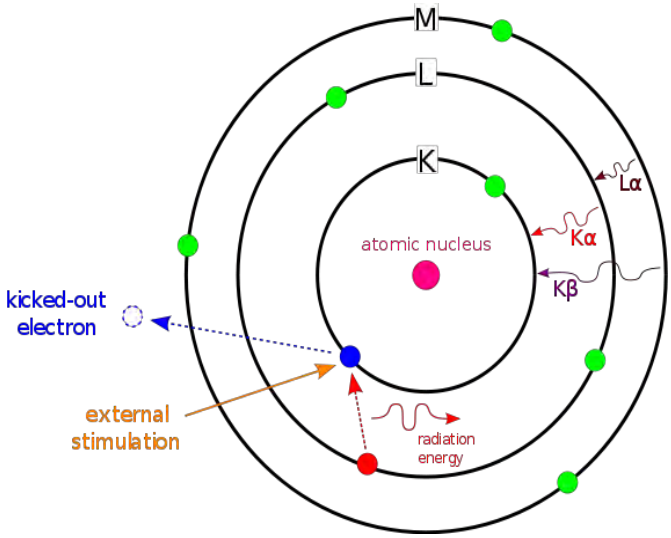

Fig. 2.12: Principle of EDS

Four primary components of the EDS setup are

1. the excitation source (electron beam or x-ray beam)
2. the X-ray detector
3. the pulse processor
4. the analyzer.

Electron beam excitation is used in electron microscopes, scanning electron microscopes (SEM) and scanning transmission electron microscopes (STEM). X-ray beam excitation is used in X-ray fluorescence (XRF) spectrometers. A detector is used to convert X-ray energy into voltage signals; this information is sent to a pulse processor, which measures the signals and passes them onto an analyzer for data display and analysis.

1.8 Objectives of the research

Development of NPs/polymer (gel) system and its characteristics are the prime interest of this work which may open the possibilities of using S NPs in biomedical applications. The possible outcome may include the following

1. To establish a suitable method for Synthesis of Sulphur Nanoparticles (SNPs), Polyaniline (PANI), *S* NPs–PANI nanocomposite, n-isopropyl acrylamide (NIPA) gel and S NPs-NIPA gel.
2. To determine the surface properties (surface area, surface morphology and material dimension) of the S NPs/polymer (gel) systems.
3. To examine loading and release of NPs from polymer/gel matrices.
4. Evaluation of antimicrobial (antibacterial and antifungal) activity of SNPs, PANI and *S*NPs-PANI nanocomposite
5. Developing a highly effective SNPs-PANI nanocomposites antimicrobial agent for treating microbial infections, particularly resistant infections.
6. Comparison the antibacterial and antifungal activity of S NPs, PANI and S NPs-PANI nanocomposites with antibiotics.

Chapter 2

Experimental

2.1 Materials and Probes

2.1.1 Chemicals

All the chemicals used in this research were analytical grade and used as received without any further purification except aniline which was distilled prior to use. All solutions were prepared by using double distilled water .The chemical and reagents used in this experiment are listed bellow

a) Sodium thiosulfate [Merck Germany]
b) Oxalic acid [Merck, Germany]
c) Aniline [E. Merck, Germany]
d) Ammonium peroxydisulfate [Merck, Germany]
e) Sulfuric acid [Merck, Germany]
f) N-isopropylacrylamide (NIPA) [Kohjin Co; Tokyo, Japan]
g) N, N-Methylene bis acrylamide (BIS) [Acros Organics Geel, Belgium]
h) 2,2- Azo-bis-isobutyrylnitrile (AIBN) [Kanto chemical Co; Japan]
i) Cetyl trimethyl ammonium bromide (CTAB). [Merck, Germany]
j) Potassium hydroxide [Merck, Germany]

2.1.2 Instruments

a) UV visible recording spectrophotometer [UV-1602, Shimadzu, Great Britain]
b) Potentiostat/ Galvanostat [HABF 501, Hokuto Denko, Japan]
c) Oven [Binder- Germany]
d) Scanning electron microscope [JEOL JSM-7600F,Japan]
e) X-ray Diffractrometer [Philips, Export Pro, Holland]
f) Infra red spectrophotometer [IR-470, Shimadzu, Japan]
g) Centrifuge machine [Hermle, 2200A, Germany]
h) Sonicator [Model 50T, VWR Scientific , USA]
i) Digital balance [FR-200, Japan]
j) Oven [Thermo, UK]
k) Thermo gravimetric analyzer [TGA 40, Shimadzu , Japan]
l) All types of beaker, volumetric flask. Conical flask, pipette, burette, measuring cylinder, reagents bottles were made of Pyrex glass England.

2.2 Methods

2.2.1 Synthesis of Sulfur Nanoparticles (*S* NPs) Electrochemically

The electrosynthesis was carried out in a standard single Pyrex electrochemical cell containing three-electrode arrangement. **Fig 2.1** shows the three electrodes system in an electrochemical cell. In this setup, steel electrode served as the working electrode having surface area 0.5 cm^2 and the Hg/Hg_2Cl_2 (environment of 3 M KCl) as the reference one**.** The platinum sheet (surface area 0.5 cm^2) was employed as the counter electrode either constant or sweep cyclic potential mode performed in aqueous solution containing sodium thiosulfate (0.5 M) and KOH (0.5 M). Prior to electrolysis, the platinum and steel electrodes were cleaned smoothly by washing with deionized water followed by rubbing with alumina. Finally, the electrode was cleaned by cycling for 10–15 times in 0.5 M sulfuric acid solution between +0.6 and −0.6 V at 50 mV s^{-1} scan rate. The synthesis was carried out at a constant potential (3V) for 1 hour under mild stirring.

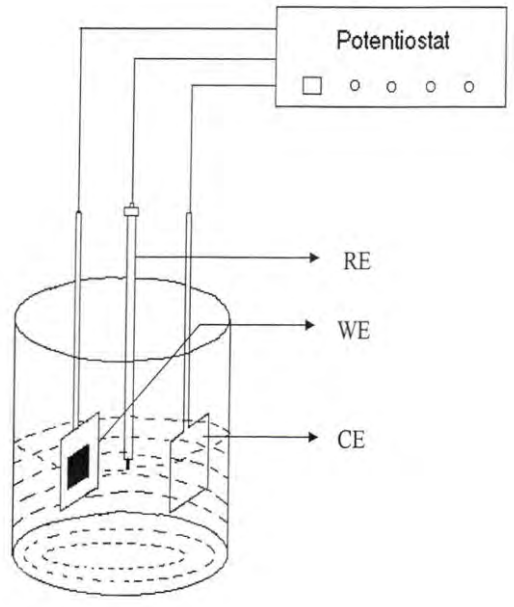

Fig.2.1 Schematic representation of the three electrodes system in an electrochemical cell.

In a solution sodium thiosulfate substrate could be first reduced at the surface of cathode and, in the next step, the produced sulfide ions was oxidized to elemental sulfur at the anode. At high electrode potential, elemental nano sulfur goes to solution from anode to give colloidal

solution. In order to collect the S NPs, the obtained colloidal solution was centrifuged at 4000 rpm and the NPs obtained after centrifuge was washed several times with deionized water and dried in an oven at 60-70°C for 4 hours. The temperature was fixed for all experiments.

2.2.2 Synthesis of Sulfur Nanoparticles (*S* NPs) Chemically

The synthesis of S NPs was carried out by dissolving Sodium thiosulphate (5 mM) and Oxalic acid (5 mM) acid solutions in presence of CTAB (0.69 mM) under mild stirring. In an acidic solution, sodium thiosulphate undergoes through a disproportionation reaction to give colloidal solution of S NPs and sulfonic acid according to the following reaction

$Na_2S_2O_3 + C_2H_2O_4 = C_2H_2O_2\text{-}Na + S\downarrow + H_2O + SO_2$

$SO_2 + H_2O = H_2SO_3$

In order to collect the S NPs, the obtained colloidal solution was centrifuged at 4000 rpm and the NPs obtained after centrifuge was wash several times using deionized water and dried in an oven at 60-70°C for 4 hours.

2.2.3 Synthesis of Polyaniline

2.2.3.1 Electrochemically

The electrosynthesis of PANI was carried out in a standard single Pyrex electrochemical cell containing three-electrode arrangement. In this setup, stainless steel (SS) having geometrical surface area 0.5 cm^2 served as the working electrode, 0.5 cm^2 platinum foil (Pt) counter electrode and the Hg/Hg_2Cl_2 (environment of 3 M KCl) as the reference one. The potential was employed as either constant or sweep cyclic potential mode performed in aqueous solution containing aniline (0.5 M) and 0.1 M sulfuric acid solution were used as electrolytes. Prior to each experiment, the Platinum and steel electrodes were cleaned smoothly by washing with deionized water followed by rubbing with alumina.

Finally, the electrode was cleaned by cycling for 10-15 times in 0.5 M sulfuric acid solution between + 0.6 and - 0.6 V at 100 mV s^{-1} scan rate. In this experiment working electrode SS was act as anode and counter electrode Pt act as cathode. The synthesis was carried out either by sweeping the potential between - 0.4 V to and 1.5V at a scan rate of 100 mVs^{-1} or at a

constant potential of +1.5 V vs SCE. After polymerization, the potential of PANI film coated SS electrode was held at 0.0V until cathodic current disappeared to dedopped the PANI deposit. The PANI as deposited and dedoped, was washed several times using distilled water to remove any traces of monomer or any others reactants or byproducts that might be produced during electrolysis. PANI sample were obtained electrochemically either as thin film grafted on SS electrode or as thick deposit, which can be scratched off the SS electrode, rinsed and dried. The dried PANI sample were crushed to powder and used for different analysis.

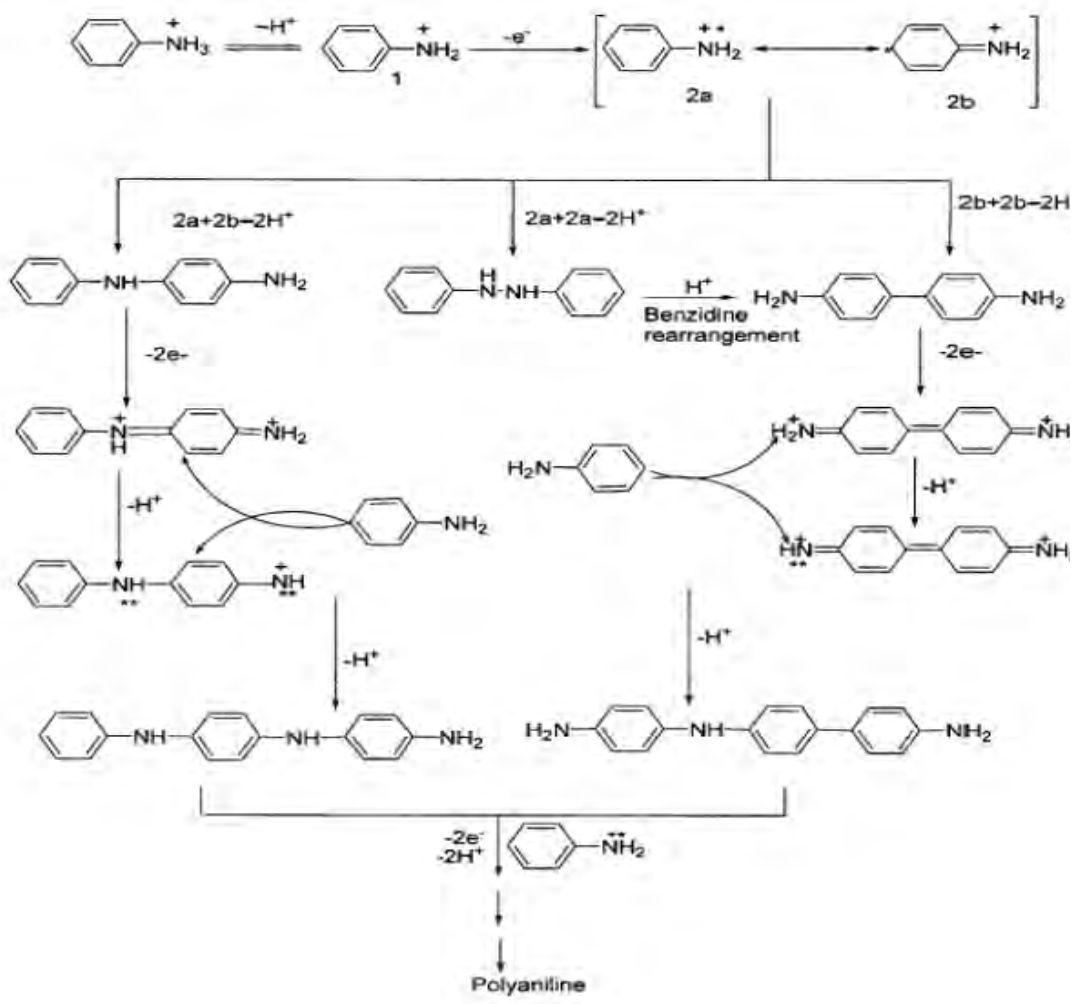

Fig.2.2. Reaction scheme for electrocmical formation of PANI.

2.2.3.2 Chemically

In a typical synthesis experiment of PANI, the aniline monomer 5 ml dissolve in 1.0 M HCl solution containing 2.2 M Ammonium peroxydisulfate was slowly added drop wise into the aniline HCl solution with constant mechanical stirring at a reaction temperature of 0-5 °C for 1 hour. The reaction mixture was stirred for an additional 2 h at 0-5 °C and then the resulting

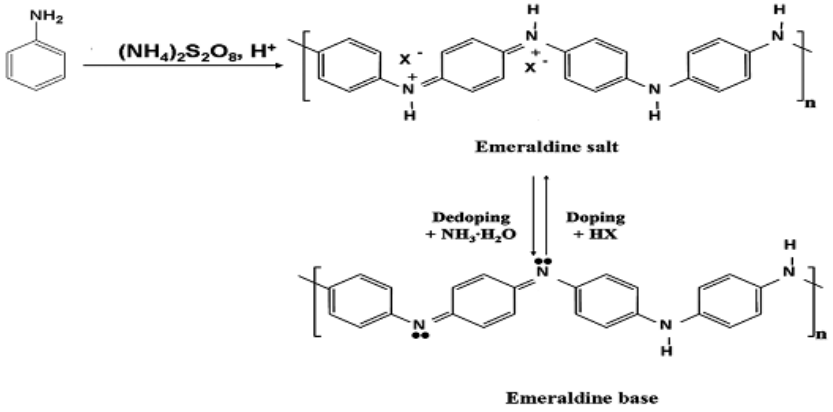

Fig. 2.3. Reaction scheme for synthesis of PANI chemically.

green suspension, indicating the formation of insoluble polyaniline in its emeraldine salt (ES) form, was then filtered with Whitman filter paper through vacuum and washed several times with distilled water. The powder obtained was dried at 50 °C for 24 h.

2.2.4. Dispersion of SNPs onto Polyanilline

2.2.4.1. Chemical oxidation process

The composite of PANI with SNPs was synthesized by in situ chemical oxidation polymerization. In a typical synthesis experiments, 0.05 gm of SNPs were dissolved in 0.1 M DMSO solution and ultrasonicated over 1h, then transferred into a flask with an ice bath. Aniline monomer (2mL) also dissolves in 1.0 M HCl solution was added to S NPs suspension. A 100 ml 1.0 M HCl solution containing 2.2 M Ammonium peroxydisulfate was slowly added drop wise into the suspension with constant mechanical stirring at a reaction temperature 0-5°C for 1 h. the reaction mixture was stirred for an additional 2 h at 0-5°C and then resulting green suspension indicating the formation of insoluble SNPs-PANI nanocomposites, was then filtered and rinsed several times with distilled water. The powder obtain was dried under a vacuum at 50°C for 24 h.

2.2.4.2 Electrochemical process

The synthesis of SNPs PANI nanocomposite was carried out in acidic media where aniline monomer exists as an anilinium cation at a constant stirring in presence of disperses S NPs. The polymerization was done electrochemically by applying potential between -0.4 V to and +1.5 V vs SCE at a scan rate of100 mV/s or at a constant potential of +1.5 V vs SCE. After polymerization, the potential of SNPs-PANI nanocomposite film coated SS electrode was held at 0.0V until cathodic current disappeared to dedopped the SNPs-PANI nanocomposite deposit. The SNPs-PANI nanocomposite as deposited and dedoped, was washed several times using distilled water to remove any traces of monomer or any others reactants or byproducts that might be produced during electrolysis. SNPs-PANI nanocomposite sample were obtained electrochemically either as thin film grafted on SS electrode or as thick deposit, which can be scratched off the SS electrode, rinsed and dried. The dried SNPs-PANI nanocomposite were crushed to powder and used for different analysis.

2.2.5. Synthesis of N-isopropylacrylamide (NIPA) gel

NIPA gels were prepared by free radical polymerization of NIPA monomer in presence of hydrophobic crosslinker BIS (N, N-Methylene bis acrylamide). In a typical procedure, 0.12 gm N-isopropylacrylamide and 2.2 mol % BIS were dissolved in 5 ml DMSO solution. Then nitrogen gas was bubbled through the solution for 30 min, prior to addition of initiator AIBN, to remove any dissolved Oxygen and then initiator, AIBN (2,2- Azo-bis-isobutyrylnitrile) were added at concentrations each of 0.015 g/mL. Finally, the solution was transferred to the 12 cm^2 glass slides separated by Teflon spacers and glass microcapilary tube with an inner diameter of 270 μm to obtain slab and cylindrical gel respectively. Then the solution containing cell kept in an oven at 60-70°C for 24 h. At this temperature gelation began and after complete gelation, the gel was transferred from cell to a Petri disc and wash several times with DMSO followed by water to remove unreacted substances.

2.2.6 Dispersion of S NPs onto NIPA Gel

The composite of NIPA with SNPs was synthesized by in situ polymerization process. In a typical synthesis experiments, 0.05 gm of SNPs were dissolved in 0.1 M 5 mL DMSO and

ultrasonicated over 1h, then transferred into a flask. N-isopropylacrylamide (0.12 gm) monomer and 2.2 mol % BIS were added to S NPs suspension. Then nitrogen gas was bubbled through the solution for 30 min, prior to addition of initiator AIBN, to remove any dissolved Oxygen and then initiator, AIBN were added at concentrations each of 0.015 g/mL. Finally, the solution was transferred to the 12 cm^2 cells through a syringe and kept the solution containing cell in an oven at 60-70°C for 24 h. At this temperature polymerization began and after complete gelation, the gel was transferred from cell to a Petri disc and wash several times with DMSO followed by water to remove unreacted substances.

2.2.7 Spectral Analysis

2.2.7.1. Infrared Spectral (IR) analysis

IR spectra of all the dried samples, SNPs, PANI, PANI/ SNPs composite were recorded on an IR spectrometer in the region of 400-4000 cm^{-1}. IR spectra of solid samples were frequently obtained by mixing and grinding a small amount of materials with dry and pure KBr crystals. Through mixing and grinding were done in a mortar by a pestle. The powdered mixture was then compressed in a metal holder under a pressure of 8-10 tons to make a pellet. The pellet was then placed in the path of IR beam for measurements.

2.2.7.2 Ultraviolet visible (UV) spectroscopy

Optical spectra of solid sample were recorded in their solution states. the solution of S NPs, PANI, PANI/S NPs composites were made by dissolving small amount of each solid in 50 ml of either aqueous of DMF solvents. The dissolution employed 30 min, sonication in an ultrasonic bath to allow appreciable extent of dissolution. The sample solutions exhibited deep color in some cases. Thus, to ensure preferred dilution of the sample solution for this spectral measurement, the solution were diluted with the solvent to a visible extent in such a way that the optical density remains within the range 1.0-2.0. The sample solution was placed in the sample holder while the reference holder was filled with the corresponding solvents. The UV-Vis spectral analysis of the sample solutions employed a double beam spectrophotometer attached with a synchronized personal computer (PC) for recording the spectral data. All the analysis was performed at room temperature to within 30 (±2) °C.

2.2.7.3 Scanning Electron Microscopy (SEM)

Scanning electron microscopic technique was adapted to analyze the surface morphology of the samples. The synthesized SNPs, PANI, PANI/ SNPs, NIPA and SNPs-NIPA gel samples were utilized for SEM analysis. The samples were dried under vacuum before subjected to their surface analysis. The samples were loaded to the SEM chamber where these were kept under evacuation of 10^{-3} to 10^{-4} torr for ~30 min. Then a very thin layer of gold, few nanometers thick, was sputtered onto the sample surface to ensure electrical conductivity of the sample surface under studied. In case of n-isopropylacryl amide gel (NIPA) the equilibrium swollen hydro gel sample in water at room temperature were quickly frozen in liquid N_2 and then fractured carefully there. Then the samples were then freeze dried under vacuum at -52^{o} C for 3 days. The sample was then placed in the main chamber to view its surface image. A JSM-6700 F SEM arrangement was employed for this analysis. The image of the internal surface morphology was recorded in a pc that interfaced with the main SEM system. The operation system performed all the analysis under in situ vacuum condition.

2.2.7.4 X-ray diffraction (XRD) analysis

SNPs, PANI, PANI/ SNPs, NIPA and SNPs-NIPA gel were analyzed for their X-ray diffraction pattern in the powder state. The powder samples were pressed in a square aluminium sample holder (40 mm x 40 mm) with a 1mm deep rectangular hole (20 mm x 15 mm) and pressed against an optical smooth glass plate .The upper surface of the sample was labeled in the plane with its sample holder. The holder was then placed in the diffractometer.

2.2.7.5 Energy dispersive X-ray (EDX) analysis

Elemental analyses of the synthesized S NPs, PANI, PANI/ SNPs were performed by EDX analysis. The dried powders of the sample were dispersed on a 1 cm x 1 cm conducting steel plate. The steel plates were then placed on a conducting carbon glued strip and a very thin gold layer was sputtered on the sample to ensure the conductivity of the sample surface. The sample was then placed in the main SEM chamber integrated with the EDX machine.

2.2.7.6 Thermo gravimetric Analysis (TGA)

The analyzer usually consist of a high - precision balance with a pan (generally platinum) loaded with the sample. A different process using a quartz crystal microbalance has been devised for measuring smaller samples on the order of a microgram versus milligram with TGA. The sample of placed in a small electrically heated oven with a thermocouple to accurately measure the temperature. The atmosphere was purged with an inert gas to prevent oxidation or other undesired reaction. A computer was used to control the instrument. Analysis was carried out by raising the temperature of the sample gradually and plotting weight (%) against temperature. The temperature in many testing routinely reaches 1000°C or greater. After the data were obtained, curve smoothing and other operations were done to find the exact points of inflection. A method known as high resolution TGA was employed to obtained greater accuracy in areas where the derivative curve peaks. In these methods, temperature increased slows as weight loss increases. This was to more accurately identify the exact temperature where a peak occurs.

2.2.8. Determination of antibacterial susceptibility of S NPs PANI and S NP-PANI nanocomposite

2.2.8.1 Bacterial and fungal strains

Clinically important diarrhoeal pathogens such as *Vibrio cholerae* O1, *Salmonella* Typhi and non-diarrhoeal important bacterial pathogens (*Pseudomonas auruginosa, Escherchia coli*, *Acnetobactor* spp., *Enterobacter* spp., *Staphylococcus aureus* and *Streptococcus pneumoniae*) were included in the study for antibacterial susceptibility testing in the International Centre for Diarrheal Disease Research, Bangladesh (icddr,b). Clinically important fungal species such as *Candida*, *Scedosporium* spp.; and *Scytalidium* spp.,were included in the antifungal susceptibility testing.

2.2.8.2 Determination of antimicrobial susceptibility by modified Kirby-Baur method

Susceptibility of isolates to different antimicrobial agents was measured in vitro by employing the modified Kirby-Bauer [137] method. This method allows for the rapid determination of the efficacy of a drug by measuring the diameter of the zone of inhibition that results from diffusion of the agent into the medium surrounding the disc. Mueller Hinton

agar (MHA) medium (300 g beef infusion l^{-1}, 17.5 g casamino acids l^{-1}, 1.5 g starch l^{-1} and 17 g agar l^{-1}) and antibiotic discs [Ciprofloxacin (5 µg), Cotrimoxazole (25 µg), Tetracycline (30 µg)] were used for determining antimicrobial susceptibility of the isolates. Four to five bacterial colonies were inoculated into 3 ml of Mueller Hinton broth (MHB) and incubated at 37°C for three hours. The broth culture was adjusted to 0.5 McFarlon ($8X10^8$ CFU/ml of broth. A cotton swab was dipped into broth containing young culture of bacteria and was streaked evenly in three directions over the entire surface of the MHA plate for uniform inoculums to obtain confluent growth. The plate was then allowed to dry for 3 to 5 minutes. Antibiotic impregnated discs were then applied to the surface of the inoculated plates with sterile forceps. Within 15 min after the discs were applied, the plates were inverted and placed in an incubator at 37°C. After 16 to 18 h of incubation, inhibition zone diameter around disc was measured in mm.

2.2.8.3 Determination of antibacterial susceptibility of S NPs, PANI and S NP-PANI nanocomposite by well diffusion test

Susceptibility of isolates to S NPs, PANI and S NP-PANI composite was measured in vitro by employing well diffusion method. This method allows for the rapid determination of the efficacy of a drug by measuring the diameter of the zone of inhibition that results from diffusion of the agent into the medium surrounding the well. Mueller Hinton agar (MHA) medium (beef extract 2 g, l^{-1}, acid hydrolysate of casein 17.5 g l^{-1}, starch 1.5 g l^{-1} and agar 17 g l^{-1}). Four to five bacterial colonies were inoculated into 3 ml of Mueller Hinton broth (MHB) and incubated at 37°C for three hours. The broth culture was adjusted to 0.5 McFarland standards ($8X10^8$ CFU/ml of broth). A cotton swab was dipped into broth containing young culture of bacteria and was streaked evenly in three directions over the entire surface of the MHA plate for uniform inoculums to obtain confluent growth. The plate was then allowed to dry for 3 to 5 minutes. Wells were made into MHA. S NPs, PANI and S NP-PANI nanocomposite were then applied to the wells of the inoculated plates with micropipette. Within 5 min after the plates were placed in an incubator at 37°C. After 16 to 18 h of incubation, inhibition zone diameter around well was measured in mm.

2.2.8.4. Determination of antifungal susceptibility of S NPs, PANI and S NP-PANI composite by well diffusion test

Susceptibility of fungal isolates to S NPs, PANI and S NP-PANI composite was measured in vitro by employing well diffusion method [138]. The well diffusion test was performed using MHA containing 10% glucose (MHAG). The inoculum used was prepared using the yeasts from a 24-hour culture on blood agar or MHAG, a suspension was made in a sterile saline solution (0.85%). The turbidity of the suspension was adjusted with a concentration of 0.5 McFarland standards (0.5-2.5×103). 20 ml of MHAG was melted, cooled to 55 ◦C and then inoculated with 1ml of the fungal culture suspension. The inoculated agar was poured into the assay Petri dish, and allowed to cool down on a leveled surface. Once the medium had solidified, four wells, each 10mm in diameter, were cut out of the agar, and 100 µl, 150 µl, 200 µl and 250 µl of S NPs, PANI and S NP-PANI were placed into wells and incubated at 37 ◦C for 24 hours and zone diameter of inhibition around well was measured in mm.

Chapter 3

Results & Discussions

3.1 Characterization of S NPs

3.1.1. X-ray diffraction (XRD) Analysis

The XRD analysis of sulfur nanoparticles synthesized by electrochemically and chemically is shown in **Fig. 3.1** and **Fig.3.2.** The position and intensities of the diffraction peaks of all samples were compared with the with standard α-sulfur particle diffraction pattern [139]. From **Fig. 3.1** and **Fig.3.2** it were seen that the presence of strong and sharp diffraction peaks indicating the obtained nanoparticles was highly crystalline nature. The determination of the mean particle diameter (D) was done by the XRD analysis using Debye-Scherrer formula,

$$D = \frac{k\lambda}{\beta Cos\theta} \qquad (3.1)$$

where, D is the crystallite size, k is the Scherrer constant usually taken as 0.89, λ is the wavelength of the X-ray radiation (0.154056 nm for Cu Kα), and β is the full width at half maximum of the diffraction peak measured at 2 θ.

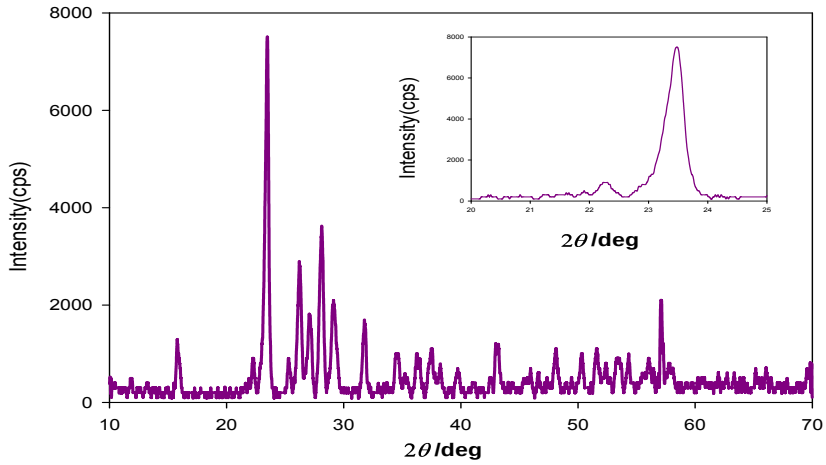

Fig.3.1 XRD pattern of S NPs by Electrochemically.

All detectable peaks could be indexed to S orthorhombic phase with S_8 structure, without obvious characteristic reflection peaks from other impurities, revealing the high purity of the as-synthesized products. The estimated crystallite size of the samples prepared in electrosynthesis and chemical synthesis (from line broadening of the most intense diffraction peak) were approximately 50 nm and 65 nm.

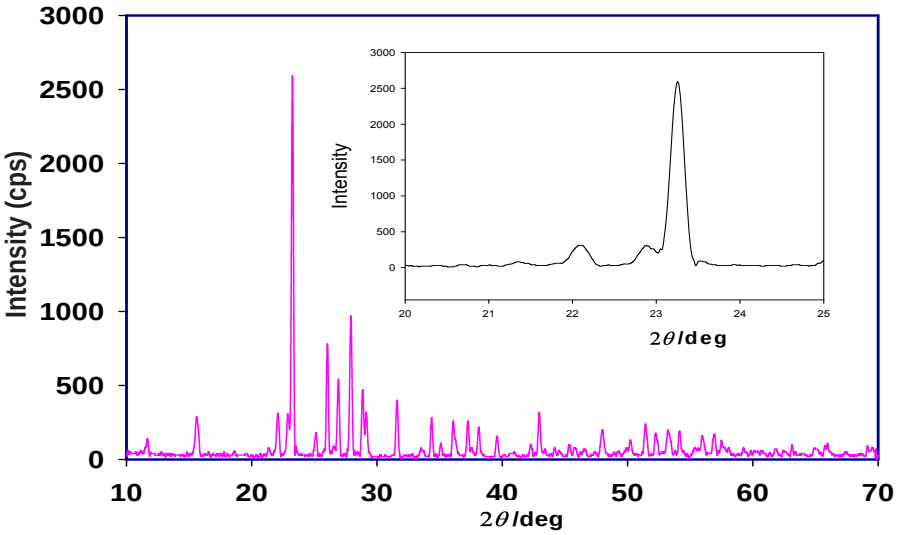

Fig.3.2 XRD pattern of S NPs by chemically.

3.1.2. Scanning Electron Microscopy (SEM)

Fig 3.3 shows the scanning electron microscopy (SEM) images of the SNPs synthesized by electrolysis of thiosulfate solutions and by chemically of acid catalyzed precipitation reaction. From **Fig 3.3(a, b)** it was seen that the particles were spherical in shape and also showed

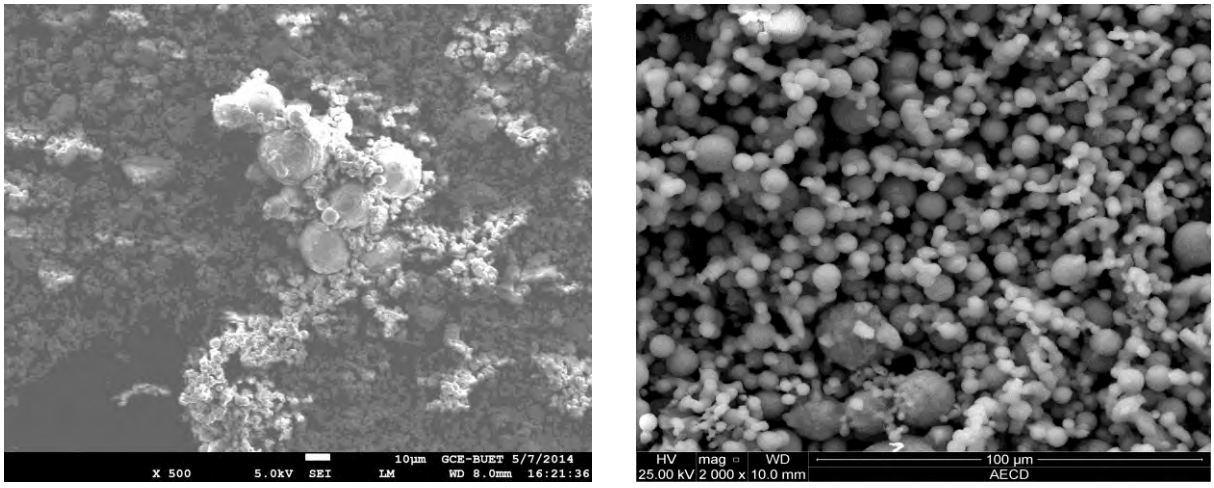

Fig.3.3 SEM image of S NPs synthesized (a) electrochemically and (b) chemically.

loose aggregation. Closer focusing on the aggregated structures showed that each aggregate is a collection of tinier particles showed solid compact particles of all less than 100 nm in size, around 55±10 nm on average. Though not completely homogenous, the size distribution is uniform, with no huge crystals of bulk sulphur.

3.1.3. Energy dispersive X-ray (EDX) analysis

The synthesized nanoparticles were characterized by EDX method for the evaluation of their composition and purity. **Fig.3.4 and Fig.3.5** shows the spectrum of the EDX analysis of as prepared solid SNPs synthesized by electrochemically and chemically at four different locations. The peak observed at 2.31 keV was for Kα line of the elemental S nanoparticles in both methods. It is evident from the peaks that the product was only SNPs and no other impurity was present. The percentage of S NPs at different locations was determined from the intensity of the lines and the results are summarized in **Table 3.1.** Thus from the chemical composition obtained from the EDS spectra at different location, it can be concluded that the mass (%) of synthesized product was 100 indicating high purity of S NPs. EDX spectra of SNPs synthesized by electrochemically at four different locations is following

EDX spectra at +001 location

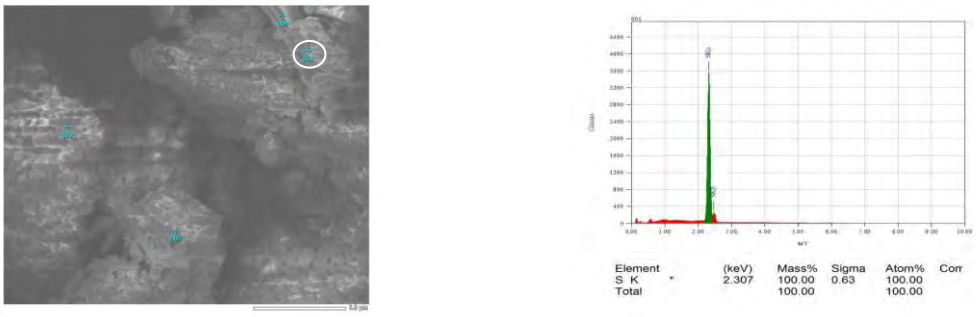

Fig.3.4 (a) EDX analysis of SNPs at + 001 position by electrochemically.

EDX spectra at +002 position

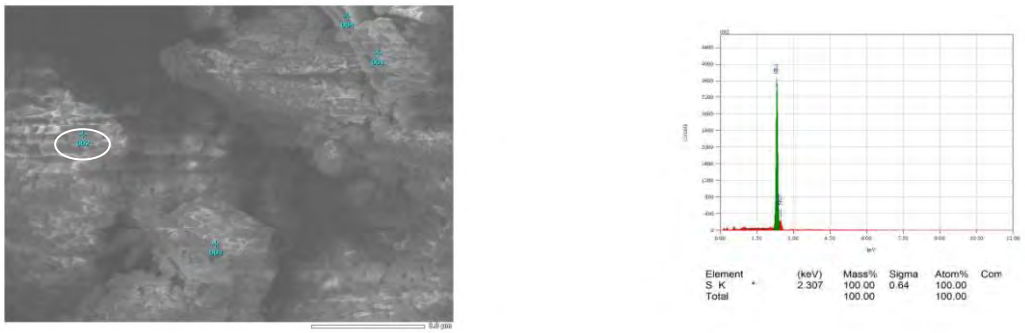

Fig.3.4 (b) EDX analysis of SNPs at + 002 position by electrochemically.

EDX spectra at +003 position

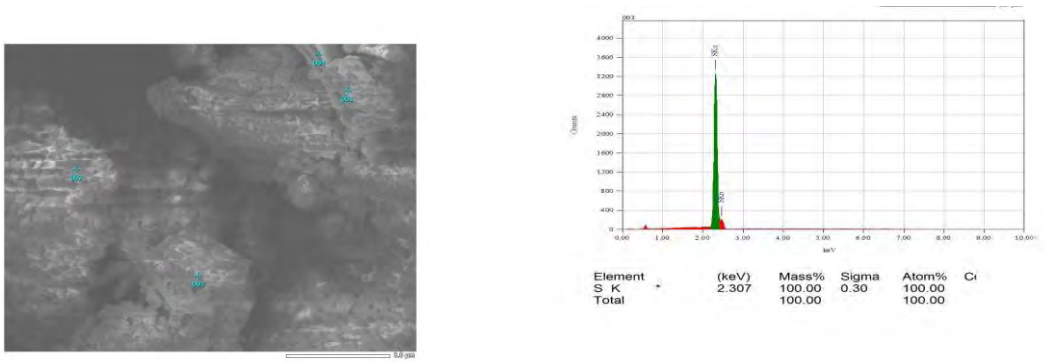

Fig.3.4(c) EDX analysis of SNPs at + 003 position by electrochemically.

EDX spectra at +004 position

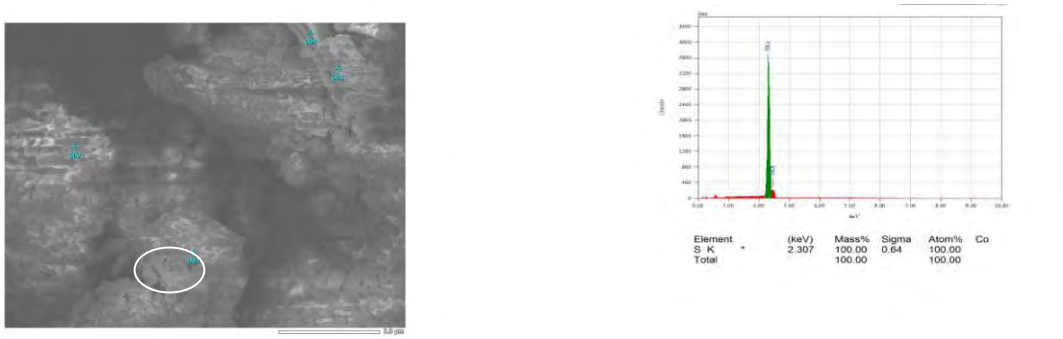

Fig.3.4 (d) EDX analysis of SNPs at + 004 position by electrochemically.

EDX spectra of SNPs synthesized by chemically at four different locations is following

EDX spectra at+001 location

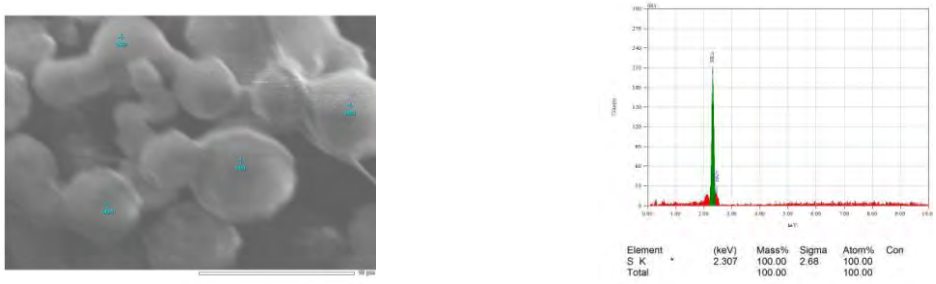

Fig.3.5 (a) EDX analysis of SNPs at + 001 position by chemically.

EDX spectra at+002 location

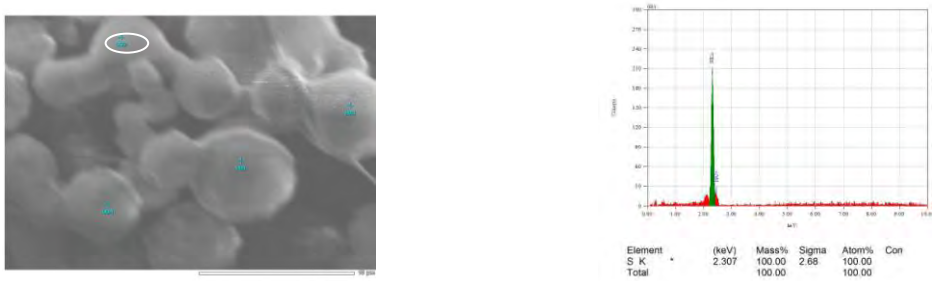

Fig. 3.5(b) EDX analysis of SNPs at + 002 position by chemically.

EDX spectra at+003 location

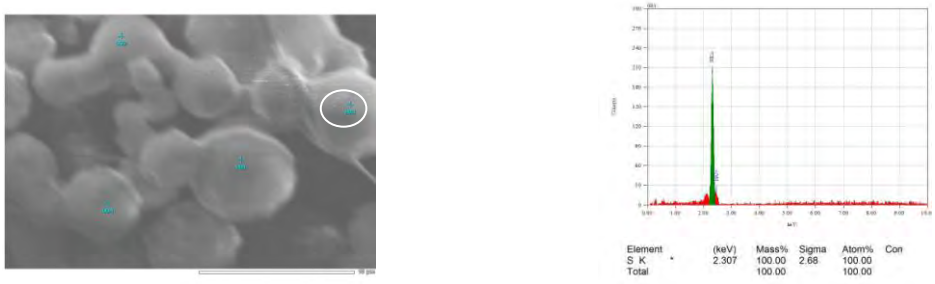

Fig.3. 5(c) EDX analysis of SNPs at + 003 position by chemically.

EDX spectra at+004 location

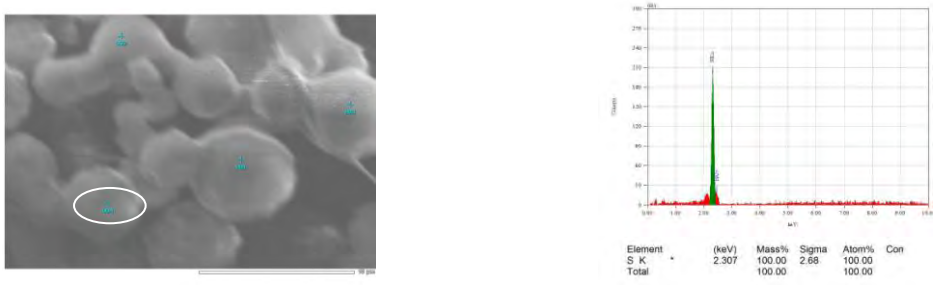

Fig.3. 5(d) EDX analysis of SNPs at + 004 position by chemically.

Table 3.1 Elemental composition of as prepared solid S NPs

Sample	Location	Peaks Observed (keV)	Mass (%)	Atom (%)	Tentative chemical formula
S NPs	**1**	**2.31**	**100**	**100**	**S NPs**
	2	**2.31**	**100**	**100**	**SNPs**
	3	**2.31**	**100**	**100**	**SNPs**
	4	**2.31**	**100**	**100**	**SNPs**
Total			**100**	**100**	**SNPs**

The results of XRD, SEM and EDX analysis, it was seen that the electrochemically synthesized SNPs was uniform and smaller in size. Therefore, the rest of the studies electrochemically synthesized product of SNPs was used.

3.1.4. Thermogravimatric analysis (TGA)

Thermo gravimetric analysis (TGA) is one of the thermal analysis techniques used to quantify weight change and thermal decomposition of the sample**.** The measurement is normally carried out in air or in an inert atmosphere, such as Helium or Argon, and the weight is recorded as a function of increasing temperature. **Fig.3.6** shows the TGA curves of pure S NPs. From **Fig.3.6** it was observed that a very sharp weight change was observed at

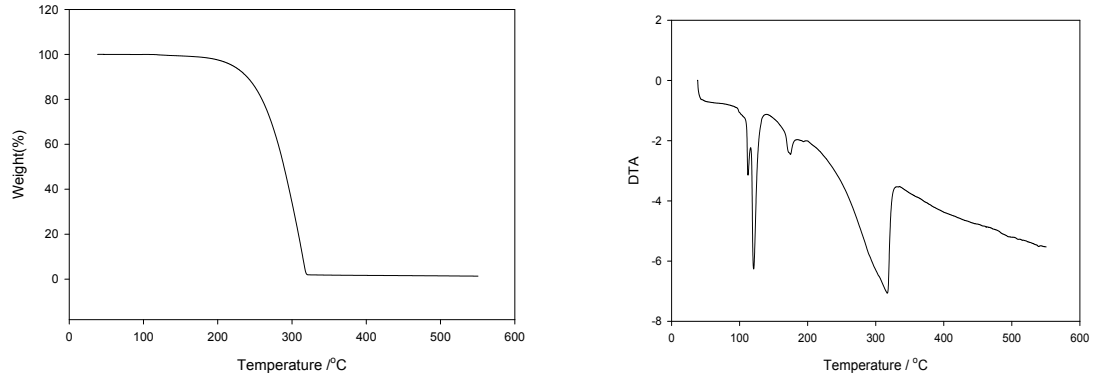

Fig.3.6. TGA and DTA graph of S NPs synthesized by electrochemically.

320°C and can be ascribed to the elimination of Sulfur to Sulfur dioxide. From **Fig.3.6** it was also observed that weight loss occurred in one step as there is no other impurity present .Therefore, the total process sulfur burned to sulfur dioxide, the weight % is change to zero. From DTA curve negative peak is obtained which indicates that the conversion is endothermic in nature.

3.1.5. Electrochemical study of SNPs

In electrosynthesis process was studied by cyclic voltameric methods. Cyclic voltametric studies on the thiosulfate were performed by using a steel electrode ((SS) as working electrode in a solution containing 0.5 M $Na_2S_2O_3$ and 0.5 M KOH. In thiosulfate ion two sulfur atoms are not equivalent; the unique chemistry of the thiosulfate ion, $S_2O_3^{2-}$ or SSO_3^{2}, which is responsible for the reducing properties and complexing abilities of thiosulfates. **Fig 3.7** shows the cyclic voltammogram of background in KOH. From **Fig** it was also seen that there was no characteristics oxidation and reduction peaks.

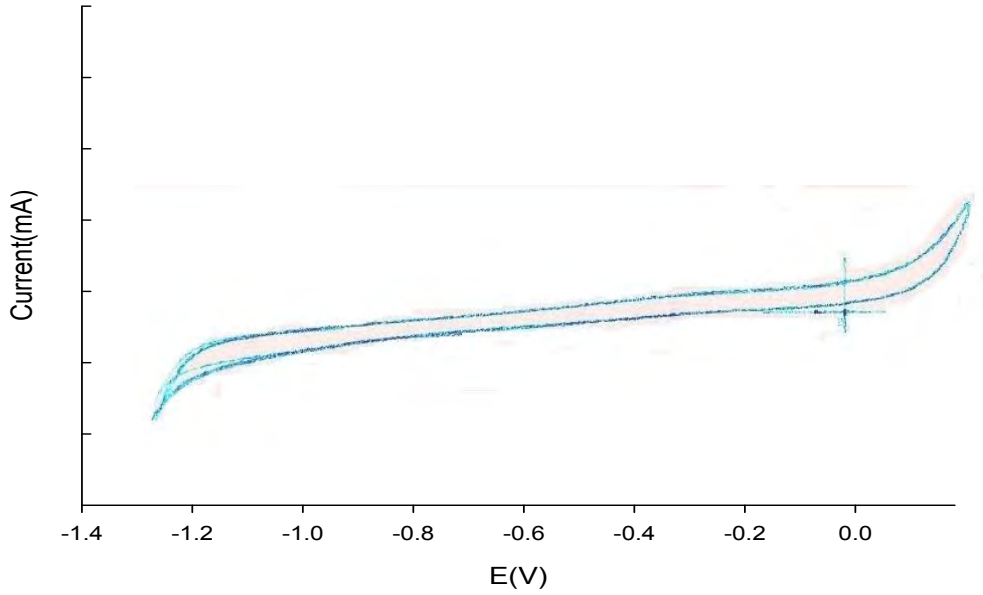

Fig. 3.7 Cyclic voltammogram of background in KOH.

Fig 3.8 shows the resulting cyclic voltammogram of formation of SNPs, the reduction of thiosulfate ion is occurred at about −1.08 V, while in the reverse scan, a weaker anodic peak due to the oxidation of sulfide ions is observed at about −0.8 V. This behavior shows that, at the steel electrode, at potentials not exceeding the potential of hydrogen evolution, the thiosulfate is reduced to sulfide and sulfite ions. Then, the produced sulfide ions in the previous step (initial reduction of thiosulfate) can be removed from aqueous solution by oxidation either to elemental sulfur or to oxyanions such as sulfate ion.

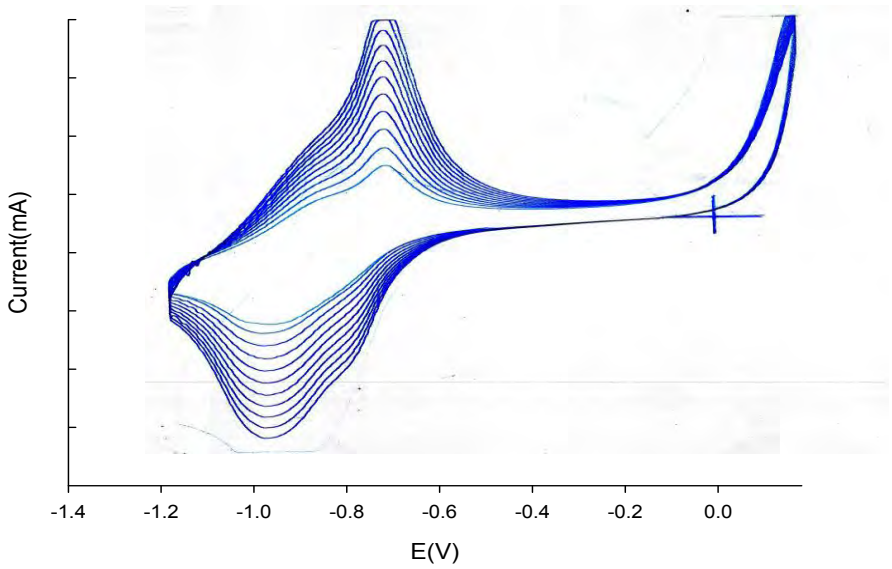

Fig.3.8 Cyclic voltammogram of reduction of $Na_2S_2O_3$ to formation of SNPs.

The reduction of thiosulfate ion is described by the equation

$$S_2O_3^{2-} + 2e = S^{2-} + SO_3^{2-} \quad (3.2)$$

At electrode potential not exceeding the potential of hydrogen evolution, the thiosulfate is reduced to sulfide and sulfite ions. S^{2-} in aqueous media has the following possible reactions as:

$$S^{2-}(l) \rightarrow S\,(s) + 2e^- \quad (3.3)$$

$$S^{2-}(l) + 8\,OH^-(l) \rightarrow SO_4^{2-}(l) + 4H_2O(l) + 6e^- \quad (3.4)$$

In this case, sodium thiosulfate substrate could be first reduced at the surface of cathode and, in the next step, the produced sulfide ions will be oxidized to elemental sulfur at the anode.

3.1.5.1 Doping dedoping process of SNPs

The electrochemical doping dedoping process of SNPs coated film electrode was examined by cyclic voltametry in aqueous solution of KOH (0.5M). In this case SNPs coated working electrode was allowed to sweep between the potential of +0.2 to -1.2 V at a scan rate of 100 mVs^{-1}(**Fig.3.9**). The light yellow color of the film turned to white when potential sweep

approached to the cathodic direction at ca. +0.0 V where dedoping of electrolyte occurs. In this case an oxidation and redrox peak disappears indicating that electroactive species was absent in the electrolytic solution.

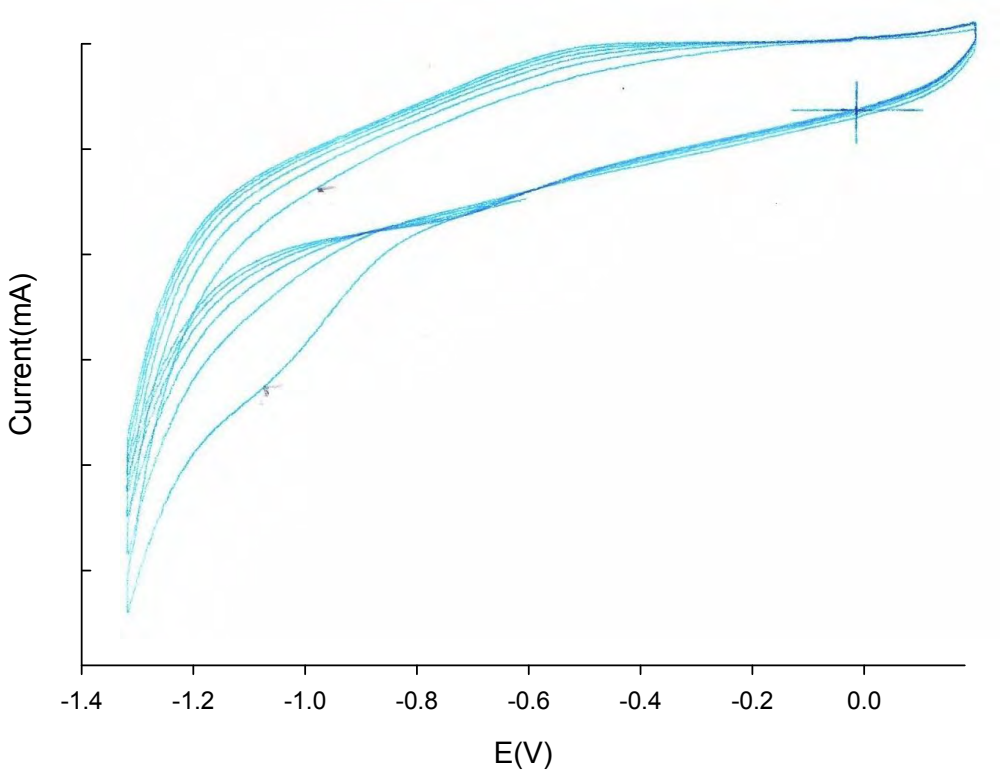

Fig.3.9 Doping- dedoping process of SNPs.

3.2 Characterization of PANI

3.2.1 Scanning electron microscopy (SEM)

SEM Analysis is used to study morphology and the external form of the prepared materials. Chemical composition and morphological structure of a material strongly depend on the mode of synthesis, be it chemical and electrochemical, synthesis condition such as pH, concentration of reactant and product, chemical nature of the oxidant, oxidation potential etc.

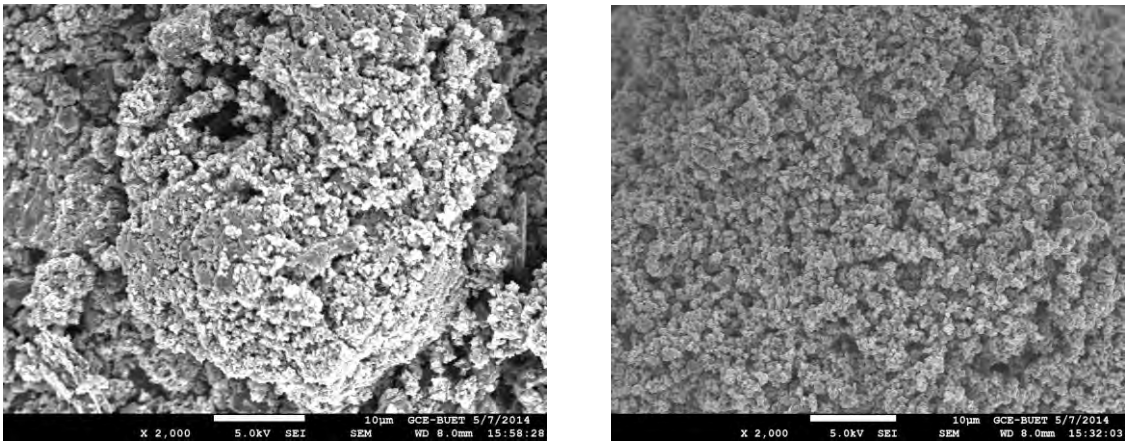

Fig.3.10 SEM micrograph of PANI synthesizes by (a) chemically and (b) electrochemically.

Fig 3.10(a) shows the SEM images of the PANI synthesized by electrochemically. From **Fig 3.10(a)** it was seen that the surface morphology in this case appears to be rather less uniform, small, and spherical and showed loose aggregation. **Fig. 3.10(b)** shows the SEM images of the PANI synthesized by chemically. It was seen from **Fig** that a grain like morphology appears and the grain seems to be aggregated to a bigger deposit and randomly pilled on the substrate and the surface is not uniformly covered. Moreover, the deposits seem to be three dimensional structures with plenty of pores and the pores and directionality obviously provide greater surface area and surface activity. The present SEM observations clearly suggest that PANI surface prepared by electrochemically clearly different from the PANI when prepared chemically. From the observed dissimilar morphological features of the PANI samples, it is expected that their surface activity could be different.

3.2.2 Energy dispersive X-ray (EDX) analysis

EDX analysis is an analytical technique used for the elemental analysis and chemical composition of the sample. From elemental analysis it is possible to investigate all the elements contained in the PANI. **Fig 3.11** shows the EDX spectra of PANI synthesized by

chemically and electrochemically. EDX experiment was run through four different positions. The percentages of the elements were determined from the intensity of the lines and the results are summarized in Table 3.2 and 3.3. Thus from the chemical composition of obtained from EDX spectra, it was concluded that the prepared both sample are PANI and no other impurity were present. The elemental analysis of PANI was done at 3 different locations (electrochemically and chemically) by EDX method which is given bellow. The results show that synthesized PANI in both processes (electrochemically and chemically) were produced pure products and no others impurity were present.

For location +001

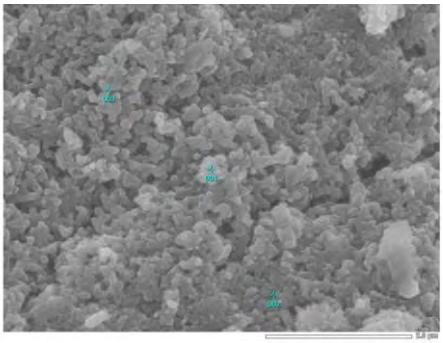

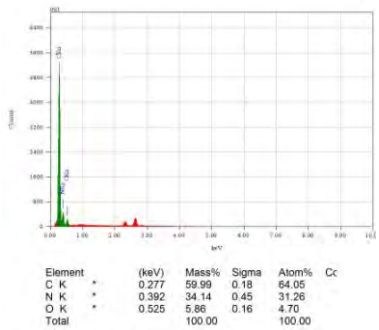

Element		(keV)	Mass%	Sigma	Atom%	Cc
C K	*	0.277	59.99	0.18	64.05	
N K	*	0.392	34.14	0.45	31.26	
O K	*	0.525	5.86	0.16	4.70	
Total			100.00		100.00	

Fig 3.11(a) EDX spectra of PANI at location +001 synthesized by electrochemically.

For location +002

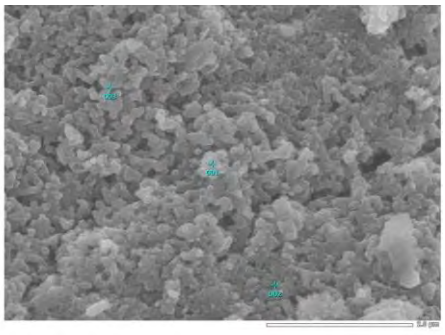

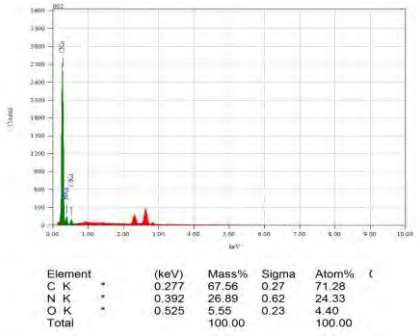

Element		(keV)	Mass%	Sigma	Atom%	(
C K	*	0.277	67.56	0.27	71.28	
N K	*	0.392	26.89	0.62	24.33	
O K	*	0.525	5.55	0.23	4.40	
Total			100.00		100.00	

Fig 3.11(b) EDX spectra of PANI at location +002 synthesized by electrochemically.

For location +003

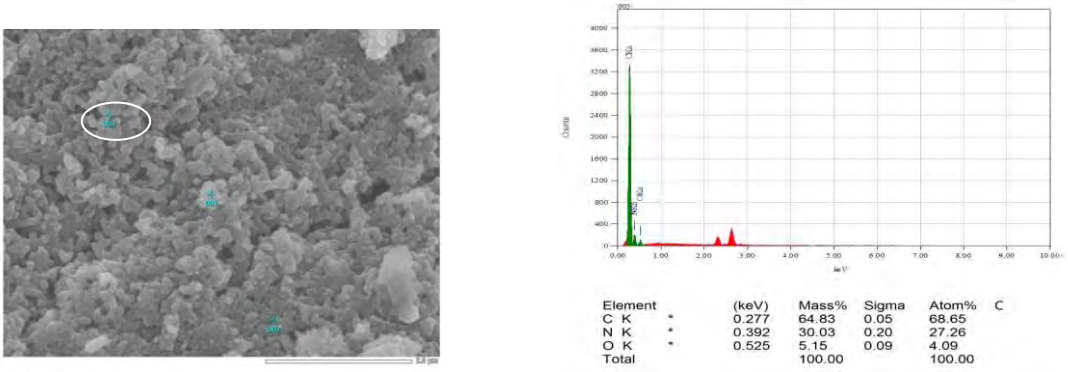

Fig 3.11(c) EDX spectra of PANI at location +003 synthesized by electrochemically.

EDX spectra of PANI synthesized by chemically

For location +001

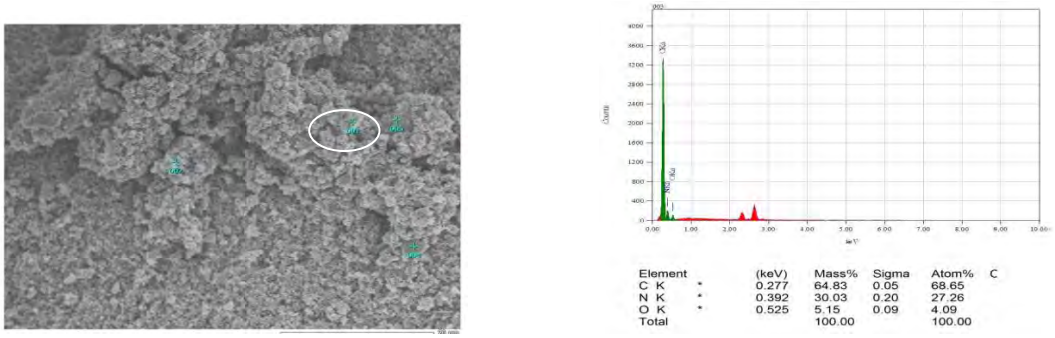

Fig.3.12 (a) EDX spectra of PANI at location +002 synthesized by chemically.

For location +002

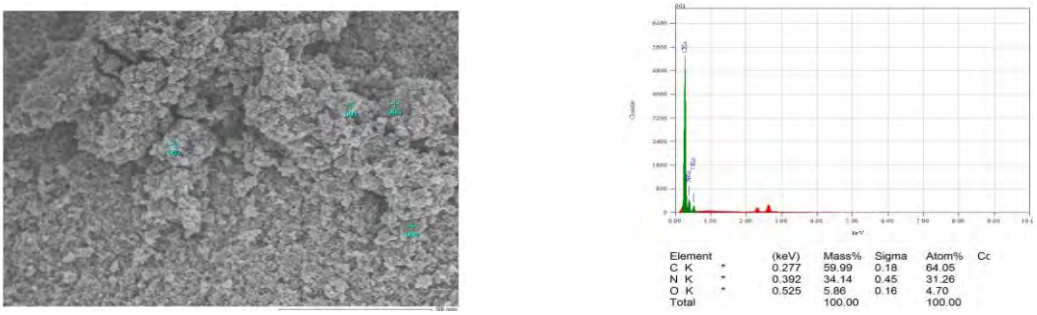

Fig.3.12 (b) EDX spectra of PANI at location +002 synthesized by chemically.

For location +003

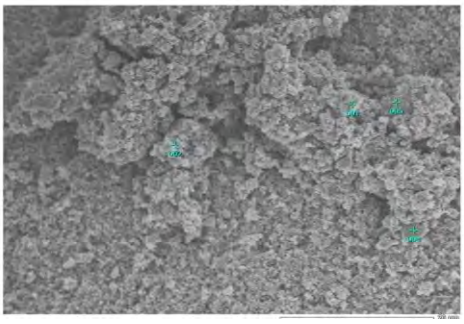

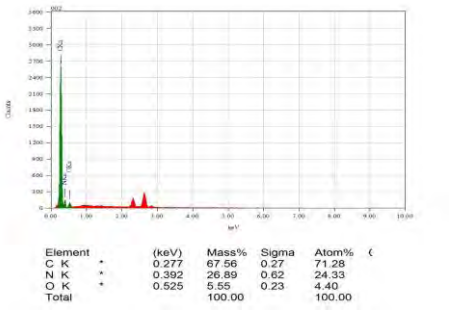

Fig. 3.12(c) EDX spectra of PANI at location +003 synthesized by chemically.

Since electrochemical process provide homogenous surface and provide better results. Therefore, rest of the analysis, electrochemically obtained samples was used.

Table 3.2 Elemental composition of PANI synthesized by electrochemically

Sample	Location	Peaks Observed (keV)	Mass (%)	Atom (%)	Tentative chemical formula
S NPs	C	0.277	59.99	64.04	PANI
	N	0.392	34.14	31.26	
	O	0.525	5.86	4.70	
Total			100	100	

Table 3.3 Elemental composition of PANI synthesized by chemically

Sample	Location	Peaks Observed (keV)	Mass (%)	Atom (%)	Tentative chemical formula
S NPs	C	0.277	67.56	71.28	PANI
	N	0.392	26.89	24.33	
	O	0.525	5.55	4.40	
Total			100	100	

3.2.3 X-ray diffraction (XRD) analysis of PANI

XRD provide information about the intermolecular arrangement i.e; the level of crystallinity of a material. **Fig.3.13** shows the XRD pattern of the synthesized PANI. The PANI shows only a broad amorphous scattering around 2θ = 25°.The presence of strong and broad diffraction peaks in **Fig.3.13** indicates that the obtained PANI was amorphous in nature. Most of the conductive polymers are reported to be extremely poor crystalline [141]. During

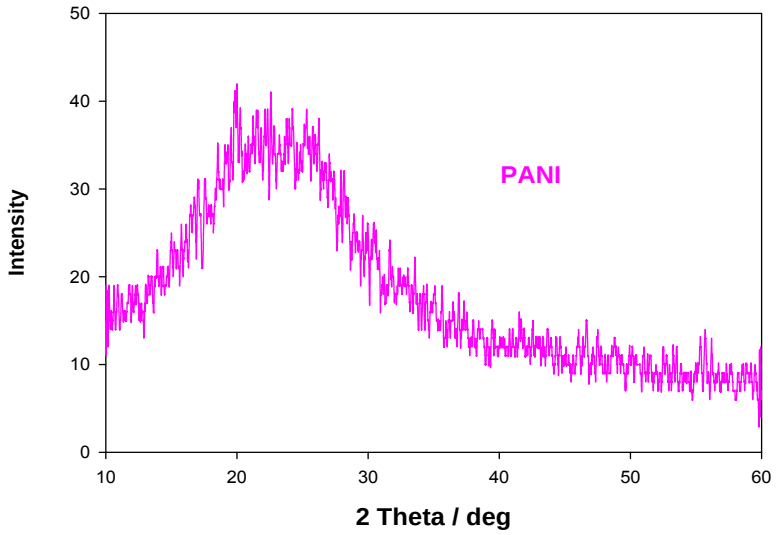

Fig.3.13 XRD pattern of PANI.

polymerization, although most of the aniline units are linked through the 1, 4 positions, a significant unit are coupled through other positions. This introduces defects in the hypothetical linear chain arrangement of the polymer and also causes some cross linking of the polymer and consequently results in a significant decrease in the crystallinity and leads to diffuse diffraction pattern as exhibited in **Fig.**

3.2.4 Thermogravimetric analysis (TGA)

Thermogravimetric analysis (TGA) is one of the thermal analysis techniques used to quantify weight change and thermal decomposition of the sample. TGA measures the amount and rate (velocity) of change in the mass of a sample as a function of temperature or time in a controlled atmosphere. The measurements are used primarily to determine the thermal and/or oxidative stabilities of materials as well as their compositional properties. The technique can analyze materials that exhibit either mass loss or gain due to decomposition, oxidation or loss of volatiles (such as moisture). Thermal degradation of PANI was explained by thermogravimetry. The resulting mass change Vs temperature curve provides the information

concerning the thermal stability and composition of the initial sample, intermediates and the residue. This technique provides sufficient information to calculate the amount of dopant present in the PANI backbone and to study the thermal decomposition of the polymer. The results of the TGA of the PANI are presented in **Fig.3.14**. PANI showed two main weight loss stages. The first step weight loss is associated with the loss of moisture. PANI always shows high moisture loss because it is highly hygroscopic in nature and some moisture still remains even after vacuum drying. A slow and somewhat gradual weight loss was observed for these polymers at 550°C are due to the structure decomposition of PANI backbone. PANI samples were not completely destroyed because in nitrogen atmosphere carbonization of polymer takes place leaving a marked residue. PANI synthesized in the present work show very good thermal stability. The results of the DTA spectrum reveals that for the PANI sample, the peak descends at 87 and 285°C; that implies to endothermic nature.

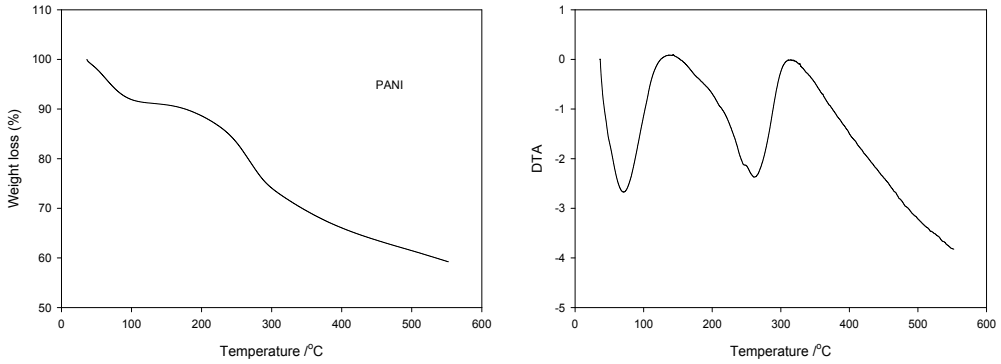

Fig.3.14. TG and DTA analysis of PANI.

3.3. Characterization of SNPs-PANI nanocomposite

3.3.1 X-ray diffraction (XRD) analysis

XRD is extensively used in material identification. It is a non destructive, very simple and rapid technique for powder and other microcrystalline samples. The XRD pattern of PANI (blue color) and SNPS-PANI nanocomposite (pink color) was shown in **Fig.3.15.** The SNPs-PANI nanocomposite showed peaks at 2θ = 19, 20, 25.05, 27 corresponding to the interface distances d = 34.617, 4.659, 4.425, 3.545 and 3.293 A°, respectively. The peaks from 20 to 27° are attributed to the momentum transfer and periodicity, perpendicular to the chain direction. From Fig it was also observed that strong and broad diffraction peaks appears indicating that SNPs-PANI nanocomposite was also amorphous in nature as PANI. The XRD pattern of SNPs-PANI nanocomposite shows sharp and well defined peaks, which indicate the presence of SNPs in the polymer chain. The inter planar distance and crystallite size are estimated by Bragg‟s law and Debye Scherer equation.

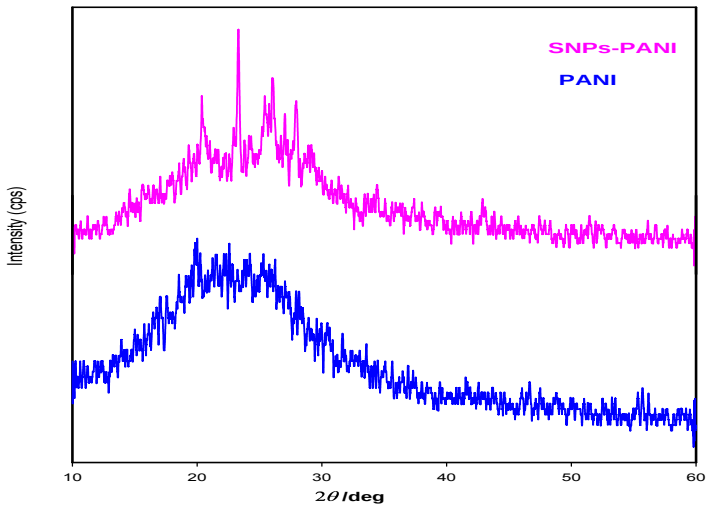

Fig.3.15 Combined XRD pattern of PANI and SNPs-PANI nanocomposite.

3.3.2 Scanning Electron Microscopy (SEM)

Fig 3.16 shows the SEM image of S NPs-PANI nanocomposite. The SEM image of S NPs-PANI clearly indicates that the polymer possess three dimentional structure with plenty of pores and also less uniform surfaces. The pores and dimensionality provide greater surface area and thus surface activity. Moreover, the pores of the PANI prevent aggregation of SNPs onto nanocomposte.

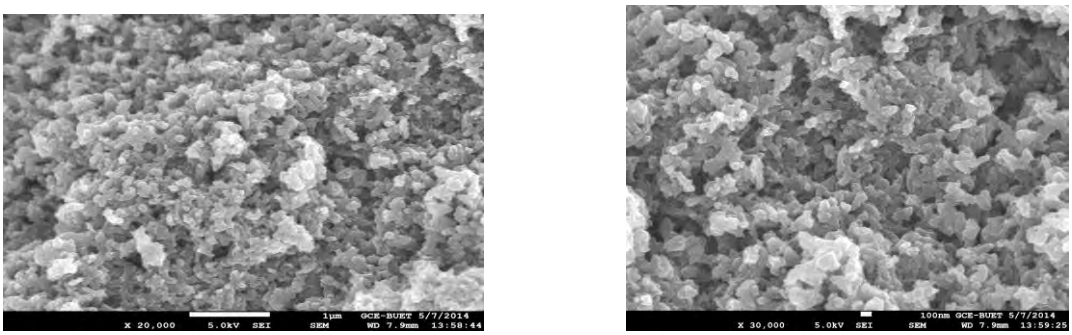

Fig.3.16 SEM image of S NPs- PANI composite at different magnification.

3.3.3 Energy dispersive X-ray (EDX) analysis

EDX analysis was performed to confirm the atomic composition (%) and purity of the synthesized nanoparticles. **Fig.3.17** showed the C, S, O and N EDX mapping images of the SNPS-PANI nanocomposite, suggesting that elemental S was present in the as-prepared product. As evidenced by the data, the product contains C, S, O and N and does not contain any impurities. EDS spectra of SNPs-PANI nanocomposite synthesized by electrochemically at four different locations is following

EDXspectra of SNPs-PANI nanocomposite at +001 location

Fig 3.17(a) EDX spectra of SNPs-PANI nanocomposite at +001 location.

EDX spectra at +002

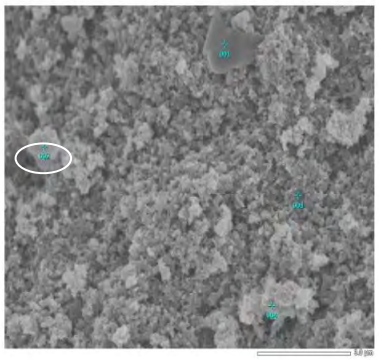

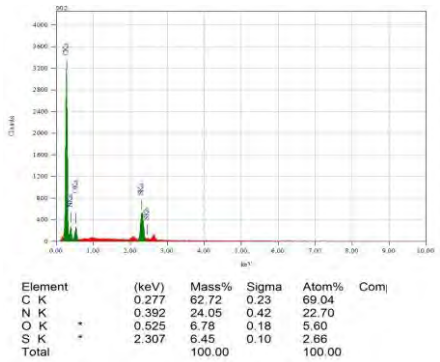

Element		(keV)	Mass%	Sigma	Atom%	Com
C K		0.277	62.72	0.23	69.04	
N K		0.392	24.05	0.42	22.70	
O K	*	0.525	6.78	0.18	5.60	
S K	*	2.307	6.45	0.10	2.66	
Total			100.00		100.00	

Fig 3.17(b) EDX spectra of SNPs-PANI nanocomposite at +002 location.

EDX spectra at +003 location

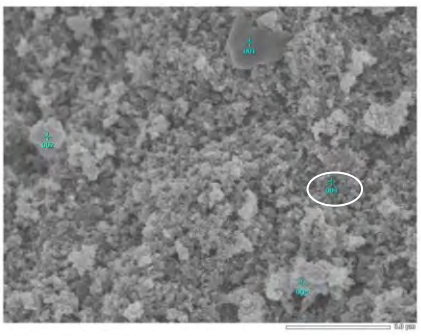

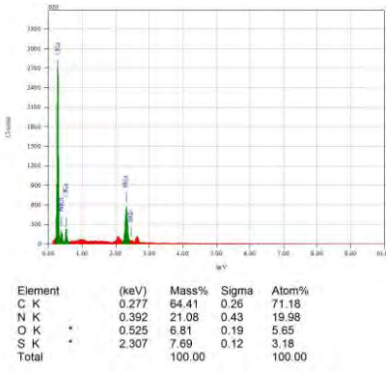

Element		(keV)	Mass%	Sigma	Atom%
C K		0.277	64.41	0.26	71.18
N K		0.392	21.08	0.43	19.98
O K	*	0.525	6.81	0.19	5.65
S K	*	2.307	7.69	0.12	3.18
Total			100.00		100.00

Fig 3.17(c) EDX spectra of SNPs-PANI nanocomposite at +003 location.

EDX specta at +004 location

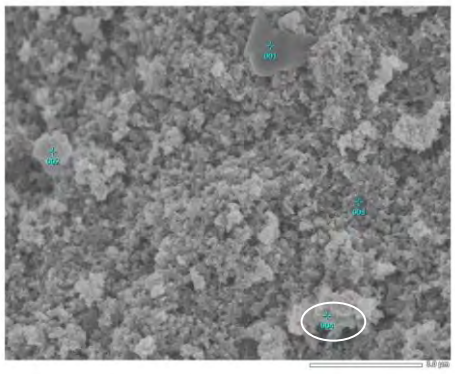

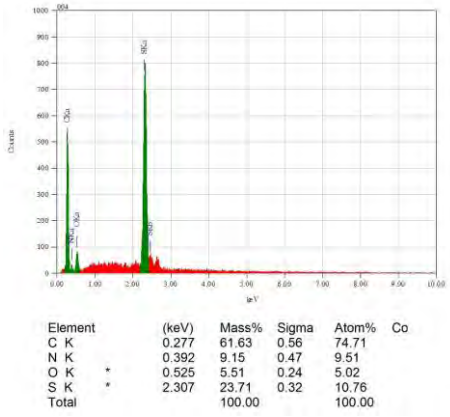

Element		(keV)	Mass%	Sigma	Atom%	Co
C K		0.277	61.63	0.56	74.71	
N K		0.392	9.15	0.47	9.51	
O K	*	0.525	5.51	0.24	5.02	
S K	*	2.307	23.71	0.32	10.76	
Total			100.00		100.00	

Fig 3.17(d) EDX spectra of SNPs-PANI nanocomposite at +004 location.

3.3.4 Thermogravimatric analysis (TGA)

Knowledge of thermal stability of SNPs-PANI nanaocomposite under various thermal conditions is important for their use in many practical applications. Thermal degradation of SNPs-PANI is explained by thermogravimetry. Thermogravimetry is the change in mass of sample as a function of temperature when it is subjected to controlled temperature program. The resulting mass change Vs temperature curve provides the information concerning the thermal stability and composition of the initial sample, intermediates and the residue. This

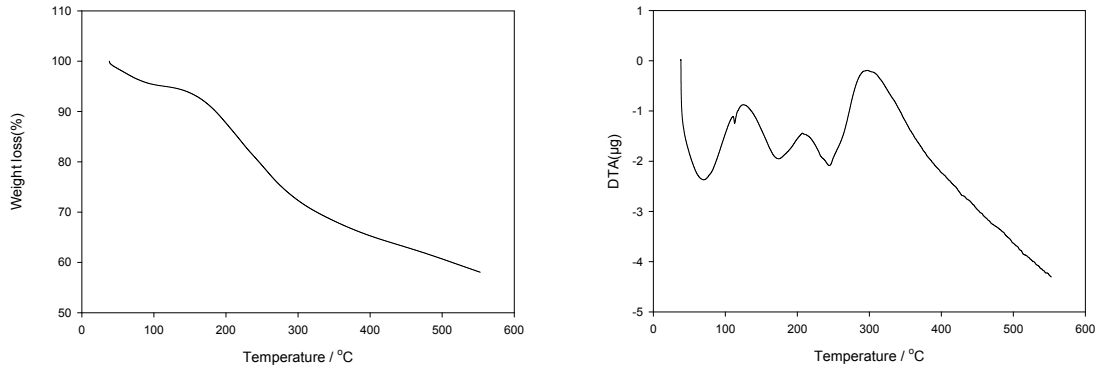

Fig.3.18. TG and DTA analysis of SNPs-PANI nanocomposite.

technique provides sufficient information to presence of SNPs in the PANI backbone and to study the thermal decomposition of the polymer. As shown in **Fig.3.18,** the weight loss of SNPs-PANI starts from 80 °C and completely decreasing all evaporation of SNPs-PANI at 550°C. Therefore, the sulfur content in SNPs-PANI was calculated to be 55.9%. From the results of the DTA spectrum reveals that for the SNPs-PANI sample, three endothermic peaks appear indicating the presence of SNPs in nanocomposite.

3.3.5 Infrared spectral analysis

Fig 3.19 shows the IR spectra of PANI and SNPs-PANI nanocomposite synthesized by electrochemically. The stretching vibrations observed at 1576 and 1497 cm^{-1} were assigned to the C=C stretching deformation of quinoid and benzenoid rings, the bands at 1,550 cm^{-1} due to N-H bendings, 1302 cm^{-1} attributed to the C–N stretching of secondary aromatic amine, 1139 cm^{-1} attributed to the aromatic C–H in-plane bending, as well as 826 cm^{-1} related to the out-of-plane deformation of C–H in the 1, 4-disubstituted benzene ring were observed for PANI . The band at 3380 and 3272 is assigned to asymmetrical and symmetrical stretching vibrations of N-H.

Bands for the SNPs-PANI nanocomposite sample in the high wavenumber region have been observed, corresponding to the N–H stretching (3400–3200 cm^{-1}), together with the aromatic C–H stretching vibration (3000–2850 cm^{-1}). The quinonoid ring absorbs at 1596 cm^{-1} and the benzenoid ring absorbs at about 1500 cm^{-1}. The band at 1300 cm^{-1} is assigned to the C–N stretching of the secondary aromatic amine and the band at 1244 cm^{-1} is related to the protonated C–N group. The absorption bands at 1120 and 1044 cm^{-1} are due to the aromatic C–H in-plane bending modes overlapped with S–N bond stretching arising from SNPs in SNPs-PANI nanocomposite. The out-of-plane deformations of C–H in the 1, 4-substituted benzene ring result in the band at 870 cm^{-1} [142]. The infrared spectrum at low frequencies of the composite confirmed the presence of nanoparticles in the polymer, in particular showing the band at 225 cm^{-1}.

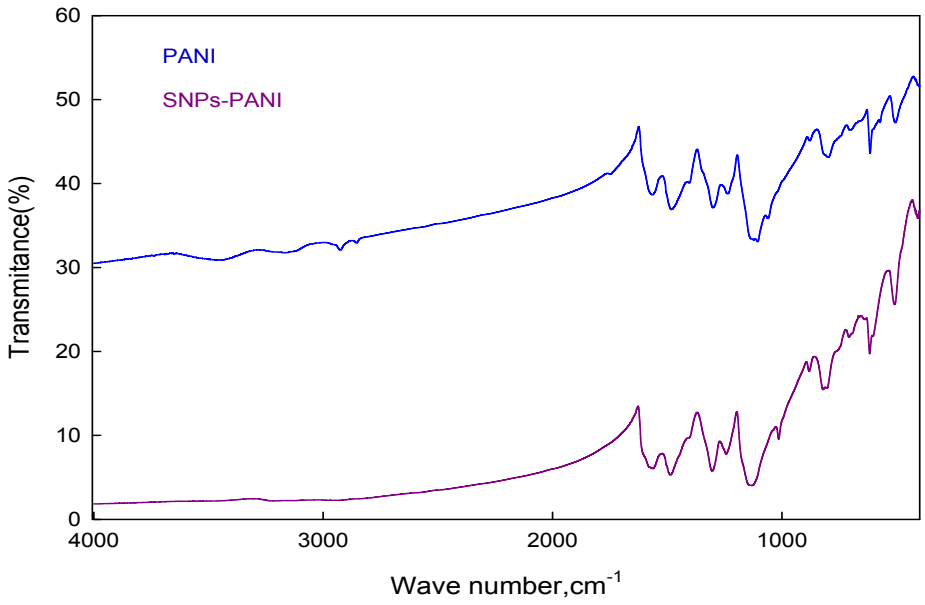

Fig.3.19 Combined IR spectra of PANI and SNPs-PANI nanocomposite.

3.3.6 Ultraviolet-Visible spectroscopy

Fig. 3.20 illustrates the UV- visible spectra of PANI and SNPs-PANI recorded in DMSO solution at room temperature. The absorption spectrum shows two remarkable peaks at 274 nm and 361 nm and a week shoulder at 630 nm. The peak observed at 361 nm correspond to the inter band π-π*(valance band to conduction band) transition, peak at 274 nm corresponds to bezenoid to quinoid transition (π-π*) indicating the synthesized polymer is polyaniline in oxidized form while the other peaks at around 630 nm may be responsible for PANI conductivity by forming polaron and bipolaron as mid gap state [92]. In fact polaron state is a radical cation i.e. contains one electron whereas bipolaron is a dication, i.e. electronless. At low doping level, polaron formation takes while at highly doped states, bipolaron formation predominates. Therefore because of greater stability a bipolaroan is favoured over polaroan. The presence of SNPs in the SNPs-PANI nanocomposite leads to a small red shift of the absorption.

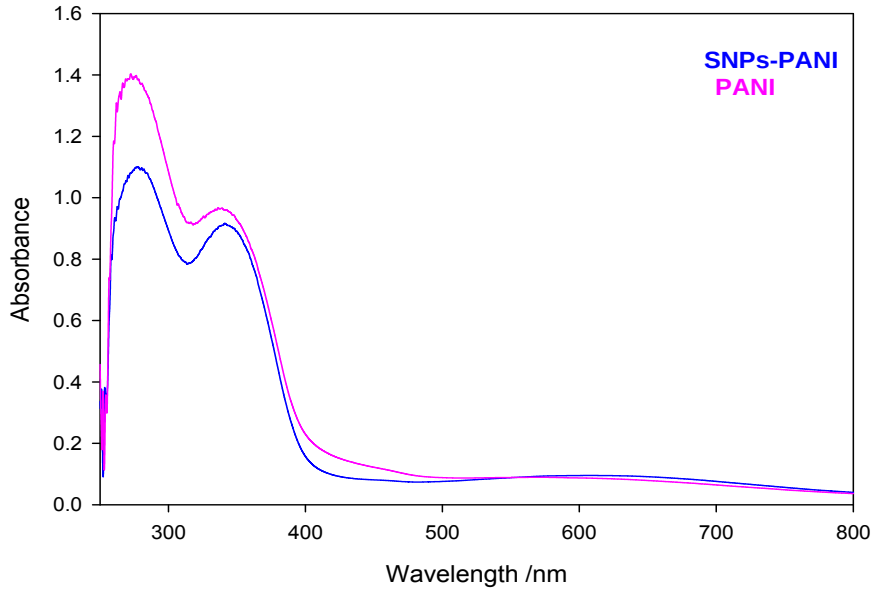

Fig. 3.20 Combined UV visible spectra of PANI and SNPs-PANI nanocomposite.

3.4. Characterization of NIPA and SNPs-NIPA gel

3.4.1 X-Ray diffraction (XRD) analysis

Fig. 3.21 illustrates the combined XRD (X-ray diffraction) pattern of NIPA gel and SNPs-NIPA gel. Three broad peaks centered at $2\theta = 10^{o}$, 22^{o} and 45^{o} were observed, showing the resulting NIPA gel was semicrystalline nature. Moreover, it has been demonstrated that the two broad peaks are ascribed to the periodicity parallel and perpendicular to the polymer chain [144]. In XRD patter of SNPs-NIPA gel, only peak intensity was increased and there is no other distinct change was observed. Moreover, SNPs-NIPA gel was also semicrystalline nature.

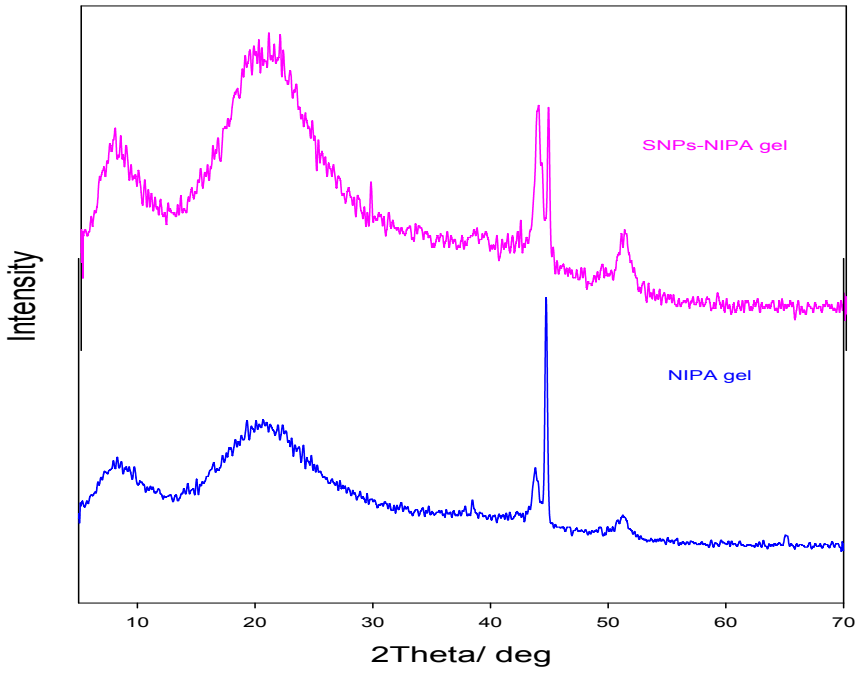

Fig.3.21 Combined XRD of NIPA gel and SNPs-NIPA gel.

3.4.2 Scanning Electron Microscopy (SEM) of NIPA gel

Fig. 3.22 shows the SEM image of poly N-isopropyl acrylamide poly (NIPA) microgels. It was clearly observed from the **Fig** that the gel had porous structure with three dimensional networks. Moreover, the bright sport in the micrograph indicates the microgel particles prepared are rather mono-dispersed spherical Particles. This mono dispersed porous spherical particle gives the gel ability to act as a drug carrier.

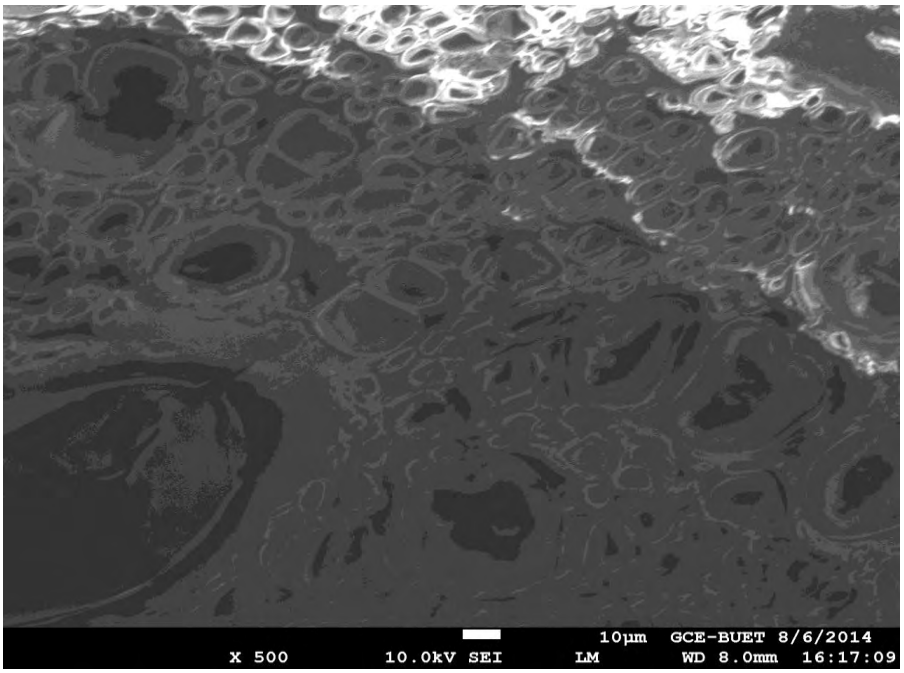

Fig.3.22. SEM images of poly (NIPA) microgels.

3.4.3 Energy dispersive X-ray (EDX) analysis of NIPA gel

EDX is an analytical technique used for the chemical analysis and characterization of a sample. Elemental analysis of the as prepared poly NIPA gel has been performed by employing EDX method. From elemental analysis it is possible to investigate all the elements contained in poly NIPA gel. **Fig. 3.23** shows the EDX spectra of NIPA gel at four different locations. The peaks observed at 0.2 kV, 0.39kV and 0.52 kV were for Carbon, Nitrogen and oxygen respectively. EDX spectra of NIpa gel at four different locations is following

EDX spectra of NIPA gel at +001 location

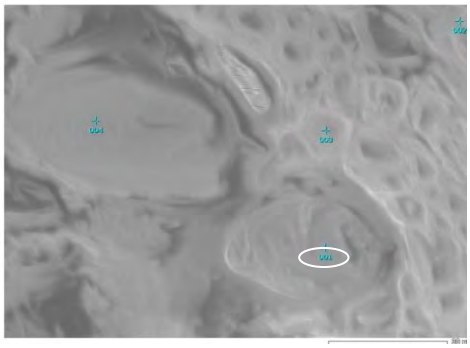

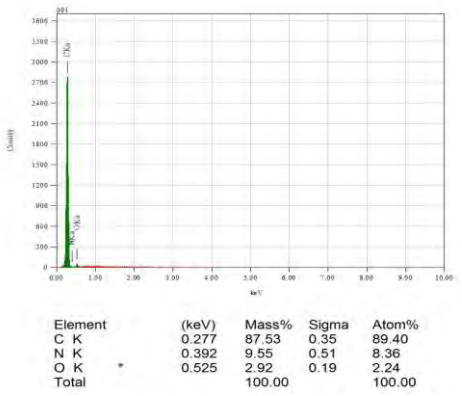

Element	(keV)	Mass%	Sigma	Atom%
C K	0.277	87.53	0.35	89.40
N K	0.392	9.55	0.51	8.36
O K	0.525	2.92	0.19	2.24
Total		100.00		100.00

Fig.3.23 (a) EDX spectra of NIPA gel at +001 location.

EDX spectra of NIPA gel at +002 location

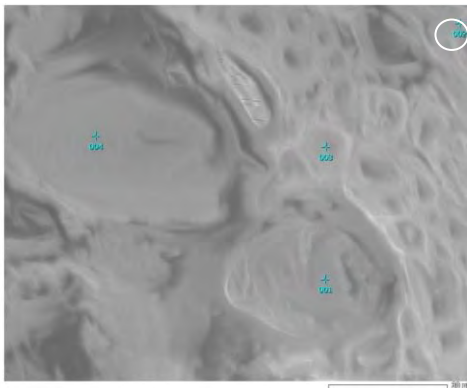

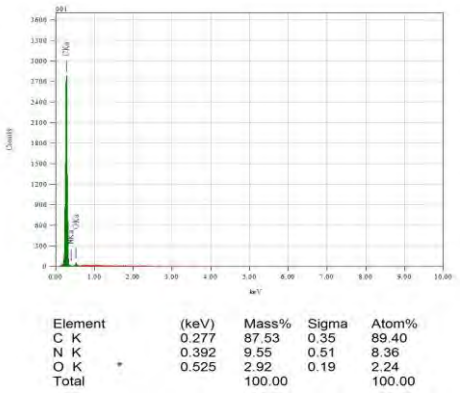

Element	(keV)	Mass%	Sigma	Atom%
C K	0.277	87.53	0.35	89.40
N K	0.392	9.55	0.51	8.36
O K	0.525	2.92	0.19	2.24
Total		100.00		100.00

Fig.3.23 (b) EDX spectra of NIPA gel at +002 location.

EDX spectra of NIPA gel at +003 location

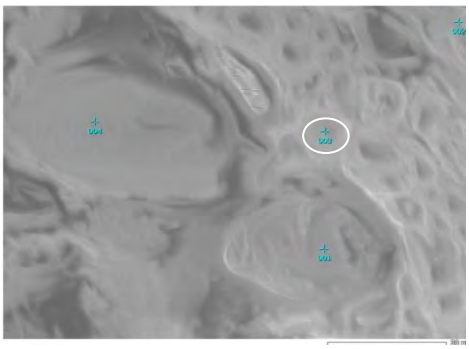

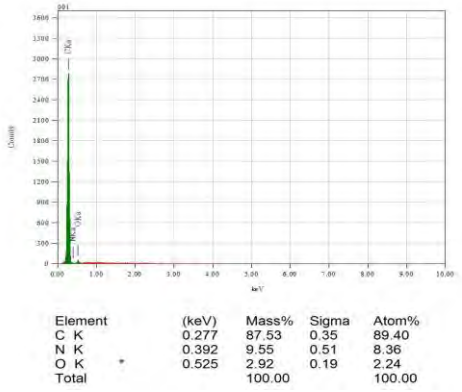

Element	(keV)	Mass%	Sigma	Atom%
C K	0.277	87.53	0.35	89.40
N K	0.392	9.55	0.51	8.36
O K	0.525	2.92	0.19	2.24
Total		100.00		100.00

Fig.3.23(c) EDX spectra of NIPA gel at +003 location.

EDX spectra of NIPA gel at +004 location

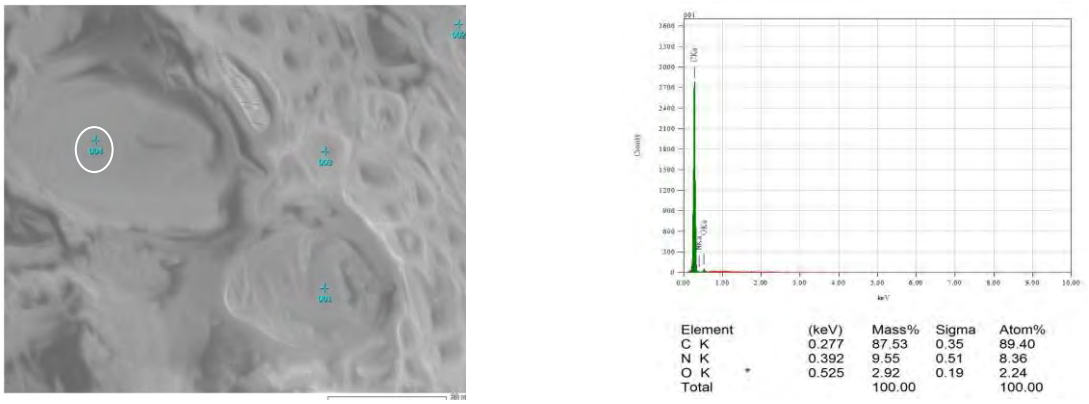

Fig.3.23 (d) EDX spectra of NIPA gel at +004 location.

4.4.4 SEM image of S NPs-NIPA nanocomposite

Fig.3.24 shows the SEM image of SNPs-NIPA nanocomposite. It was clearly observed from the **Fig.3.24** that the gel had also porous monodispersed spherical particles structure with three dimensional networks as like poly NIPA gel. This monodispersed spherical gel network may be preventing the agglomeration of S NPs in the composite. But both NIPA gel and SNPs-NIPA nanocomposite were give similar appearance in the micrograph. So, difficult to find out any identical morphology of SNPs-NIPA nanocomposite. Consequently, some other way of identification is necessary for the existence of S NPs in the gel network.

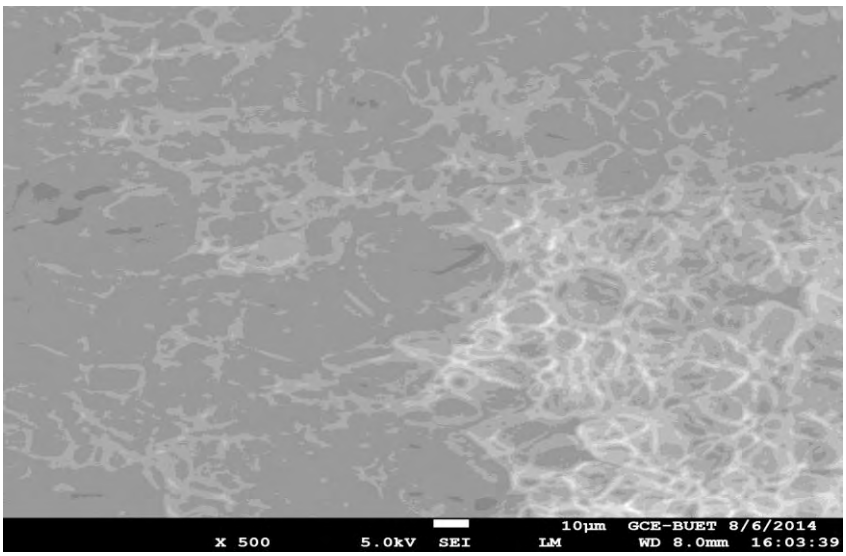

Fig.3.24 SEM images of poly SNPs- NIPA gels.

3.4.5 Energy dispersive X-ray (EDX) analysis of S NPs-NIPA nanocomposite

From elemental analysis it is possible to investigate all the elements contained in S NPs-NIPA gel. **Fig.3.25** shows the spectrum of the EDX analysis of as prepared S NPs-NIPA nanocomposite. As can be seen from the peaks observed at 0.2 kV, 0.39kV, 0.52 kV and 2.3 kV were for Carbon, Nitrogen, oxygen and SNPs respectively. The percentage of poly NIPA-S NPs nanocomposite at different locations was determined from the intensity of the lines and the results are summarized in **Table 3.4.** It is evident from the peaks that no other impurity was present in the poly NIPA- SNPs microgel. EDX analysis of as prepared S NPs-NIPA nanocomposite were taken at four different locations which is following

EDX spectra of SNPs-NIPA gel at +001 location.

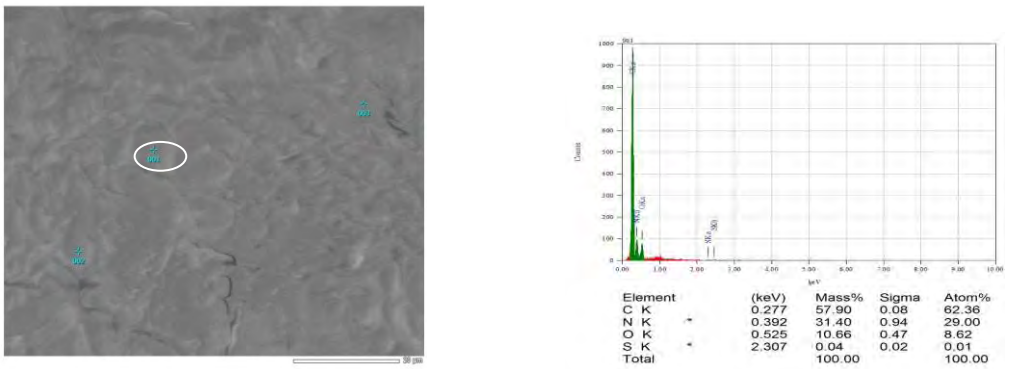

Fig.3.25 (a) EDX spectra of SNPs-NIPA gel at +001 location.

EDX spectra of SNPs-NIPA gel at +002 location.

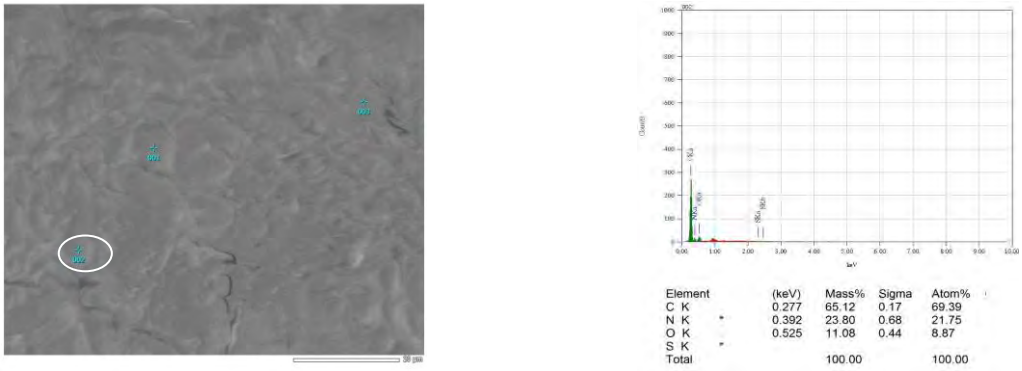

Fig.3.25 (b) EDX spectra of SNPs-NIPA gel at +002 location.

EDX spectra of SNPs-NIPA gel at +003 location

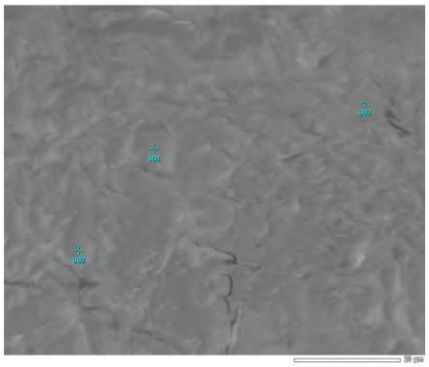

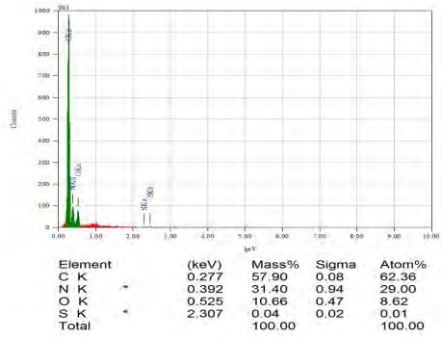

Fig.3.25(c) EDX spectra of SNPs-NIPA gel at +003 location.

EDX spectra of SNPs-NIPA gel at +004 location

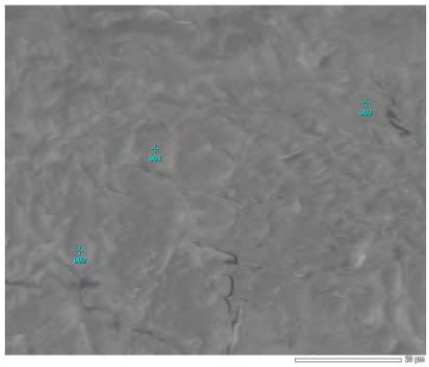

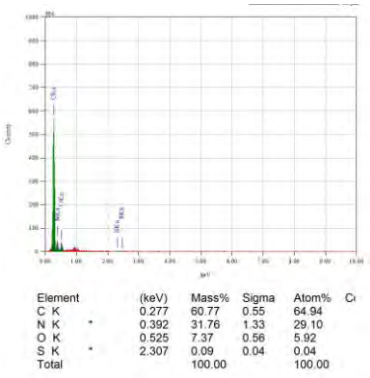

Fig.3.25 (d) EDX spectra of SNPs-NIPA gel at +004 location.

Table 3.4 Elemental composition of SNPs-NIPA gel

Sample	Location	Peaks Observed (keV)	Mass (%)	Atom (%)	Tentative chemical formula
S NPs -NIPA	C	0.277	57.90	62.36	SNPs-NIPA
	N	0.392	31.40	29.00	
	O	0.525	10.66	8.62	
	S	2.307	0.04	0.01	
Total			100	100	

3.5 Drug release capacity of SNPs-NIPA gel with temperature

The existence of both hydrophilic and hydrophobic groups makes NIPA hydrogel show the remarkable temperature-sensitive property. The temperature sensitivity of the synthesized nanoparticles was also measured using the UV-Vis spectrometer. When the temperature was increased above 34^0C, crystals disappeared and the hydrogel became blurry. Increasing the temperature further (35^0C), the NIPA hydrogel obviously started to shrink. This was because the water inside the hydrogel had been expelled out of the network due to the strengthened hydrophobic effect. Keeping increasing the temperature would make the hydrogel become smaller and smaller until all the water inside the hydrogel was expelled out of the network. When the temperature was decreased back to the room temperature, the crystals could still come back and the hydrogel could recover its original shape [123]. However, SNPs give UV visible spectra at 225 nm. **Fig. 3.26** shows the UV spectra of SNPs. SNPs-NIPA hydrogel released SNPs with increasing temperature $(25\text{-}40)^0$C and the amount of released SNPs was measured by measuring absorbance of SNPs (Fig).

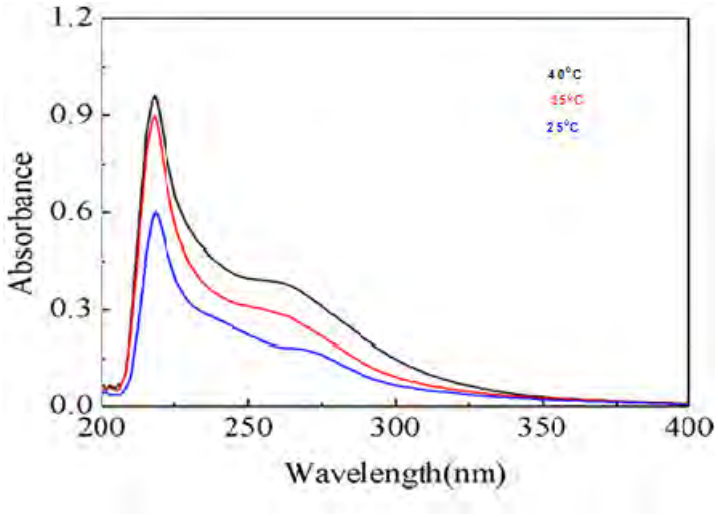

Fig.3.26 UV visible spectra of SNPs at (a) 25^0C (b) 35^0C (c) 40^0 C.

NIPA gel is biodegradable and can be used as drug carrier in human body safely [120]. The majority of current drug formulations represent lyophobic colloids, such as suspensions, emulsions, powders, crosslinked gels, etc. NIPA gel system may be suitable for a drug delivery system which rapidly release controlled amount of some hydrophobic drug by on-off of external stimuli such as increasing temperature.

3.6. Drug delivery by doping de-doping process

3.6.1 Doping de-doping process of PANI

Electrochemical synthesis of PANI was carried out by anodic oxidation of aniline onto stainless steel (SS) electrode. Typical CV of electrochemical polymerization of aniline is shown in **Fig.3.27.** On sweeping the potential from -0.4 to + 1.5 V vs SCE, a sharp rise in the current is seen at a potential +1.35 V indicating the oxidation of aniline to yield PANI. A thin deep blue film is seen on the SS electrode surface. As the sweeping repeated; in the second and subsequent cycles the peaks current increases further indicating the formation of more deposits of PANI on the electrode surface. The cyclic voltammogram (Fig.3.26) of PANI also shows cathodic peak at +0.6 V. Both cathodic and anodic peaks appear in the CV of PANI suggesting that the presence of electro active region on the PANI film [140]. **Fig.3.28** shows cyclic voltammogram of background in H_2SO_4. From Fig it was observed that no characteristics oxidation and reduction peaks indicating that no electro active species is present in the solution at this potential range.

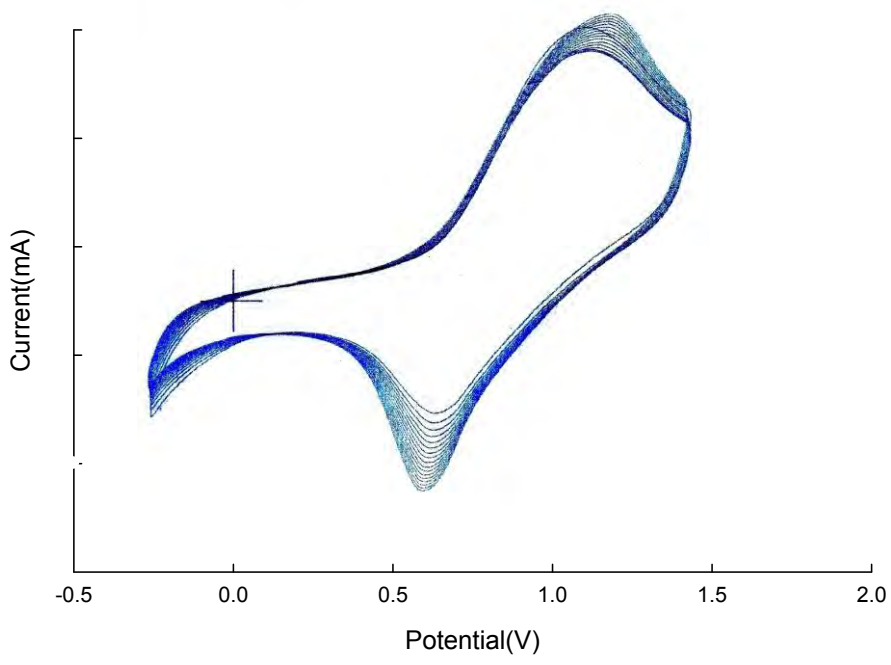

Fig.3.27. Doping dedoping process of PANI.

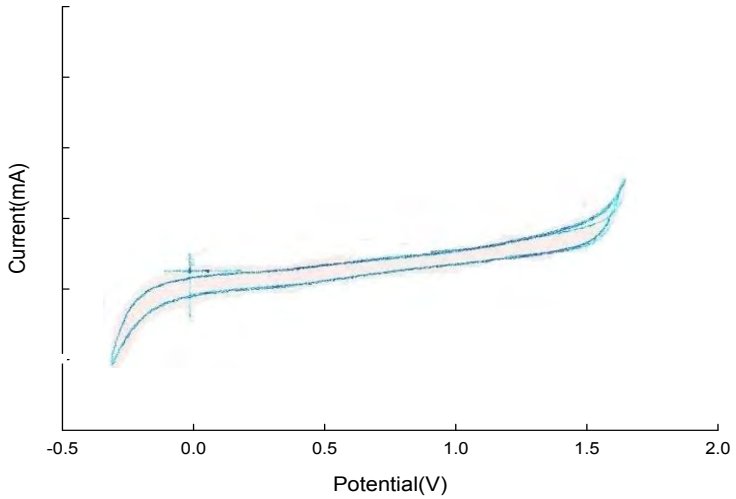

Fig.3.28 Cyclic voltammogram of background in H_2SO_4

3.6.2 Doping de-doping process of PANI coated film electrode

The electrochemical doping dedoping process of PANI coated film electrode was examined by cyclic voltametry in aqueous solution of H_2SO_4 (1M). For this case a cell consists of the PANI coated working electrode was allowed to sweep between the potential -0.4to +1.5V at a scan rate of 100 mVs^{-1}(**Fig.3.29**). The deep blue color of the film turned to greenish yellow when potential sweep approached to the cathodic direction at ca. +0.0 V or lower where dedoping of electrolyte occurs. In this case an oxidation and redrox peak disappears indicating that anilne monomer absent in the electrolytic solution.

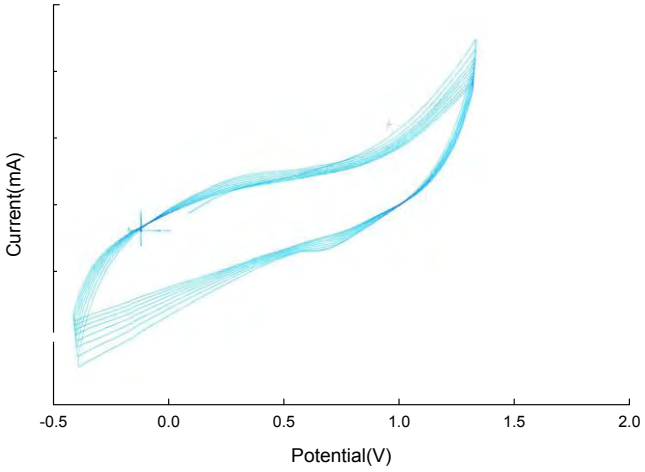

Fig.3.29. Doping dedoping process of PANI coated film electrode.

Mechanism of electrochemical formation of PANI. Reaction scheme for electrocmical formation of PANI is in following

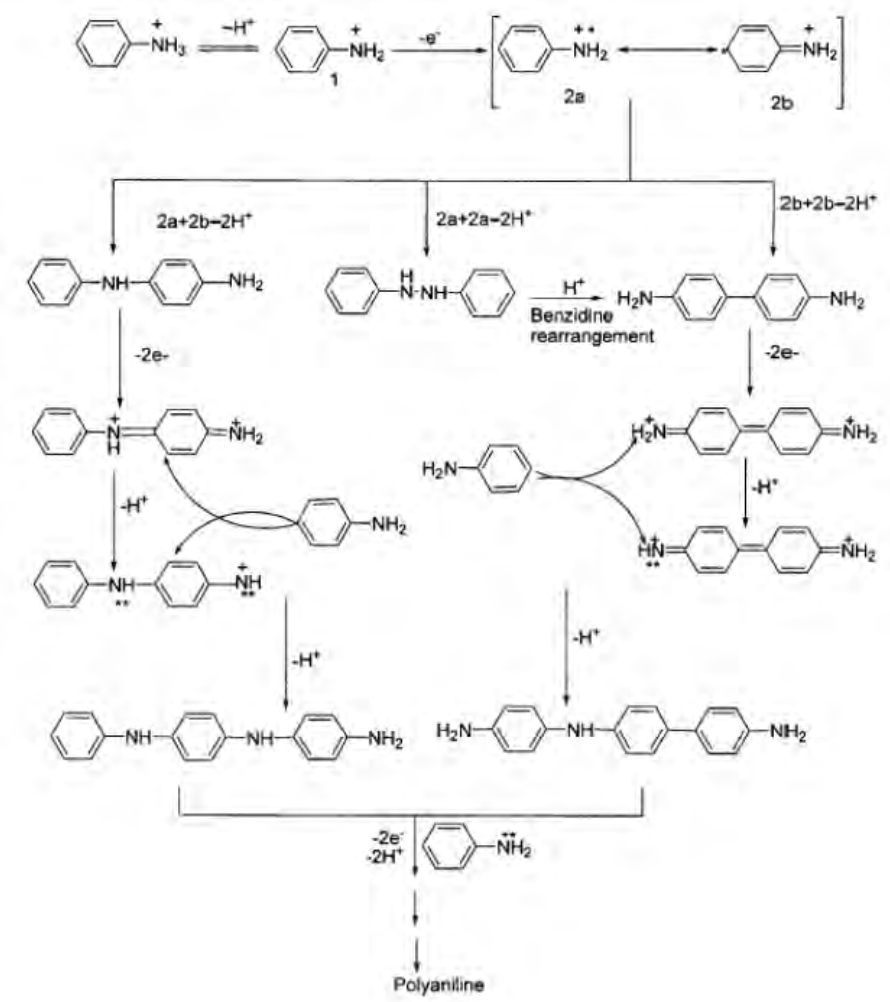

.

3.6.3 Doping de-doping process of SNPs-PANI nanocomposite

The doping-dedoping process of SNPs-PANI nanocomposite was examined by cyclic voltametry. **Fig.3.30** shows the cyclic voltammogram of SNPs-PANI nanocomposite in the potential range -0.5 to +1.5 V at a scan rate of 100 mVs^{-1}. It was seen from **Fig** that one peak appear at +01.1 V in the anodic sweeping and another peak at +0.5 V for catholic sweeping suggesting that the presence of electro active region in the SNPs-PANI nanocomposite film. From **Fig** also it was also observed that the anodic and cathodic peak potential of SNPs-PANI nanocomposite was decreased than PANI indicating that presence of SNPs in nanocomposite.

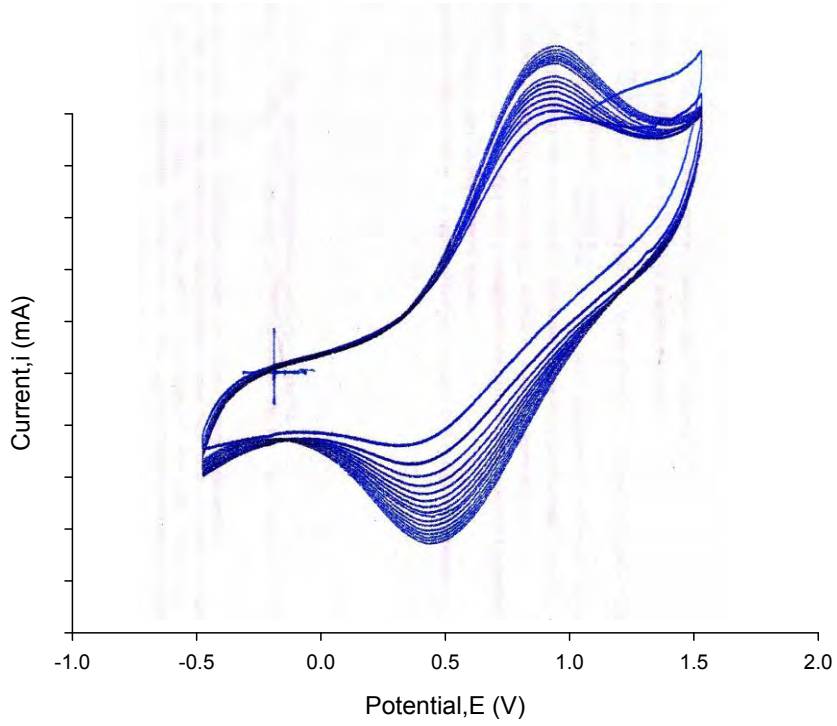

Fig.3.30. Doping-dedoping process of SNPs-PANI nanocomposite.

3.6.4 Doping de-doping process of SNPs-PANI coated film electrode

The electrochemical doping dedoping process of **SNPs-PANI** coated film electrode was examined by cyclic voltametry in aqueous solution of H_2SO_4 (1M). For this case a cell consists of the PANI coated working electrode was allowed to sweep between the potential -0.4to +1.5V at a scan rate of 100 mVs^{-1}(**Fig. 3.31**). The deep blue color of the film turned to greenish yellow when potential sweep approached to the cathodic direction at ca. +0.0 V or lower where dedoping of electrolyte occurs. In this case an oxidation and redrox peak

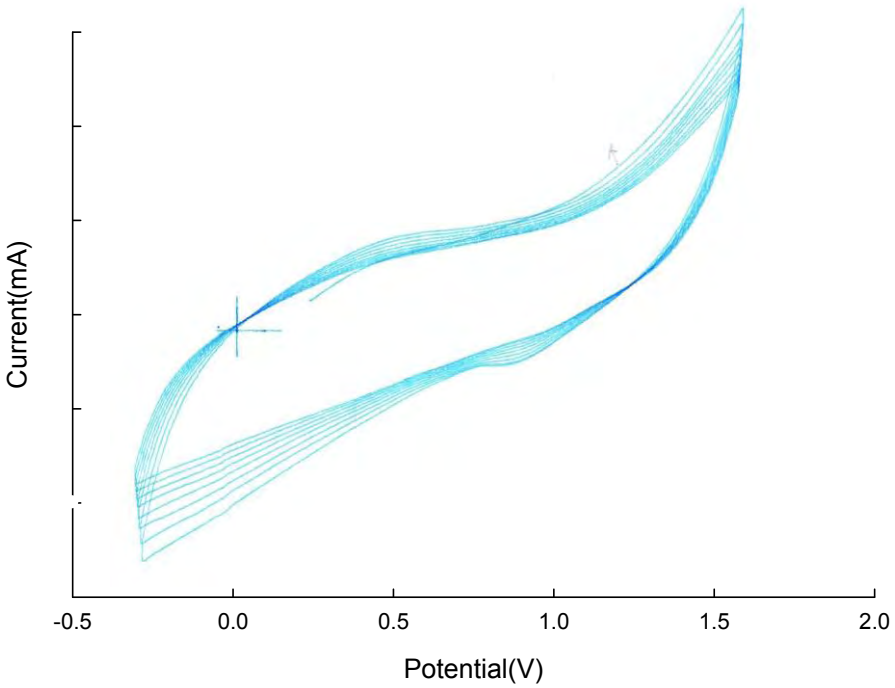

Fig. 3.31. Doping de-doping process of SNPs-PANIcoated film electrode.

disappears indicating that anilne monomer and/or electroactive species was absent in the solution.

Conducting polymer PANI has been tried as drug-delivering systems and release drugs with changing potential. Conducting electroactive polymers have been considered for drug delivery due to their unique redox properties, which allow controlled ionic transport through the polymer membrane. Electrochemical switching of the polymer is accompanied by the movement of counter ions, so-called dopant ions, in and out of the membrane for charge balance [140]. However, by depoing process of SNPS-PANI, it was concluded that incorporated SNPs released from PANI. However, due to promising application possibilities in human body, it is necessary to the investigation of cytotoxicity of PANI. The biocompatibility of PANI has recently been tested [140,141] and results in different study show that PANI possesses cytotoxicity [142]. Therefore, for in vitro application in human body derivatives of PANI is needed which will be biodegradable and safe for human body.

3.7 Antimicrobial activity of SNPs, PANI and SNPs-PANI nanocomposite

3.7.1. Antibacterial susceptibility test results of SNPs, PANI and SNPs/PANI Composite agar by well diffusion test

Two important and common diarrhoeal pathogens and six important and common non-diarrhoeal bacterial pathogens were tested by standard disc diffusion method. Overall bacterial species susceptible to antibiotics are also susceptible to SNPs and more susceptible to PANI/SNPs showing a good correlation. *Vibrio cholerae* O1 and *Salmonella* Typhi showed resistant to some antibiotics (cotrimoxazole, ciprofloxacin) and many nondiarrhoeal pathogens showed resistant to different antibiotics **(Table 3.5).**

Table 3.5 Antibacterial activity (zone diameter) of SNPs, PANI and SNPs/PANI (1:4 ratio) composite by agar well diffusion test and comparison with reference antibiotics tested by disc diffusion method

Bacteria Isolates	SNPs	PANI	SNPs-PANI	Cotrimoxazole*	Ciprofloxacin*	Ceftriaxone*
	Zone of inhibition in mm (mean of their replicates)					
Vibrio cholerae O1	16.5	17.0	27.5	7.0	26	ND
Salmonella Typhi	7.0	13.0	24.5	28.0	28	30
Pseudomonas spp.	<7.0	12.0	29.0	ND	36	19
Acnetobactor spp.	<7.0	12.0	30.0	ND	28	20
E. coli	8.0	19.0	25.5	27.0	28	19
Enterobacter spp.	7.5	14.0	18.0	ND	ND	11
Staphylococcus aureus	8.0	18.0	28.0	<7.0	≤10	<7
Streptococcus pneumoniae	9.0	13.0	25.0	<7.0	20	ND

❖ 150 (SNPs 30 µg and polyaniline(120 µg) nanoparticles used for all isolates

*Antibiotics were tested by disc diffusion method for comparison

*Red color indicates resistant to antibiotics, blue color indicates Intermediate and black color indicates susceptible to antibiotics for bacterial pathogens

Three important bacterial species that were resistant to cotrimoxazole showed moderate to high antibacterial activities to SNPs and PANI-SNPs whereas one species (*Enterobacter* spp.) resistant to cotrimoxazole showed poor activity (7.5 mm) to SNPs and good activity (18.0 mm) to PANI-SNPs. When the bacterial pathogens were tested for susceptibility to SNPs, majority (75%) of bacterial pathogens were susceptible (inhibition zone diameter > 16 mm)

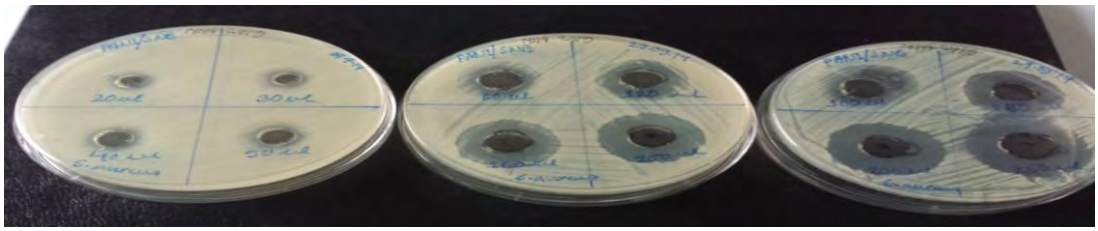

Fig.3.32 Inhibition zone for SNPs-PANI nanocomposite at different dose against *Staphylococcus aureus*

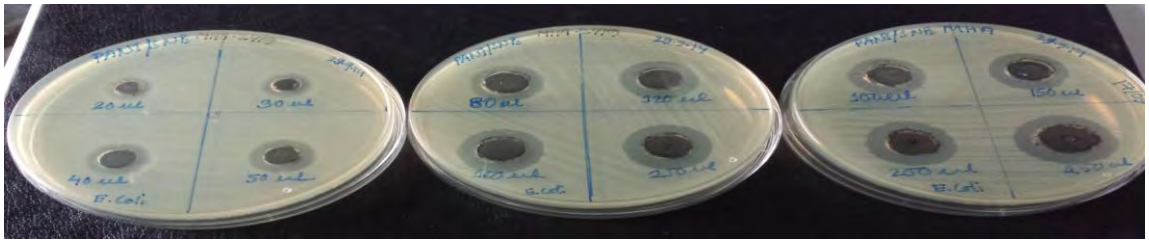

Fig.3.33 Inhibition zone for SNPs-PANI nanocomposite at different dose against *E.Coli.*

to S NPs. It showed high in-vitro activity against *Staphylococcus aureus* that were resistant to all three (cotrimoxazole, ciprofloxacin and ceftriaxone) antibiotics tested. PANI-S NPs showed high antibacterial activities (inhibition zone diameter > 18-30 mm) against all diarrhoeal and non-diarrhoeal pathogens tested (**Table 3.5**) On the basis of quantitative analysis, 150 µg PANI-SNPs composite contains 30 µg SNPs and 120 µg polyaniline nanoparticles which showed more antibacterial activities (inhibition zone diameter range ≥ 18-29 mm) than 150 µg SNPs (inhibition zone diameter > 7.5- 23.5 mm) and 150 µg (PANI inhibition zone diameter > 16 mm) showing synergistic activities of the composite. Comparison of antibacterial susceptibility test results of antibiotics with those of SNPs, PANI and SNPs-PANI composite showed that SNPs-PANI were more efficient/ active against all pathogenic bacteria tested in our study including susceptible and resistant bacteria. Moreover, SNPs-PANI nanocomposite showed dose dependent response against all pathogenic bacteria.

Fig.3.32 shows the Inhibition zone for SNPs-PANI nanocomposite at different dose against *Staphylococcus aureus*. It was observed that with increasing concentration inhibition zone was also increased. **Fig.3.33** shows the Inhibition zone for SNPs-PANI nanocomposite at different dose against *E.Coli.* From Fig it was seen that with increasing concentration inhibition zone was also increased.

3.7.2. Antifungal susceptibility test results of SNPs, PANI and SNPs/PANI Composite agar by well diffusion test

Antifungal activities of SNPs, PANI and SNPs-PANI composite are shown in **Table 3.6**. Antifungal activities were observed to be dose dependant for all nanoparticles tested.

Table 3.6 Antifungal activities (zone diameter) of SNPs, PANI and SNPs/PANI (1:4 ratio) composite determined by agar well diffusion method

Nanoparticles Tested		**Fungal spp., tested (No. of isolates)**		
Names	**Amount (**μg)	*Candida* spp., (10)	*Secdosporium* spp., (2)	*Scytalidium* spp., (2)
		Zone of inhibition in mm (mean of their replicates**)**		
SNPs	100	13	10	13
	150	17	11	14
	200	21	14	16
	250	24	16	17
PANI	100	14	10	12
	150	19	11	15
	200	22	13	18
	250	24	14	20
SNPs-PANI*	100	19	11	15
	150	23	13	17
	200	26	15	20
	250	28	17	22

*PANI-SNPs present in 1:4 ratio, i, e, 100 μg contains 20 μg SNPs and 80 μg PANI,
150 μg contains 30 μg and 120 μg PANI so on.

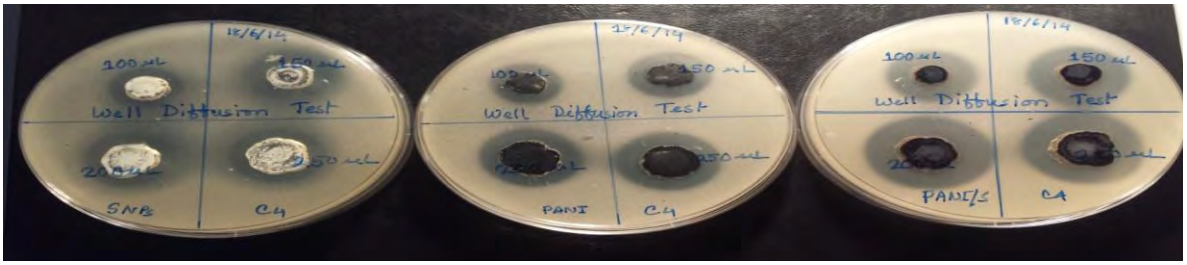

Fig.3.34 Inhibition zone for SNPs, PANI and Inhibition zone for SNPs, PANI and SNPs-PANI nanocomposite against *Candida* spp.

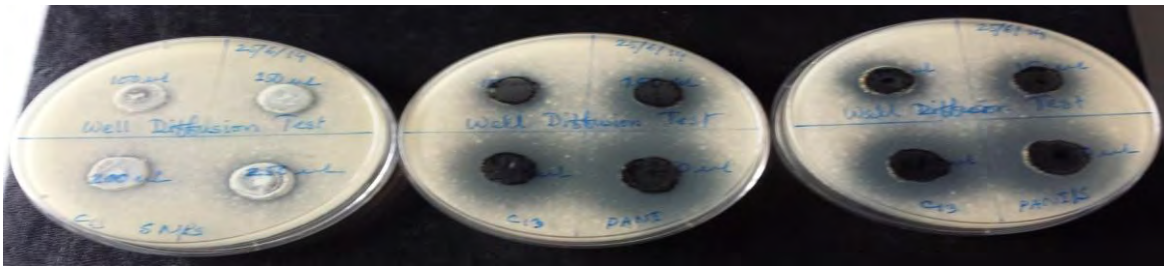

Fig 3.35 Inhibition zone for S NPs, PANI and S NPs- PANI nanocomposite against Secdosporium ***spp.***

Fig 3.34 and 3.35 showed the Inhibition zone for SNPs, PANI and SNPs-PANI nanocomposite against *Candida* spp and *Secdosporium* spp. From **Fig** it was observed that SNPs-PANI nanocomposite have highest antifungal activity than SNPs and PANI.

Conclusion

In summary, Sulfur nanoparticles (SNPs) were synthesized by electrochemically and chemically by reduction of sodium thiosulfate and by acid catalyzed precipitation of sodium thiosulfate in presence CTAB respectively. Conductive polymer Polyaniline (PANI) and PANI-SNPs nanocomposite were also synthesized by electrochemically and chemically. Electrochemically synthesized products of S NPs, PANI and S NPs- PANI nanocomposite showed lower particle size, uniform morphology and higher activity than chemically synthesized products. This is due to the difference in synthesis method and hence difference in the efficiency of reduction / oxidation or polymerization and different ways of arrangement of polymer chains. S NPs, PANI and S NPs- PANI have good thermal stability. PANI has been tried as drug-delivering systems and release drugs with changing potential but PANI dispersions possess cytotoxicity. Therefore, for in vitro application in human body derivatives of PANI is needed which will be biodegradable and safe for human body. However, NIPA and SNPs-NIPA gel have remarkable temperature-sensitive property. The hydrogel release SNPs with increased temperature $(25\text{-}40)^0$C. NIPA gel is biodegradable and can be used as drug carrier in human body safely. Additionally, antibacterial test were done by synthesized SNPs, PANI and PANI- SNPs nanocomposite. The obtained results showed that PANI-SNPs nanocomposite enhanced the antibacterial antifungal activity than SNPs and PANI.

References

[1] E. Boisselier, D. Astruc, "Gold nanoparticles for nanomedicine: preparations, imaging, diagnostics, therapies and toxicity". *J. Chem. Soc. Rev.,* **38,** 1759-1782, 2009.

[2] Q. A. Pankhurst, N. K. T. Thanh, S. K. Jones, J. Dobson, "Applications of Magnetic Nanoparticles in Biomedicine". *J. Phys. D: Appl. Phys.*, **42,** 58-61, 2009.

[3] T. Jamieson, R. Bakhshi, D. Petrova, R. Pocock, M. Imani, A. M. Seifalian, "Biological applications of quantum dots". *J. Biomater.,* **28,** 4717- 4732, 2007.

[4] M. Kolar, K. Urbanek, T. Latal, "Antibiotic selective pressure and development of bacterial resistance". *Int J Antimicrob.,* **17,** 357- 363, 2001.

[5] S. Pethkar, R. C. Patil, J. A. Kher, K. Vijayamohanan, " Deposition and characterization of CdS Nanoparticles/Polyaniline composite films". *J. Thin Solid Films,* **949,** 105-109, 1999.

[6] L. I. Nianfeng, L. E. I. Ting, L. I. U. Yong, H. E. Yuehui, Z. Yangde, "Electrochemical preparation and characterization of gold-polyaniline core-shell nanocomposites on highly oriented pyrolytic graphite". *Trans. J. Nonferrous Met. Soc. China,* **20,** 2314-2319, 2010**.**

[7] J. S. Kim, E. Kuk, K. N. Yu, J. H. Kim, H. J. Lee, S. H. Kim, Y. K. Park, C. Y. Hwang, Y. K. Kim, Y. S. Lee, D. H. Jeong and M. H. Cho, "Antimicrobial effects of silver nanoparticles". *Nanomed. Nanotechnol., Biol. Med.,* **3,** 95-101, 2007.

[8] Q. Li, S. Mahendra, D. Y. Lyon, L. Brunet, M. V. Liga, D. Li and P. J. J. Alvarez, "Antimicrobial nanomaterials for water disinfection and microbial control: potential applications and implications". *Water Res.,* 42, 4591–4602, 2008.

[9] M. Raffi, S. Mehrwan, T. M. Bhatti, J. I. Akhter, A. Hameed, W. Yawar and M. M. Hasan, "Antibacterial characterization of silver nanoparticles against E. coli ATCC-*15224". Ant. Microbiol*., **60**, 75–80, 2010.

[10] L. Zhang, D. Pornpattananangkul, C. M. J. Hu, C. M. Huang, "Development of Nanoparticles for Antimicrobial Drug Delivery". *Current Medicinal Chemistry*, **17**, 585-594, 2010.

[11] S. Baruah and J. Dutta, "Paper modified with ZnO nanorods–antimicrobial in Agriculture" *Environ. Chem. Lett.,* **7**, 191–204, 2009.

[12] S. Pal, Y. K. Tak and J. M. Song, "Antiviral Properties of Silver Nanoparticles on a Magnetic Hybrid Colloid" .*Appl. Environ. Microbiol.,* **73**, 1712–1720, 2007.

[13] M. A. Aguilar-Mendez, E. S. Martın-Martınez, L. Ortega- Arroyo, G. Cobian-Portillo and E. Sanchez-Espındola, "The preparation of Ag-TiO_2 nanocomposites". *J. Nanopart. Res*., **13,** 2525–2532, 2011.

[14] P. Gong, H. Li, X. He, K. Wang, J. Hu, W. Tan, S. Zhang and X. Yang, "Preparation of stable colloidal suspension of uniform silver nanoparticles and their antibacterial activities". *Nanotechnology*, **18**, 285604, 2007.

[15] M. A. A. Mendez, E. S. M. Martınez, L. O. Arroyo, G. C. Portillo, E. S. Espındola, "Conduction mechanism in polymer nano-composite electrolyte system". *J. Nanopart. Res.,* **13,** 2525–2532, 2011.

[16] C. M. Rico, S. Majumdar, M. Duarte-Gardea, J. R. Peralta- Videa and J. L. Gardea-Torresdey, "Interaction of nanoparticles with edible plants and their possible implications in the food chain". *J. Agric. Food Chem.,* **59**, 3485–3498, 2011.

[17] P. Gajjar, B. Pettee, D. W. Britt, W. Huang, W. P. Johnson and A. J. Anderson, "**Antifungal Activity of Silver and Copper Nanoparticles on Two Plant Pathogens, *Alternaria alternata* and *Botrytis cinerea".*** *J. Biol. Eng.*, ***3***, 1-13, *2009*.

[18] K. Jagajjanani Rao , S. Paria, "Use of sulfur nanoparticles as a green pesticide on *Fusarium solani* and *Venturia inaequalis* phytopathogens". *RSC Adv.***,** 3, 10471-10478, 2013.

[19] G. Borkow , A. Monk, " Fighting nosocomial infections with biocidal non-intrusive hard and soft surfaces". *World J Clin Infect Dis.,* **2**, 77-90. 2012.

[20] A. S. Deshpande, R. B. Khomane, B. K. Vaidya, R. M. Joshi, A. S. Harle and B. D. Kulkarni, "The Efficancy of Micron and Nanoscale Sulfur the Schutte Fungi" *Nanoscale Res. Lett.,* **3**, 221–229, 2008.

[21] H. Inoue, G. Kawano, H. Nagasawa and S. Sakuda, " Identification of Indole Derivatives as Self-Growth Inhibitors of *Symbiobacterium thermophilum*, a Unique Bacterium Whose Growth Depends on Coculture with a *Bacillus* sp". *Appl. Environ. Microbiol.***, 68,** 4809–4811, 2002.

[22] R. M. Cooper and J. S. Williams, "Elemental sulphur as an induced antifungal substance in plant defence". *J. Exp. Bot.,* **55**, 1947–1953, 2004.

[23] G. Liu, P. Niu, L. Yin, H. M. Cheng. "α-Sulfur Crystals as a Visible-Light-Active Photocatalyst". *J. Am. Chem. Soc.,* **134**, 9070−9073, 2012.

[24] Y. Sheng Su, A. Manthiram, "A facile in situ sulfur deposition route to obtain carbon-

wrapped sulfur composite cathodes for lithium–sulfur batteries". *J. Electrochim. Acta,* **77,** 272-278, 2012.

[25] R. G. Chaudhuri, S. Paria. "Synthesis of sulfur nanoparticles in aqueous surfactant solutions". *J. Colloid Interf. Sci.,* **343,** 439-446, 2010.

[26] E. Granot, E. Katz, B. Badnar, I. Willner, "Enhanced bioelectrocatalysis using Au nanoparticle/polyaniline hybrid systems in thin films and microstructured rods assembled on electrodes".*J. Chem. Mater.,* **17,** 4600-4609, 2005.

[27] Y. Qiang, J. Antony, A. Sharma, J. Nutting, D. Sikes, D. Meyer, "Highly magnetic core-shell nanoparticles with unique magnetization mechanism". *J. Nanoparticles Research*, **8**, 489–496, 2006.

[28] C. Hayashi, "Method of manufacturing ultrafine particles and their application". *Phys. Today* **40,** 44-51, 1987.

[29] H. Gleiter, "Nanocrystalline Materials". Prog. *Mater. Sci.* **33,** 223-229, 1989.

[30] R. Uyeda, "Preparation of palladium ultrafine particles in reverse micelles". *Prog. Mater. Sci*. **35,** *1*–96, 1991.

[31] I. Sondi, B. Salopek-Sondi, "Susceptibility constants of Escherichia coli and Bacillus subtilis to silver and copper nanoparticles". *J. Colloids Interface Sci.* **275,** 177-182, 2004.

[32] V. Gupta, A. Kumar, "Nanosilver Products-A Review". *Chem Sci Rev Lett*, **3**, 717-727, 2014.

[33] F. Furno, K.S. Morley, B. Wong, B. L Sharp, P. L. Arnold, S. M. Howdle, R. Bayston, P. D. Brown, P. D. P. Winship, H. J. Reid, "Silver nanoparticles and polymeric medical devices: a new approach to prevention of infection". *J. Antimicrob. Chemother.,* **54,** 1019–24, 2004.

[34] S. Kim, H.J. Kim, "Polyethylene and biodegradable mulches for agricultural applications: a review". *Int. Biodeterioration Biodegrad.,* **57,** 155–62, 2006.

[35] E. Sachlos, D. Gotora, J. T. Czernuszka, "Collagen scaffolds reinforced with biomimetic composite nano-sized carbonate-substituted hydroxyapatite crystals and shaped by rapid prototyping to contain internal microchannels". *Tissue Eng.* **12,** 2479, 2006.

[36] O. C. Farokhzad, J. Cheng, B. A. Teply, I. Sherifi, S. Jon, P. W. Kantoff, J. P. Richie,

R. Langer, "Nanomedicine: developing smarter therapeutic and diagnostic modalities". *Proc. Natl Acad. Sci.* USA **103,** 6315-6320, 2006.

[37] P. K. Stoimenov, R. L. Klinger, G. L. Marchin, K. J. Klabunde, "Controllable preparation of Nano-MgO and investigation of its bactericidal properties". *Langmuir,* **18,** 6679-6686, 2002.

[38] A. Panacek, L. Kvitek, R. Prucek, M. Kolar, R. Vecerova, N. Pizurova, V. K. Sharma, T. Nevecna, R. Zboril, "Antibacterial activity and toxicity of silver–nanosilver versus ionic silver". *J. Phys. Chem.,* B **110,** 16248-16253, 2006.

[39] C. W. Waren, S. Nie, "Probing the cytotoxicity of semiconductor quantum dots".*Science,* **281,** 2016-2018, 1998.

[40] A. Vaseashta, D. Dimova-Malinovska, "Microwave-assisted rapid extracellular synthesis of stable bio-functionalized silver nanoparticles from guava (Psidium guajava) leaf extract". *Sci. Technol. Adv. Mater.,* **6,** 312-318, 2005.

[41] R. Langer, "Designing materials for biology and medicine". *Science* **293,** 58-59, 2001.

[42] J. M. Dang, K. W. Leong, "Natural polymers for gene delivery and tissue engineering" Advanced Drug Delivery Reviews, **58,** 487–499, 2006.

[43] C. Baker, A. Pradhan, L. Pakstis, D. J. Pochan, S. I. Shah, "Synthesis and antibacterial properties of silver nanoparticles". *J. Nanosci. Technol.,* **5,** 244-249, 2005.

[44] A. C. Templeton, W. P. Wuelfing, R.W. Murray, "Controlled and reversible formation of nanoparticle aggregates and films using Cu^{2+}-carboxylate chemistry". *Acc. Chem. Res.,* **33,** 27, 2000.

[45] M. C. Daniel, J. R. Aranzaes, S. Nlate, D. Astruc, "Gold-nanoparticle-cored Polyferrocenyl Dendrimers: Modes of Synthesis and Functions as Exoreceptors of Biologically Important Anions and Re-usable Redox Sensors". Journal of Inorganic and Organometallic Polymers and Materials, **15,** 107-119, 2005,

[46] T. Hasobe, H. Imahori, P.V. Kamat, T.K. Ahn, S.K. Kim, D. Kim, A. Fujimoto, T. Hirakawa, S. Fukuzumi, Photovoltaic cells using composite nanoclusters of porphyrins and fullerenes with gold nanoparticles. *J. Am. Chem. Soc.,* **127,** 1216,

2005.

[47] A. Caballero, M. Cruz, L. Hernán , M. Melero, J. Morales, E. Rodríguez Castellon, *"*Nanocrystalline materials obtained by using a simple, rapid method for rechargeable lithium batteries". *J. Power Sources,* 150,192–201, 2005.

[48] J. Barkauskas , R. Juskenas, V. Mileriene, V. Kubilius, "Effect of sulfur on the synthesis and modification of carbon nanostructures". Materials Research Bulletin, 42, 1732–1739, 2007.

[49] Y. Zhao, J.M. Hong, J.J. Zhu, Microwave-assistedself-assembled ZnS nanoballs, *J. Crystal Growth,* **270**, 438–445, 2004.

[50] L. F. Xi, Y. M. Lam, "Synthesis and characterization of CdSe nanorods using a novel microemulsion method at moderate temperature". *J. Colloid and Interface Science,* **316**, 771–778, 2007.

[51] N. Ishida, M. Kobayashi, "Interaction forces measured between poly (*N*-isopropylacrylamide) grafted surface and hydrophobic particle". J. Control. Release, **297**, 513–519, 2006.

[52] *R.B. Manna*, A. *Mandale*, *A. B. Kulkarni*, *"Synthesis* and *characterization* of dodecanethiol- capped cadmium sulride nanoparticles in a Winsor II microemulsion of *diethyl ether/AOT/water"*. *Langmuir, **18**, 8237-8240, 2002*.

[53] L. Kienle, V. Duppel, S. Schlecht, "Modified magnetic properties of paramagnetic (Zn, Mn) **S** at reduced dimensions". *Soild State Sci.*, **6**, 179-183, 2004.

[54] P. P. Chin, J. Ding, J. B. Yi, B. H. Liu, "A Review of Methods for Synthesis of Nanostructured Metals with Emphasis on Iron Compounds". *J. Alloy. Compd.,* **390**, 255-268, 2005.

[55] F. Qi, K. Hirofumi, O. Kenta, "Manganese oxide porous crystals". *J. Mater. Chem.*, **9**, 319-333, 1999.

[56] R. Feynman, "Applications of nanoparticles in biology and medicine". *J. Science*. **254**, 1300-1301, 1991.

[57] W. J. Parak, D. Gerion, T. Pellegrino, D. Zanchet, C. Micheel, C.S. Williams, R. Boudreau, M.A. Le Gros, C.A. Larabell, A.P. Alivisatos, "Site-Specific Ligation Of DNA-Modified Gold Nanoparticles". *J. Nanotechnology*, **14**, 15-27, 2003.

[58] G. M. Whitesides, "Applications of nanoparticles in biology and medicine". *J. Natur.*

Biotechno., **21**,1161-1165, 2003.

[59] F. M. Gutierrez, P. L. Olive, A. Banuelos, E. Orrantia, N. Nino, E. M. Sanchez, F. Ruiz, H. Bach, Y. A. Gay. "A Study on the Antibacterial Activity Of Zno Nanoparticles". *J. Nanomedi.,* **6**, 681-688, 2010.

[60] K. Dunn, V. E. Jones, "The role of Acticoat with nanocrystalline silver in the management of burns". *Burns*. **30**, 2004, 1–9.

[61] M. Sametband, S. Shukla, T. Meningher, S. Hirsh, E. Mendelson, R. Sarid, A. Gedanken, M. Mandelboim, "Effective multi- strain inhibition of influenza virus by anionic gold nanoparticles". *J. Med. Chem. Commun.* **2**, 421-423, 2011.

[62] A. M. Schrand, M. F. Rahman, S. M. Hussain, J. J. Schlager, D. A. Smith, A. F. Syed, "The use of Gold Nanoparticles in Diagnostics and Detection". *J. Nano. Nanobiotechn.*, **2**, 544–568, 2010.

[63] S. Pethkar, R. C. Patil, J. A. Kher, K. Vijayamohanan, "Conducting polymer-based nanostructurized materials--electrochemical aspects". *J. Thin Solid Films,* **949**, 105-109, 1999.

[64] L. I. Nianfeng, L. E. I. Ting, L. I. U. Yong, H. E. Yuehui, Z. Yangde, "Electrochemical preparation and characterization of gold-polyaniline core-shell nanocomposites on highly oriented pyrolytic graphite". *J. Nonfer. Met. Soc. China.* **20,** 2314−2319, 2010.

[65] T. Takigawa, K. Urayama, Y. Morino, T. Masuda, "Simultaneous Swelling and Stress Relaxation Behavior of Uniaxially Stretched Polymer Gels". *Polymer Journal,* **25,** 929-937, 1993.

[66] K. Khannap, S. C. Singhn, A. K. Viswanath, "Synthesis of Ag/polyaniline nanocomposite via an in situ photo-redox mechanism". *J. Mater. Chem. Phys.,* **92**, 214−219, 2005.

[67] Y. J. Sheng, X. X. Shuang, X. Y. Lian, Y. Wu, C. Zhao, "Synthesis and characterization of Ag/polyaniline core-shell nanocomposites based on silver nanoparticles colloid". *J. Mater Lett.*, **61**, 2794−2797, 2007.

[68] Y. Sheng Su, A. Manthiram," A facile in situ sulfur deposition route to obtain carbon-wrapped sulfur composite cathodes for lithium–sulfur batteries". *J. Electrochim. Acta,* **77**, 272– 278, 2012.

[69] S. R. Choudhury, S. Basu , "Polyethylene glycol-stabilized sulphur nanoparticles: an effective antimicrobial agent against multidrug-resistantbacteria". *J Antimicrob. Chemother.* **67**,1134-1137,2012.

[70] R. G. Chaudhuri, S. Paria, "Synthesis of sulfur nanoparticles in aqueous surfactant solutions". *J. Colloid Interf. Sci.* **343,** 439–446, 2010.

[71] A. Taylor, P. Robert, T. Otanicar, Y. Herukerrupu, B. Fabienne, R. Gary, R. Hawkes, E.Jiang, X. C. Sylvain, "Feasibility of nanofluid-based optical filters". *J. Appli. Opti.,* **52,** 1413–22, 2013.

[72] X. Huang, A. Mostafa, E. Sayed, "Gold nanoparticles: Optical properties and implementations in cancer diagnosis and photothermal therapy". Journal of Advanced Research, **1**, 13–28, 2010.

[73] A. H. Lu, W. Schmidt, N. Matoussevitch, H. Bönnemann, B. Spliethoff, B. Tesche, E. Bill, W. Kiefer, F. Schüth, "Nanoengineering of a Magnetically Separable Hydrogenation Catalyst". *Angewandte Chemie International Edition,* **43**, 4303–4306, 2004.

[74] J. Sun, S. L. Simon, "Nanoscale thermal analysis for nanomedicine by nanocalorimetry". *J. Thermo. Acta.,* **463,** 32-40, 2007.

[75] B. Revaz, B. L. Zink, F. Hellman, "Si-N membrane-based microcalorimetry: heat capacity and thermal conductivity of thin films". *Thermochim. Acta*, **432**,158–168, 2005.

[76] H.Y. Miao, J.T. Lue, S.Y. Chen, S. K. Chen, M. S. Ouyang, "Growth of carbon nanotubes on transition metal alloys by microwave-enhanced hot-filament deposition". *Thin Solid Films,* **484** ,58–63, 2005.

[77] B. Peng, Y. Yao, and J. Zhang, "Effect of the Reynolds and Richardson Numbers on the Growth of Well-Aligned Ultralong Single-Walled Carbon Nanotubes". *J. Phys. Chem. C*, **114**, 12960–12965, 2010.

[78] B. O. Dabbousi, J. R. Viejo, F. V. Mikulec, J. R Heine, H. Mattoussi, R. Ober, K. F. Jensen, M. G. Bawendi, "(CdSe)ZnS Core−Shell Quantum Dots: Synthesis and Characterization of a Size Series of Highly Luminescent Nanocrystallites". *J. Phys. Chem. B*, **101,** 9463-9475, 1997.

[79] M. Rivera Diaz, P. E. V. Mejia, "Nanoparticles as Drug Delivery Systems in Cancer Medicine:Emphasis on RNAi-Containing Nanoliposomes". *Pharmaceuticals*, **6,** 1361-1380, 2013.

[80] I. Sondi , B. S. Sondi , "Silver nanoparticles as antimicrobial agent: a case study on E. coli as a model for. Gram-negative bacteria". J Colloid Interface Sci., **275**,177-182, 2004.

[81] J. F. Healy, *Pliny the Elder on science and technology*, Oxford University Press, pp. 247–249, 1999.

[82] M. Bea, *"* Nanosilver Products - A Review". *J. Chem. Revi.* **64,** 429–451, 1964.

[83] Greenwood Norman, E. Alan. *Chemistry of the Elements* (2nd ed.) pp. 645–662, 1997.

[84] C. C. Boswell, D. K. Friesen. "Elemental sulfur fertilizers and their use on crops and pastures". *Fertilizer research*, **35**, 127-149, 1993.

[85] P. S. Rao, D. N. Sathyanarayana, In *Advanced Functional Molecules and Polymers,* Gordon & Breach, Tokyo, 2001**.**

[86] A. Mostafaei , A. Zolriasatein, "Synthesis and characterization of conducting polyaniline nanocomposites containing ZnO nanorods" . *Progress in Natural Science: Materials International*, **22**, 273–280, 2012.

[87] F. Ahmed, S. Kumar, N. Arshi, M. S. Anwar, L. S. Yeon, G. S. Kil, D.W. Park, B. H. Koo, C. G. Lee, "Preparation and characterizations of polyaniline (PANI)/ZnO nanocomposites film using solution casting method". *Thin Solid Films*, **519**, 8375–8378, 2011.

[88] J. Yue, A. J. Epstein, "Synthesis of self-doped conducting polyaniline". *J. Am. Chem. Soc.*, **112** , 2800–2801, 1990.

[89] J. Vivekanandan, V. Ponnusamy, A. Mahudeswaran, P. S. Vijayanand, "Synthesis,

characterization and conductivity study of polyaniline prepared by chemical oxidative and electrochemical Methods". *Archives of Applied Science Research*, 3 ,147-153, 2011.

[90] J. Stejskal, R. G. Gilbert, "Polyaniline. Preparation of a conducting polymer". *J. Pure Appl. Chem.* **74,** 857-867, 2002.

[91] N. Li, J. Lee, L. Ong, "A polyaniline and nafion® composite film as a rechargeable battery", *Journal of Applied Electrochemistry*, **22**, 512-516, 1992.

[92] N. Gospodinova and L. Terlemezyan, "Conducting polymers prepared by oxidative polymerization: polyaniline". *Progress in Polymer Science*, **23**, 1443-1484, 1998.

[93] Z. Liu, S. Poyraz, Y. Liu, X. Zhang, "Seeding approach to noble metal decorated conducting polymer nanofiber network". ***Nanoscale***, **4**, 106-109, 2012.

[94] L. E. I. Ting, "Preparation of novel core-shell nanoparticles by electrochemical synthesis". *J. Trans Nonferrous Met Soc China*, **17**, 1343−1346, 2007.

[95] A. Greiner, J. H. Wendorff, A. L. Yarin, E Zussman ,"Biohybrid nanosystems with polymer nanofibers and nanotubes". *Applied Microbiology and Biotechnology,* **71**, 387–93, 2006.

[96] P.Henrique, C. Camargo, K. G. Satyanarayana, F. Wypych. "Nanocomposites: Synthesis, Structure, Properties and New Application Opportunities". *Materials Research*, **12**, 1-39, 2009.

[97] M. G. Kanatzidis, C.G. Wu, H. O. Marcy, C. R. Kannewurf, "Conductive Polymer Bronzes: Intercalated Polyaniline in V_2O_5 Xerogels". *J. Am. Chem. Soc*. **111,** 4139-4141, 1989.

[98] S. Pande, H. Swaruparani, M. D. Bedre, R. Bhat, R. Deshpande, A. Venkataraman**. "**Synthesis, Characterization and Studies of PANI-MMT Nanocompoisites". *Nanoscience and Nanotechnology,* **2**, 90-98, 2012.

[99] M. L. Cantu and P. G. Romero, "The Organic-Inorganic Polyaniline/V_2O_5 System: Application as a High-Capacity Hybrid Cathode for Rechargeable Lithium Batteries". *Journal of The Electrochemical Society,* **146**, 2029-2033, 1999.

[100] Bashir Ahmad, S. Abbas, Z. Iqbal, S. Bashir, J. Ali, "Synthesis of Cross Linked PVP Hydrogels and its Use for the Control Release of Anti-Asthmatic Drugs". *Middle-*

East Journal of Scientific Research, **14**, 273-283, 2013.

[101] P.C. Thomas, B. H. Cipriano, S. R. Raghavan, "Nanoparticle-crosslinked hydrogels as a class of efficient materials for separation and ion exchange". *Soft Matter*, **7**, 8192–8197, 2011.

[102] D. Browarzik, "A new thermodynamic model of volume changes in temperature-sensitive polymer gels". *Journal of Molecular Liquids,* **198**, 149–156, 2014.

[103] M. Zrıinyi, D. Szabo, H. G. Kilian, "Kinetics of the shape change of magnetic field sensitive polymer gels". *Polymer Gels and Networks,* **6**, 441–454, 1998.

[104] A. Suzuki, T. Tanaka, "Phase transition in polymer gels induced by visible light". *Nature*, **346**, 345-347, 1990.

[105] D. E. Discher, P. Janmey, Y. L. Wang, "Tissue Cells Feel and Respond to the Stiffness of Their Substrate". *J. Science,* 310, 1139–43, 2005.

[106] A. S. Hoffman, "Applications of thermally reversible polymers and hydrogels in therapeutics and diagnostics". *J. Control. Rel.*, **6**, 297–305, 1987.

[107] L. C. Dong, A. S. Hoffman , "Synthesis and application of thermally reversible heterogels for drug delivery" *Journal of Controlled Release,* **13**, 21–31, 1990.

[108] K. Sawahata, M. Hara, H. Yasunaga, Y. Osada, "Electrically controlled drug delivery system using polyelectrolyte gels". *Journal of Controlled Release,* **14**, 253–262, 1990.

[109] N. A. Peppas, A. R. Khare, "Preparation, structure and diffusional behavior of hydrogels in controlled release". *Advanced Drug Delivery Reviews,* 11, 1–35, 1993.

[110] H. Matsuoka, K. Fujimoto, H. Kawaguchi, "Monodisperse microspheres exhibiting discontinuous response to temperature change". *Polymer Gels and Networks,* 6, 319–332, 1998.

[111] T. Amiya, Y. Hirokawa, Y. Hirose, Y. Li, T. Tanaka, "Reentrant phase transition of *N*-isopropylacrylamide gels in Towards a mixed solvents". *J. Chem. Phys.* **86**, 2375–2379, 1987.

[112] A. Serres, M. Baudys, S.W. Kim, "Temperature and pH sensitive polymers for human calcitonin delivery". *J. Pharm. Sci.,* **13**, 196–201, 1996.

[113] C. S. Brazel, N. A. Peppas, "Synthesis and characterization of thermo- and chemo-

mechanically responsive poly(*N*-iso- propylacrylamide-*co*-methacrylic acid) hydrogels, Macro conventional and environmentally-sensitivemolecules". *Journal of Controlled Release,* **28**, 8016–8020, 1995.

[114] J. Kim, J. Yoon, R. C. Hayward, "Dynamic display of biomolecular patterns through an elastic creasing instability of stimuli-responsive hydrogels". *Nature Materials* **9**,159–164, 2010.

[115] J. H. Holtz, S. A. Asher, "Polymerized colloidal crystal hydrogel films as intelligent chemical sensing materials". *Nature,* **389**, 829-832, 1997.

[116] N. A. Peppas, K.B. Keys, M. T. Lugo, A. M. Lowman, "Poly (ethylene glycol)-containing hydrogels in drug delivery". *Journal of Controlled Release*, **62**, 81–87, 1999.

[117] H. Ichijo, R. Kishi, O. Hirasa, Y. Takiguchi, "Separation of organic substances with thermoresponsive polymer hydrogel". *J. Polymer Gels and Networks,* **2**, 315–322, 1994.

[118] L. Guo , J. Nie, B. Du, Z. Peng, B. Tesche, K. Kleinermanns, "Thermoresponsive polymer-stabilized silver nanoparticles". *J. Colloid and Inter. Sci.*, **319** 175–181, 2008.

[119] F. E. Hamed, N. Dave, J .Liu, "Stimuli-responsive releasing of gold nanoparticles and liposomes from aptamer-functionalized hydrogels". *Nanotechnology*, **22**,494-499, 2011.

[120] Y. Qiu, K. Park, Environment-sensitive hydrogels for drug delivery. Advanced Drug Delivery Reviews, **53**, 321–339, 2001.

[121] J. R. Crison, S.Y. Lin, A. S. Fox, G. L. Amidon, "Physical chemical properties effecting drug transport through poly-(ethylene oxide) hydrogels". *Control. Release Bioact. Mater.*, **21**, 483–484, 1994.

[122] A. Suzuki, T. Tanaka, "Phase transition in polymer gels induced by visible light". *Nature,* **346**, 345-347, 1990.

[123] N. Bait, B. Grassl, C. Derail, A. Benaboura, "Hydrogel nanocomposites as pressure-sensitive adhesives for skin-contact applications". ***Soft Matter***, **7**, 2025-

2032, 2011.

[124] Guohua Chen & Allan S. Hoffman, Graft copolymers that exhibit temperature-induced phase transitions over a wide range of pH, *Nature,* **373**, 49 -52, 1995.

[125] X. Yin, A. S. Hoffman, P. S. Stayton, "Poly (N-isopropylacrylamide-co-propylacrylic acid) copolymers that respond sharply to temperature and pH". *Biomacromolecules*, **7,** 1381-1385, 2006.

[126] J. C. Garbern, A. S. Hoffman, P. S. Stayton, "Injectable pH- and temperature-responsive poly (N-isopropylacrylamide-co-propylacrylic acid) copolymers for delivery of angiogenic growth factors". *Biomacromolecules*, **11**, 1833–1839, 2010.

[127] C. L Zhu, C H. Lu, X. Y. Song, H. H. Yang , X. R. Wang, "Bioresponsive controlled release using mesoporous silica nanoparticles capped with aptamer-based molecular gate". *J Am Chem Soc*., **133**, 1278-1281, 2011.

[128] S. Rattan, T. Sehgal, "Stimuli-Responsive Polymeric Membranes through Graft Copolymerization of N-Isopropylacrylamide onto Polycarbonate Track Etched Membranes for Biomedical Applications". *Procedia Chemistry*, **4**, 194–201, 2012.

[129] H. Yan, K. Tsujii, "Potential Application of Poly (*N*-isopropylacrylamide) Gel Containing Polymeric Micelles to Drug Delivery Systems". *Colloids and Surfaces B: Biointerfaces*, **46**, 142-146, 2005.

[130] F. E. Hamed, N. Dave, J. Liu, "Stimuli-responsive releasing of gold nanoparticles and liposomes from aptamer-functionalized hydrogels". *Nanotechnology,* **22**,494-511, 2011.

[131] P. Wang, T. P. Johnston, "Kinetics of sol-to-gel transition for Poloxamer polyols". *J. Appl. Polym. Sci.* **43**, 283– 292, 1991.

[132] L. He, Q. Zuo, S. Xie, Y. Huang , W. Xue, Intelligent hydrogels for drug delivery system. *Recent Pat Drug Deliv Formul.,* 5, 265-74, 2011.

[133] A. S. Hoffman, "Thermal cycling effects on the bioreactor performances of immobilized β-galactosidase in temperature-sensitive hydrogel beads". *J. Control. Release,* **6**,297–305, 1987.

[134] A. S. Hoffman, A. Afrassiabi, L. C. Dong, "A novel approach for preparation of pH-

sensitive hydrogels for enteric drug delivery". J. Control. Release, **4**, 213–222, 1986.

[135] L.E. Bromberg, "Transport of monocharged ions through environment-sensitive composite membranes based on poly- electrolyte complexes". *J. Membr. Sci.,* **62**,117–130, 1991.

[136] C. L. Bell, N. A. Peppas, "Biomedical membranes from hydrogels and interpolymer complexes". *Advances in Polymer Science*, **122**, 125-175, 1995.

[137] A. W. Bauer. "Testing Antibiotic Using Disk Diffusion Assay Kirby Bauer Method". *American journal of clinical pathology,* **44**, 493-496, 1966.

[138] S. Magaldi, S. M. Essayag, C. H. Capriles, C. Perez, M. T. Colella, C. Olaizola, Y. Ontiveros, "Well diffusion for antifungal susceptibility testing". *International Journal of Infectious Diseases,* **8**, 39–45, 2004.

[139] Joint Commission on Powder Diffraction Standards. Powder diffraction file, Inorganic phase. International center for diffraction data. PA, USA. JCPDS No. 08247, p. 410.

[140] P.K. Prabhakar, S. Raj, P.R. Anuradha, S.N. Sawant, M. Doble, Biocompat-ibility studies on polyaniline and polyaniline–silver nanoparticle coatedpolyurethane composite, Colloids Surf. B: Biointerfaces **86** ,146–153, 2011.

[141] P. Humpolicek, V. Kasparkova, P. Saha, J. Stejskal, Biocompatibility of polyani-line, Synth. Met. **162**, 722–727, 2012.

[142] Y. Min, Y.Y. Yang, Y. Poojari, Y.D. Liu, J.-C. Wu, D.J. Hansford, Sul-fonated polyaniline-based organic electrodes for controlled electricalstimulation of human osteosarcoma cells, Biomacromolecules **14**, 1727–1731, 2013.